

NASA**MEMORANDUM**

FLIGHT MEASUREMENTS OF SOME OF
THE FLYING QUALITIES AND STABILITY DERIVATIVES
OF A SUPERSONIC FIGHTER AIRPLANE

By Christopher C. Kraft, Jr., Milton D. McLaughlin,
Jack A. White, and Robert A. Champine

Langley Research Center
Langley Field, Va.

~~CLASSIFIED DOCUMENT~~

This material contains information affecting the National Defense of the United States within the meaning of the espionage laws, Title 18, U.S.C., Secs. 793 and 794, the transmission or revelation of which in any manner to an unauthorized person is prohibited by law.

**NATIONAL AERONAUTICS AND
SPACE ADMINISTRATION**

WASHINGTON

December 1958

Classification canceled (~~SECRET~~) ^{7/20/66}
by authority of NASA classification Change Notice #10-1
of authorizing change

Linda Beathie-GS2 12 September 1966
Name & Grade of Officer making change

2 cals removed 20 Jan 64 for

NATIONAL AERONAUTICS AND SPACE ADMINISTRATION

MEMORANDUM 10-7-58L

TECH LIBRARY KAFB, NM



0063048

FLIGHT MEASUREMENTS OF SOME OF
THE FLYING QUALITIES AND STABILITY DERIVATIVES
OF A SUPERSONIC FIGHTER AIRPLANE*

By Christopher C. Kraft, Jr., Milton D. McLaughlin,
Jack A. White, and Robert A. Champine

SUMMARY

Flight measurements have been made to determine the flying qualities and some of the stability derivatives of a supersonic fighter airplane. The results are presented in the form of measured flight data and pilot opinion.

The damping of the short-period longitudinal oscillations is somewhat low. The feel forces provided by the longitudinal feel system are considered good by the pilots. The longitudinal-control-system characteristics that result from the nonlinear gearing between the stick and stabilizer result in poor handling characteristics for all indicated airspeeds. It appears as though a more linear stick-to-stabilizer relationship near trim would result in improved flying qualities throughout the flight regime. Also, the longitudinal stick-fixed stability as measured by the variation of stick position with normal acceleration is adversely affected by structural deformation during accelerated maneuvers. The airplane has a high roll-to-yaw ratio but one which is within the present flying-qualities requirements. The pilots dislike the longitudinal trim system because of the difficulty experienced when trying to trim precisely and the overshoot which occurs when making a large or rapid trim correction. The roll performance of the airplane is considered adequate for Mach numbers below 0.9, but the performance deteriorates rapidly in the high Mach number, high-dynamic-pressure region.

INTRODUCTION

This paper presents an investigation of the flying qualities and measurements of some of the stability derivatives of a supersonic day fighter for both carrier-based and land-based operations. Flight tests

*Title, Unclassified.

1210

to measure the flying qualities and other characteristics of the airplane are presented in references 1 to 10. Tests of modern airplanes such as the one in the present investigation are needed to extend the present flying-qualities specifications of reference 11 to the new flight regimes covered by the high performance capabilities of this type of aircraft. In addition, the need for flying-qualities investigations is continuous to ascertain if there is a need for additional requirements to or revisions in the present requirements. This fighter airplane was extensively tested during the design stage by both wind-tunnel and rocket-model techniques. (For example, see refs. 12 to 16.) It is therefore interesting and beneficial to future design to continue the tests of this particular airplane in flight so that previous tests can be compared with flight test results.

The test airplane incorporates several new design features in its external geometry which make the airplane of general interest. Such features are leading-edge chord-extensions, leading-edge droop, high wing and low tail, and a variable-incidence wing to improve take-off and landing characteristics. Also, the longitudinal control system of this airplane combines such features as a spring, stick dampers, bob-weights sensitive to both normal and pitching accelerations to provide force feel to the pilot, and a nonlinear linkage combined with an irreversible power control system.

This report deals with the first phase of the flight investigation of the test airplane and discusses some of the handling qualities of the airplane that were obtained during pilot evaluation flights. Also, some brief test maneuvers have been made to determine some of the airplane stability derivatives.

SYMBOLS

a_y	lateral acceleration
b	wing span
\bar{c}	mean aerodynamic chord of wing
C_l	rolling-moment coefficient, $\frac{\text{Rolling moment}}{qSb}$
C_N	normal-force coefficient, $\frac{a_n W}{qS}$
C_m	pitching-moment coefficient, $\frac{\text{Pitching moment}}{qS\bar{c}}$

C_n	yawing-moment coefficient, $\frac{\text{Yawing moment}}{qSb}$
C_Y	lateral-force coefficient, $\frac{\text{Lateral force}}{qS}$
$C_{l/2}$	cycles to damp to one-half amplitude
g	acceleration due to gravity
H_p	pressure altitude
I_X	moment of inertia of airplane about X stability axis
I_Y	moment of inertia of airplane about Y stability axis
I_Z	moment of inertia of airplane about Z stability axis
I_{XZ}	product of inertia referred to X and Z stability axes
M	Mach number
m	mass of airplane
a_n	normal acceleration, g units
$\frac{pb}{2V}$	helix angle
p	rolling velocity
P	period of oscillation
q	dynamic pressure or nondimensional pitching velocity
S	wing area
$T_{l/2}$	time to damp to one-half amplitude
V	true airspeed
V_e	equivalent airspeed
W	airplane weight

α_v	vane angle
β	sideslip angle
δ_a	aileron deflection
δ_r	rudder deflection
ϕ	bank angle
$\frac{\phi}{v_e}$	rolling parameter, $\frac{57.3}{V_e} \frac{\phi}{\beta}$
Δ	increment

Stability derivatives are indicated by subscript notation; for example,

$$C_{N_\alpha} = \frac{dC_N}{d\alpha}$$

Rotary derivatives are defined as indicated by the following:

$$C_{mq} = \frac{\partial C_m}{\partial \left(\frac{qc}{2V} \right)}$$

$$C_{m\dot{\alpha}} = \frac{\partial C_m}{\partial \left(\frac{\dot{\alpha}c}{2V} \right)}$$

Subscripts:

i	indicated
c	calibrated
f	fuselage
w	wing

Dot over quantity indicates differentiation with respect to time.

DESCRIPTION OF AIRPLANE

The Chance Vought F8U-1 airplane is a high-wing, low-tail fighter airplane intended for both carrier- and land-based operations and designed for use as a supersonic day fighter. The airplane powerplant is a Pratt & Whitney J57-P-4 with afterburner. Pictures of the test airplane are shown in figure 1, a drawing of the airplane is given in figure 2, and pertinent characteristics of the airplane are presented in table I.

The test airplane has a variable-incidence wing for use during landing and take-off. The wing is moved hydraulically to an incidence of 7° in the landing condition, and in the clean condition the wing is fixed at -1° . The wing is equipped with a leading-edge flap (called leading-edge droop) which can also be operated hydraulically to three different positions. These positions are clean, cruise droop, and landing droop. The droop on each side of the wing is composed of two sections, one section extending from the root to the leading-edge chord-extension (inboard section) and the other section extending from this point to the wing tip (outboard section). (See fig. 2.) When the wing is raised to the landing position, the inboard leading edge is drooped 25° and the outboard leading edge is drooped 27° . Also, it is possible to put the droop in the landing position with an emergency air system. After this is done, the droop stays in the landing position regardless of wing position. In addition to the leading-edge droop for landing, the ailerons are deflected down 20° as a flap and the small flaps at the wing root are deflected down 20° . When the wing is raised, the horizontal tail is automatically deflected 5° leading edge up to minimize the changes in trim. The leading-edge droop can be deflected 6.8° and 7° (inboard and outboard sections, respectively) into the cruise-droop position to improve cruise and maneuver performance at subsonic and transonic speeds.

The control surfaces of the airplane are all hydraulically operated with irreversible systems and the feel forces to the pilot are supplied by artificial means. The aileron- and rudder-control feel forces are supplied by simple springs. The forces required and the deflection ranges available in the aileron and rudder control systems in the clean and landing conditions are different. The characteristics of the aileron and rudder systems are shown in figure 3. The stabilizer control system is somewhat more complex. There is a spring to provide forces in steady maneuvers and the variation of this force with stick position is shown in figure 4. It should be noted that the spring force varies linearly with stick deflection and that there is an initial preload in the feel spring of about 1 pound. The spring preload force combined with stick friction forces results in a breakout force of about 3 to 5 pounds.

Bobweights are used to provide additional forces when the airplane is in accelerated flight. There are two bobweights, one located at the stick and one at the tail, which are sensitive to both normal acceleration and pitching acceleration. In steady turns or maneuvers where the normal acceleration is fairly steady at values about $1g$, the forces from the two bobweights oppose each other and provide a force at the stick of 2.6 pounds per g . In the transient portion of a maneuver where pitching acceleration occurs, the forces from the bobweights combine to produce a force at the stick proportional to pitching acceleration of $9.3 \text{ lb/radians/sec}^2$. Additional forces are provided during stick motion by two dampers, one located at the stick and one at the tail. These dampers provide a force of 3.4 pounds per inch per second of stick deflection. A relief valve in each of the dampers is set so that a force of 30 pounds is the maximum force that can be produced by the combined dampers. In addition to the force characteristics provided in the aileron and stabilizer control systems, there is a nonlinear linkage in these control systems which results in a low gearing between surface and stick deflection near neutral and increasing gearings as the stick is deflected away from neutral. In the longitudinal control system the feel spring is in the rear portion of the fuselage just ahead of the nonlinear linkage. As a result, some stick deflection is required to take up the backlash before the stabilizer moves and this tends to accentuate the nonlinearity. These relationships are illustrated in figure 4.

The trim systems in the airplane are unique in that all three of the cockpit controls have the same neutral position regardless of the control surface position required for trim. The trim actuators are extendable links in the control systems. For example, if the pilot is holding a stick deflection, and thereby a certain stick force, in order to maintain a given airspeed and he wishes to trim the system to zero force, he must move the control stick back toward neutral as he trims the stabilizer to the position necessary to hold the desired trim speed. The same condition exists in all three controls. The trim systems are electronically controlled systems which operate through the automatic control amplifiers. Potentiometers located on the stick grip and on the left console are used to introduce signals to the trim system. The output of the trim actuators are proportional to the given potentiometer knob position. The longitudinal control system has an emergency trim system which when operated calls for the maximum trim actuator rate while the emergency switch is engaged. This type of trim system is commonly called a "beep" type of trim system.

Automatic stabilization of the airplane is provided about the yaw and roll axes in both the landing and clean conditions. The yaw damper is controlled by two independent lateral accelerometers located near the center of gravity. Two signals, one from each accelerometer, each of which supplies one-half the required magnitude are transmitted through two altitude gain changers to the amplifiers. The altitude

gain changers increase the damper gain with increasing altitude. Signals from the two amplifier channels are fed to dual electrohydraulic actuators and result in the required surface displacement through the combined stroke of both ends of the dual actuator. An aileron-rudder interconnect circuit is combined with the yaw damper system to provide rudder deflection in a roll maneuver as a function of aileron position. The rudder is used to counteract the favorable yaw produced by the ailerons. The favorable yaw decreases with increasing angle of attack; therefore, the rudder-aileron interconnect signal is passed through a stabilizer-position gain changer to attenuate the signal as the stabilizer is moved in the trailing-edge-up direction. The aileron-rudder interconnect does not function in the landing condition.

The roll damping system receives its signals from two rate gyros, one used for the clean condition and one for the landing condition. In the clean condition the gain between roll rate and aileron position is constant at 0.14° of total aileron per degree per second rate of roll. In the landing condition the initial gain is 1.4° of total aileron per degree per second rate of roll. A gain changer in the landing condition reduces the gain from 100 percent to 40 percent in the first 2 inches ($1/3$ of full travel) of lateral stick displacement and from 40 percent to 0 percent as the stick displacement is increased from 2 to 6 inches (full travel).

For these tests the center of gravity of the airplane was located at $0.263\bar{c}$ at a take-off gross weight of 26,077 pounds with the gear down. Retraction of the landing gear moves the center of gravity forward $0.003\bar{c}$.

INSTRUMENTATION

Standard NACA photographically recording instruments, synchronized with a timer, were used in the test airplane. An NACA designed airspeed head located on a boom at the nose of the airplane was used to measure total and static pressures. Also, the head contained flow-direction vanes for measuring angle of attack and sideslip angle. The following quantities were measured and recorded:

- Stabilizer position
- Aileron position
- Rudder position
- Stick position
- Rudder pedal position
- Stick force
- Rudder pedal force
- Angle of attack

Sideslip angle
Airspeed
Altitude
Three components of acceleration
Rolling velocity and acceleration
Pitching velocity and acceleration
Yawing velocity and acceleration
Wing position
Wing strut force

No calibration of the boom and airspeed head as installed in this airplane was made. The airplane manufacturer, however, has calibrated a nose boom installation similar to this installation and this calibration was used to correct the measured airspeed. A plot of the calibration is shown in figure 5. Also, figure 5 presents a comparison of this calibration with a calibration obtained from the data presented in reference 17. In addition, a point obtained from the airspeed-altimeter recorder at the time of the static-pressure jump is presented. The error in static pressure and total pressure was considered zero after the jump occurred. This one datum point appears to agree well with the data obtained from reference 17. The two calibrations are in good agreement throughout the Mach number range. It should be noted that the calibration is plotted as a function of indicated Mach number and that a discontinuity exists in the calibration curves at the time of the shock passage over the nose boom static orifices. The calibration is actually nonexistent from $M = 0.96$ to 1.02 .

A camera was installed in the cockpit to photograph a target airplane through the windshield during tracking tests. It was not practical to photograph through the pilot's gunsight but the camera was bore-sighted so that tracking errors could be determined.

The manufacturer's values of the moments of inertia I_x , I_y , and I_z were used in calculating certain stability derivatives. These moments-of-inertia values were corrected for changes in weight due to fuel consumption.

TESTS, RESULTS, AND DISCUSSION

Longitudinal Stability and Control

Stability and control characteristics in steady flight.- Flight tests were made to measure the static stability throughout the speed range in the clean condition at both 35,000 feet and about 20,000 feet. These tests were performed by trimming the airplane at some high subsonic

speed, and then by decreasing the speed and accelerating from some moderate subsonic speed to about the maximum level-flight speed. The speed changes were accomplished by varying the engine throttle. It should be noted, however, that the changes in trim with power setting are small and would not be expected to have a significant effect on the stabilizer variations with Mach number. The pilot attempted to maintain flight at 1g throughout the tests and only those data were used except for some few cases in which the data were corrected to 1g flight. These tests also provided a measure of the transonic trim change. The data for the two test altitudes are presented in figure 6. The data show positive stability for all Mach numbers except in the transonic speed range. Instability is indicated from a Mach number of 0.92 to 1.03. The stick forces associated with the transonic trim changes are small, on the order of 2 to 3 pounds, and are considered desirably small by the pilots. The abrupt change in slope of the curve of stick force plotted against Mach number at a Mach number of 0.8 is a result of the flat spot in the stick-to-stabilizer relationship together with the spring preload and stick friction. This results in the force of 2 $\frac{1}{2}$ to 3 pounds on either side of trim shown in figure 6(b).

The same type of test was performed in the landing condition by gradually decreasing the airspeed from 180 knots to about 125 knots. These data are presented in figure 7. A stable variation of horizontal tail position with speed is indicated although there is a slight tendency toward decreased stability at the lower airspeeds. It might be noted that in the landing condition the airplane begins to undergo light buffet at about an indicated airspeed of 155 knots which is considerably above the stalling speed of the airplane. The pilots objected to this high buffeting speed in the landing approach and felt that buffet could not be used as a stall warning in this configuration.

The pilots made several observations regarding the landing characteristics of the airplane. It should be noted, however, that no experience has been obtained during carrier landings. The pilots normally landed the airplane out of trim to avoid using the portion of the stick-to-stabilizer gearing where the gearing is low. The pilots feel that the continuous need to retrim the airplane both longitudinally and laterally when the airspeed is reduced from 180 to 120 knots is undesirable. Also, the pilots noted that the airplane is difficult to handle during take-offs or landings in moderate cross winds of 10 to 15 knots because of excessive heeling and weathercocking. In this particular airplane, during the landing approach the roll stabilization system is frequently turned off as a result of the roll monitoring circuit when large aileron deflections are used. This is undesirable especially during an approach in turbulent air because the roll stabilization system is the system which is most effective in damping the airplane motions. (It was later found that a malfunction of one of the gyros used for the landing condition was the source of the trouble.) Also, the pilots noted that the

restriction to 220 knots airspeed with the wing up demands very careful attention during an afterburner take-off to insure that the wing is lowered and locked before the airspeed is exceeded.

Characteristics in accelerated flight.- The maneuver characteristics of the airplane were measured by performing windup turns at various altitudes and for a range of Mach numbers. In all of the tests at supersonic speeds the cruise droop was up, but at subsonic speeds tests were made with the cruise droop both up and down. In most cases, the acceleration was increased in the windup turns until moderate buffet was encountered. Some tests were also made to determine the characteristics in rapid pull-ups and turn entries.

The stick force, stick position, and stabilizer position as a function of normal acceleration in windup turns at altitudes of about 30,000 and 35,000 feet for two calibrated Mach numbers are presented in figure 8. The data of figure 8 are typical of the data obtained during the flight program. The variation of stabilizer angle with acceleration is stable and linear in all cases. The stick-force and stick-position curves reflect the nonlinearity of the control system and the effect of fuselage bending. The breakout force required to overcome the stick friction and spring preload together with the forces resulting from the very low gearing between stick and stabilizer near neutral requires a stick force of about 3 to 5 pounds to move the stabilizer. These forces cause the initial force per g for values of normal acceleration up to about 2g to exceed the limits specified in the requirements of reference 11. The force per g for values of g in excess of 2g are well within the required limits. The data with cruise droop up indicate the same trends as those for the cruise-droop-down case, and the stabilizer angle per g is slightly less for the cruise-droop-up condition. Windup turns performed at an altitude of 20,000 feet with the cruise droop down exhibit the same characteristics as those obtained at 35,500 feet. The stabilizer angle per g, however, is decreased because of the increase in dynamic pressure. The lowest altitude for which test data are presented was 14,400 feet at a Mach number of 0.9. These data are presented in figure 9 and show that the stabilizer variation with normal acceleration is approximately linear up to the highest value of g reached. The stabilizer angle per g, however, is decreased relative to the other Mach numbers and altitudes. The curves of stick force and stick position are of special interest. Very little, if any, stick motion is required to move the stabilizer at the higher values of normal acceleration but the forces required are almost linear and reflect the force resulting from the normal-acceleration bobweights. The pilots felt that the airplane was overly sensitive at this Mach number and altitude, but for slow steady maneuvers this characteristic was not too objectionable. In general, the pilots were of the opinion that the longitudinal control is too insensitive near trim for all regions of flight with the exception of indicated airspeeds in excess of

500 knots. This causes the system to be particularly annoying while tracking or during the beginning of the landing flare from a trimmed condition. The nonlinear variation of stick-to-stabilizer relation is responsible for this deficiency and it is felt that a more linear control system, especially for moderate control displacements, would be an improvement.

A summary plot of the stabilizer angle per g in accelerated maneuvers is shown in figure 10. The data of figures 8 and 9 together with all of the measured data in accelerated maneuvers are presented in this figure. At an altitude of 35,000 feet the stabilizer angle per g decreases somewhat abruptly from about 3.5 to about 2.8 in the range of M_C from 0.92 to 0.97 and then increases rapidly as supersonic speeds are attained, reaching a maximum of about 5.3 at $M_C = 1.1$. Above this Mach number and up to about $M_C = 1.45$ the stabilizer angle per g decreases until a value about the same or slightly less than that for the subsonic condition exists. Putting the cruise droop up at subsonic speeds at 35,000 feet causes a slight decrease in stabilizer angle required. At the lower altitude of 20,000 feet, the stabilizer angle per g decreased with increasing Mach number from about 2.5 at $M_C = 0.68$ to 1.65 at $M_C = 0.865$. The minimum value of 1.5 was obtained at $M_C = 0.9$ at an altitude of approximately 14,000 feet.

A number of flight tests were made of rapid pull-ups and turn entries to obtain pilot opinions of the flight characteristics of the airplane under these conditions. Typical time histories of pull-up maneuvers are presented in figure 11. These maneuvers were of particular interest because of the longitudinal feel system. The pilots felt that the force characteristics in rapid maneuvers were very good. The force during the initial part of the maneuvers was somewhat higher than in steady turns. There was a tendency for the pilots to overshoot the desired acceleration level when rapid turns to large accelerations were made. However, this tendency was believed to be due to the nonlinear gearing and the decrease in apparent stick-fixed stability at higher g levels rather than to the force characteristics. Also, the pilots felt that there was little tendency toward pilot induced oscillations and that the feel system did not restrict the maneuvering capabilities of the airplane.

Some tests were made to measure the maneuver characteristics in the landing-approach configuration for a range of airspeeds from 200 knots down to 140 knots. These data are presented in figure 12. About the same trends of stabilizer position and force characteristics are exhibited in the landing condition as in the clean condition. In the landing condition the airplane begins to buffet at very small increments of g above 1 g and it was difficult to maintain the turn at any

given g level. This condition resulted in the amount of scatter obtained in the data. The force per g in the landing condition is somewhat large, on the order of 15 pounds per g. The stabilizer angle per g increases from about 4.5° per g at 197 knots to about 10° to 12° per g at 140 knots.

Effects of fuselage bending. - As has been noted, the data of figure 9 indicate that the relation between the stick and stabilizer motion is adversely affected by normal acceleration to such an extent that there is a large decrease in apparent stick-fixed stability; that is, at Mach numbers near 0.9, the variation of stick position with normal acceleration indicates that the airplane is neutrally stable, whereas the variation of stabilizer angle with acceleration shows that the airplane has a sizeable margin of stability. These data indicate that the longitudinal control system is affected by loading on some portions of the airplane structure or control system. In an effort to isolate the parts of the control system which are affected, instruments were installed to measure the motion of various parts of the longitudinal control system. The locations of these parts are shown schematically in figure 13. In order to measure the effects of normal acceleration on the longitudinal control system, windup turns identical to those described in the section entitled "Characteristics in Accelerated Flight" were made at different Mach numbers and altitudes, and the data obtained from these tests are presented in figure 14. The position of the stick, walking beam, structural feedback linkage, and right stabilizer in terms of an equivalent stick position are shown as a function of normal acceleration; that is, the various linkages were calibrated in terms of stick angle so that on the ground under no load all of the curves would coincide. The difference between the curves in flight indicates the deformation occurring at various points in the control system in terms of the stick angle which would be required to produce this motion under a no-load condition. The results of these tests indicate that almost all of the loading effects due to acceleration occur between the stick and the walking beam. There are slight differences between the position of the walking beam and the structural feedback linkage but these effects are small compared with the differences between that of the stick and walking beam. A comparison between the walking beam and the motion of the stabilizer also indicates only slight differences which can probably be accounted for in the accuracy of the instrumentation. It might be noted that only the output of the structural feedback linkage was measured and that some compensation for structural motion could be occurring which would not be measured by the instrumentation installed for these tests. A plot of the difference between the stick motion used to obtain a given g and the stick motion which would have been required to produce the same amount of stabilizer deflection on the ground is shown in figure 15. Data are presented for all the test conditions of Mach number and dynamic pressure. The results indicate that acceleration loads on the airplane cause the longitudinal control system to deflect the stabilizer an amount equivalent to about 0.9° of stick motion per g. This plot also indicates

that the amount of deflection is almost independent of dynamic pressure or Mach number, at least for the range of the test conditions. As shown by the previous data on windup turns, the most serious effects of the undesirable control-system motion occur at Mach numbers around 0.9 where the stabilizer angle per g is the smallest. The data obtained from these tests indicate that the control-system movement due to deformation results from bending of the forward portion of the fuselage brought about by inertia loading during accelerated maneuvers.

It might be noted that the airplane manufacturer has redesigned the longitudinal control system to account for the effects of fuselage bending. The change to the control system has not as yet been tested by the NASA, but flight tests by the manufacturer indicate that the linkage change has alleviated the problem.

In the performance of maneuvers to high acceleration some marked changes in the aerodynamic stability characteristics were found to exist at the higher values of acceleration at Mach numbers of about 1.0, 1.1, and 1.2. These decreases in stick-fixed stability can be seen in the data in figure 14 and tend to aggravate the structural deformation effects at the higher values of acceleration.

Stability derivatives as determined from dynamic stability tests.-
In order to measure the dynamic stability characteristics of the airplane, pulse stabilizer inputs were imposed on the airplane for the Mach number range of the airplane at an altitude of approximately 35,000 feet. The resulting period, time to damp to one-half amplitude, and damping ratio were obtained from the short-period oscillation. These data are presented in figure 16.

The period changed from about 2.3 seconds at $M = 0.8$ to about 1.5 seconds at $M = 0.92$ and then changes slowly to about 1.0 second at $M = 1.4$. The time to damp to one-half amplitude varies from about 1.25 seconds at low Mach numbers to about 0.8 second at $M = 1.44$. The resulting damping ratio decreases sharply from about 0.20 at $M = 0.8$ to about 0.17 at $M = 0.92$, reflecting the large change in stability at Mach numbers around 0.9. The damping ratio is about constant at a value of about 0.14 from about $M = 1.0$ to 1.4.

The pilots considered the damping of the short-period longitudinal oscillation to be low and less than desired. The poor damping did not materially affect the performance of the airplane during general flying which involved only gradual maneuvers. However, the lack of good damping does result in more work during such tasks as tracking and is particularly bothersome while tracking a maneuvering target. Some brief tests regarding the tracking capabilities of the airplane are discussed subsequently.

The variation of stability with Mach number as shown by the parameter $C_{m\alpha}$ is presented in figure 17. This parameter was obtained from the period and damping data by using the expression

$$C_{m\alpha} = -\frac{I_Y}{qS\bar{c}} \left[\left(\frac{2\pi}{P} \right)^2 + \left(\frac{0.693}{T_{1/2}} \right)^2 \right]$$

Also, shown in figure 17 is the summation of the rotary derivatives $C_{mq} + C_{m\dot{\alpha}}$. These data were obtained from the formula

$$C_{mq} + C_{m\dot{\alpha}} = \frac{2VI_Y}{qS\bar{c}^2} \left[-2 \left(\frac{0.693}{T_{1/2}} \right) + C_{N\alpha} \frac{qS}{mV} \right]$$

The lift-curve slope of the airplane was also measured from the airplane short-period oscillation by measuring the normal acceleration and angle of attack during an oscillation in pitch. The following equation was used to obtain the values shown in figure 18:

$$C_{N\alpha} = \frac{\Delta a_n W}{\Delta \alpha_v q S}$$

The lift-curve slope appears to reach a maximum of 4.5 per radian at $M = 0.92$. The slope decreases gradually above $M = 0.92$ to about 3.0 per radian at $M = 1.4$. The variation of static margin dC_m/dC_N with Mach number as obtained from the measured values of $C_{m\alpha}$ and $C_{N\alpha}$ is presented in figure 19. The airplane has a static margin of about 17.5 percent \bar{c} at Mach numbers from 0.76 to 0.85 and then changes rapidly to about 30 percent at $M = 0.96$. As the Mach number increases, the static margin gradually increases to about 33 percent \bar{c} at $M = 1.44$.

Directional Stability and Control

Stability and control characteristics in sideslip.— Sideslip data were obtained in the clean condition at altitudes of approximately 35,000 feet and 20,000 feet. Also, sideslip data were obtained for the landing configuration at airspeeds of 200 and 150 knots at 8,500 feet. The maneuvers were made at nearly constant velocity. The rudder was used to increase sideslip in one direction until a maximum deflection was reached; then, the controls were returned to neutral and the same procedure was used in the other direction. Sideslip data at several test altitudes and Mach numbers are presented in figure 20. The data consist of plots of control-surface positions for the aileron, rudder,

and horizontal tail and the pilots' control forces necessary to hold these positions as a function of sideslip angle. The aileron and rudder control-surface positions varied linearly with sideslip and were in the stable direction throughout the Mach number range of the tests. The stabilizer position did not vary with sideslip. The rudder pedal force was linear with sideslip angle and the aileron force reflected the nonlinear relationship between stick and aileron deflection. The maximum aileron force was generally less than 10 pounds. The maximum pedal force was between 150 and 200 pounds for maximum rudder deflection.

Plots of $\frac{d\delta_r}{d\beta}$ and $\frac{d\delta_a}{d\beta}$ for various Mach numbers at altitudes of approximately 35,000 feet are presented in figure 21. The increase in $\frac{d\delta_a}{d\beta}$ above $M_c = 1.0$ indicates a decrease in aileron effectiveness, as shown in a subsequent section, and a possible increase in the rolling moment due to sideslip. The parameter $\frac{d\delta_r}{d\beta}$ also increases at Mach numbers above $M_c = 1.0$. The increase in this parameter is due mainly to a large reduction in rudder effectiveness at supersonic speeds.

Sideslip data for the landing condition are presented in figure 22. Data are presented for three different airspeeds which represent a spread in normal-force coefficient from 0.44 to 0.99. In the landing configuration the available rudder travel is increased to $\pm 17^\circ$. The control-surface positions show a linear variation with sideslip for moderate angles of sideslip. The rudder force has a linear variation with sideslip and the aileron force reflects the nonlinear variation of aileron deflection with stick displacement. The amount of aileron and rudder deflection per degree of sideslip in the landing configuration is larger than that shown for the clean condition (fig. 20) at the lowest Mach numbers. At the highest normal-force coefficient (fig. 22(c)) there appears to be some decrease in the directional stability and the rolling moment due to sideslip is somewhat greater as evidenced by the variation of rudder angle and aileron angle with sideslip. Also, there is an increase in pitching moment due to sideslip as shown by the variation of stabilizer angle. This condition did not exist at the lower normal-force coefficients. Although figure 22 does not show that the maximum aileron deflection is reached, the pilots noted that maximum aileron deflection was reached before maximum rudder deflection.

Roll performance.— Although most of the regimes of flight of the airplane have been covered, no detailed flight study has yet been made of the rolling performance of the airplane. Results from a preliminary study of roll performance based on data obtained from Chance Vought Aircraft, Inc. and some flight data from the Langley Flight Research Division are presented. It should be noted that the data presented

Error

An error occurred while processing this page. See the system log for more details.

NASA data show slightly higher rolling velocities. The data of figure 24 show that below $M = 1.0$ over most of the usable range of altitude the test airplane can meet the proposed roll specification of 90° in 1 second.

Stability derivatives and other measurements determined from dynamic stability tests.— The dynamic lateral directional stability characteristics were obtained by making pulse-type inputs with the rudder and then measuring the ensuing oscillations. These tests were performed at an altitude of about 35,000 feet at various Mach numbers with the stabilization systems on and off. The period, time to damp to one-half amplitude, and the damping ratio as a function of Mach number obtained from these tests are presented in figure 25. The period for the case of stabilization system on varies from 2.6 seconds at $M = 0.76$ to about 1.8 seconds at $M = 0.95$. From $M = 0.95$ to $M = 1.3$ the period is almost constant at about 1.75 seconds. There appears to be a tendency for the period to increase slightly as the Mach number is increased beyond 1.3 but there are insufficient data to establish this trend. The pilot opinion of the damping of the lateral directional oscillation indicated that the damping was adequate for large amplitude disturbances but the damping was considered poor when small disturbances or changes in trim occur. The change in damping with amplitude may result from backlash in the yaw damping system which has been improved in later versions of this airplane. The period for the case of the stabilization system off exhibits the same trends as that for the stabilization system on, the period being about 0.1 to 0.2 second longer in most cases. The time to damp to one-half amplitude and the damping ratio show the marked effects of the stabilization systems. With the stabilization system on the time to damp to one-half amplitude is fairly constant at about 1 second up to $M = 1.3$ and the damping ratio varies from about 0.27 at $M = 0.76$ to about 0.18 at $M = 1.3$. Here again there appears to be a trend toward increased time to damp to one-half amplitude at Mach numbers above 1.3. The stabilization-system-off case shows the time to damp to one-half amplitude varies from about 2.1 seconds at $M = 0.82$ to about 1.5 seconds at $M = 1.37$ and the damping ratio is about constant at 0.13 to 0.15. The pilots considered the damping of the lateral directional oscillation to be poor with the stabilization system off.

The roll-to-sideslip ratios measured during the lateral directional oscillations are presented in figure 26. The stabilization system decreases the roll-to-sideslip ratio at all Mach numbers throughout the speed range. The percent decrease is greatest at Mach numbers from about 0.75 to 1.13. Above $M = 1.13$ the stabilization system has less effect on the roll-to-sideslip ratio but the ratio is still less than with the stabilization system off. The plot of the reciprocal of the cycles to damp to one-half amplitude as a function of the parameter $\frac{\phi}{v_e}$ is shown in figure 27. The requirements as set forth in reference 11

for the stabilization system both on and off are also shown in these plots. The airplane meets the requirements in all cases both with the stabilization system on and off. The pilots felt that the roll-to-sideslip ratio was high although not too objectionable. They felt that these high ratios would not be a serious factor during most flight conditions and would only be noticed in maneuvers made specifically to measure this characteristic.

The static directional-stability parameter $C_{n\beta}$ was determined from the period and damping data by the following expression:

$$C_{n\beta} = \frac{I_Z}{qSb} \left[\left(\frac{2\pi}{P} \right)^2 + \left(\frac{0.693}{T_{1/2}} \right)^2 \right] - C_{l\beta} \frac{I_{XZ}}{I_X}$$

The values of $C_{n\beta}$ obtained in this manner for the case of stabilization system off are presented in figure 28. The data indicate that $C_{n\beta}$ varies from about 0.14 per radian at $M = 0.83$ to 0.185 per radian at $M = 0.93$ and then decreases gradually to about 0.10 per radian at $M = 1.3$. The directional-stability parameter decreases to a low value of about 0.08 per radian at Mach numbers around 1.4.

The variation of side-force coefficient with sideslip angle $C_{Y\beta}$ was determined from the following expression:

$$C_{Y\beta} = \frac{\Delta a_y W}{\Delta \beta q S}$$

The results obtained are shown in figure 29. The side-force coefficient $C_{Y\beta}$ has very little variation with Mach number, remaining at a value of about -0.8 throughout the Mach number range. Only those data for the stabilization system off are presented.

Trim Systems

The test airplane utilizes a positional type of servocontrol in the longitudinal trim system; that is, the pilot positions a wheel on the stick which calls for a given stabilizer displacement. This is in contrast to a conventional "beep" system in which the trim actuator moves at a constant rate and stops moving when the pilot releases the trim control. Also, since the stick has the same neutral position for all conditions of flight, the pilot is required to move the stick back

toward neutral as the airplane is trimmed. The main pilot objections to the trim system would seem to result from the fact that the final trim position of the stabilizer is not reached when the pilot stops the motion of the trim wheel. Because of this time delay in stabilizer motion and the inability to anticipate the final result of the trim correction, the pilot resorts to making minute adjustments of the trim wheel. As a result, the pilot is required to use a great deal of concentration not normally associated with a conventional trim system. The trim procedure is further complicated by the nonlinear stick-to-stabilizer relationship.

Time histories which illustrate the pilot's trim procedure are shown in figure 30. The first case (fig. 30(a)) is one in which the pilot attempted to trim the airplane rapidly in a flight regime where the airplane is sensitive to small control motions. The figure shows the large oscillations that result. In the second case (fig. 30(b)) the pilot used a trim procedure more typical of the normal technique used. In this case, no large trim inputs are used and the rate of trim is minimized. However, even under these conditions the airplane oscillates in pitch. In both cases, the time history of stick position indicates the pilots moved the stick in a series of steps.

On several flights, the pilots used the emergency trim system which is a "beep" type of trim control. All the pilots felt that this system may be an improvement over the present system. However, since the control for the emergency system is located on the left console and not on the stick, it is hard to make a comparison.

In the landing configuration the pilots found it difficult to make the large trim changes required during the landing approach. This comment is a result of the limited rate of trim actuation available in the system. The pilots noted that they had to wait several seconds before being able to determine how much trim had been applied and, as a result, either overshoot or undershot the desired trim position.

The pilots consider the lateral trim system poor because of the difficulty required to trim precisely. This trim system is also complicated by the nonlinear gearing between the stick and ailerons. The lateral trim system is particularly bothersome in maneuvers such as tracking or when small directional trim changes occur such as in the transonic speed range. These directional trim changes cause disproportionately large lateral trim changes because of the large roll-to-sideslip ratios and the effects of the nonlinear gearing. The pilots considered the directional trim system satisfactory and easy to use.

The stick-force changes which occur when making changes in power, dive flap position, cruise-droop position, and wing or gear position are considered desirably low. There are some rather large trim changes

when making afterburner take-offs and attempting to reach the recommended climb speed as rapidly as possible. A large directional trim change occurs when changing altitude from sea level to about 35,000 feet. If a rapid climb to high altitude is made, the trim change is initially not as large. The final trim change, however, is the same if the high altitude is maintained for any length of time. This trim change is common to this airplane and is thought to be a result of contraction of various parts of the rudder control system as they are exposed to the colder air at high altitudes.

Some Brief Measurements of the Formation and Tracking Performance of the Test Airplane

The formation flight characteristics appear good in the range of flight conditions tested - that is, at Mach numbers about 0.9 at altitudes from 10,000 to 35,000 feet. The tracking accuracy of the airplane appeared to be adversely affected by the poor damping of the longitudinal and lateral oscillations. These opinions are based on some brief tests of tracking a subsonic airplane at an altitude of 35,000 feet with the target airplane flying at $M = 0.8$ and the test airplane flying at $M = 0.8$ and $M = 1.2$. The average standard deviation for the flights made at subsonic speeds was 3.3 mils in both azimuth and elevation in a steady tail chase. These values increased to 5.0 mils in azimuth and 6.2 mils in elevation in tracking a target maneuvering at steady g. At the supersonic speed of $M = 1.2$ in a steady tail chase, the standard deviation measured was 2.3 mils in azimuth and 2.1 mils in elevation. No tests were made in maneuvering flight at supersonic speeds. The standard deviation values for the test airplane may be compared with those for a typical straight-wing subsonic airplane which is considered to have good tracking characteristics. The standard deviation values for the subsonic airplane are 1.7 mils in azimuth and 2.2 mils in elevation in a steady tail chase and 3.8 mils in elevation in steady turns. It can be seen that the tracking characteristics of the test airplane are somewhat inferior to those of the subsonic airplane but the tactical use of the airplane and the type of weapons to be used would have to be considered before making any definite conclusions regarding the tracking performance.

Measurements of Loads in the Variable-Incidence-Wing

Strut During Operation of the Wing

The test airplane has a two-position variable-incidence wing which is set at -1° for normal flight conditions and raised to 7° in the landing condition. The wing is operated by a single hydraulic strut (fig. 1) which is capable of exerting about 2,000 pounds force in the

down cycle. Flight operations of the airplane have indicated that the force available at the strut is marginal in the down cycle. In an effort to establish the loads on the strut during the operation of the variable-incidence wing, a strain gage was installed at the base of the strut. The forces measured by this installation are estimated to be accurate to within ± 100 pounds.

Operation of the variable-incidence wing in several conditions is shown in figures 31 to 34, and operation of the leading-edge droop to the cruise and landing positions with the wing in the clean position is shown in figures 35 and 36. Finally, operation of the wing with the droop locked in the landing condition is shown in figure 37. The results of these tests indicated that it is necessary to maintain the leading-edge droop in the cruise position during the down cycle to keep the strut loads within the capabilities of the hydraulic strut. The time history of figure 34 shows that the loads in the strut reach about 2,200 pounds with the cruise droop up. The load is decreased by about 300 pounds when the droop is in the cruise position (fig. 35). Because of the large effect of droop position on the strut loads, tests were made with the droop locked in the landing condition throughout the wing cycle. These tests (figs. 36 and 37) showed that the strut loads are decreased by about 1,300 pounds when the droop is deflected to the landing position and that the strut load during a wing-down cycle does not exceed 700 pounds.

In order to circumvent the problem described previously, the manufacturer has redesigned the hydraulic actuating strut to increase the output force of the strut in both the wing-up and wing-down cycles.

CONCLUDING REMARKS

Flight-test measurements have been made of the flying qualities and some of the stability derivatives of a supersonic fighter airplane. In addition, pilot opinion of various aspects of the handling qualities is presented. The flight tests cover a range of Mach numbers up to 1.5 and an altitude range from sea level to 35,000 feet.

The damping of the short-period longitudinal oscillation is low and together with somewhat poor damping of small amplitude lateral oscillations results in relatively poor tracking performance of the airplane at subsonic speeds. The airplane in the opinion of the pilots has high roll-to-yaw ratios; however, the airplane meets the roll-to-yaw specifications of the present flying-qualities requirements. The longitudinal feel system is considered good by the pilots, but some of the longitudinal-control-system characteristics result in poor handling qualities. In particular, the nonlinear relationship between the stick and stabilizer

results in the airplane being too insensitive for all indicated airspeeds up to about 500 knots. Even above these airspeeds, it appears as though a more linear stick-to-stabilizer gearing would be an improvement. In accelerated maneuvers, structural deformation of the airplane results in motion of the stabilizer without a corresponding motion of the stick. This motion causes the apparent stick-fixed stability as measured by the stick position to become less stable and in some flight conditions, where the stabilizer angle per g is small, the airplane stability varies from neutral to unstable. The pilots dislike the longitudinal trim system because of the difficulty experienced when trying to trim precisely and the overshoot which occurs when making large or rapid trim corrections.

Langley Research Center,
National Aeronautics and Space Administration,
Langley Field, Va., May 19, 1958.

REFERENCES

1. Anon.: Model XF8U-1 Airplane, Phase I, Navy Preliminary Evaluation Report No. 1, Special Report. Project TED No. PTR AC-24101.1, Flight Test Div., U. S. Naval Air Test Center (Patuxent River, Md.), July 6, 1955.
2. Anon.: Model XF8U-1 Airplane, Naval Preliminary Evaluation, Phase I, Letter Report No. 2. Project TED No. PTR AC-24101.1, Flight Test Div., U. S. Naval Air Test Center (Patuxent River, Md.), July 14, 1955.
3. Anon.: Model XF8U-1 Airplane, Phase II, Navy Preliminary Evaluation, Report No. 1, Special Report. Project TED No. PTR AC-24101.1, Flight Test Div., U. S. Naval Air Test Center (Patuxent River, Md.), Oct. 13, 1955.
4. Anon.: Model XF8U-1 Airplane, Preliminary Evaluation, Phase II, Letter Report No. 2. Project TED No. PTR AC-24101.1, Flight Test Div., U. S. Naval Air Test Center (Patuxent River, Md.), Oct. 27, 1955.
5. Anon.: Phase IV Navy Preliminary Evaluation of the Model XF8U-1/F8U-1 Airplanes, Report No. 1. Project TED No. PTR AC-24101.1, Flight Test Div., U. S. Naval Air Test Center (Patuxent River, Md.), July 6, 1956.
6. Anon.: Phase IV Navy Preliminary Evaluation of the Model XF8U-1/F8U-1 Airplanes, Report No. 2. Project TED No. PTR AC-24101.1, Flight Test Div., U. S. Naval Air Test Center (Patuxent River, Md.), Aug. 6, 1956.
7. Anon.: Stability and Control Trials of the Model F8U-1 Airplane, Letter Report No. 1, Preliminary Evaluation Phase. Project TED No. BIS 21210, Flight Test Div., U. S. Naval Air Test Center (Patuxent River, Md.), Oct. 1, 1956.
8. Anon.: Service Suitability Trials of the Model F8U-1 Airplane, Report No. 1, Preliminary Evaluation Phase. Project TED No. BIS 21210, Service Test Div., U. S. Naval Air Test Center (Patuxent River, Md.), Oct. 1, 1956.
9. Anon.: Armament Trials of Model F8U-1 Airplane (Preliminary Evaluation Phase), Report No. 1. Project TED No. BIS 21210, Armament Test Div., U. S. Naval Air Test Center (Patuxent River, Md.), Nov. 1, 1956.

10. Anon.: Fleet Introduction Program of the Model F8U-1 Airplane, Report No. 1, Final Report. Project TED No. PTR AC-24101.3, Service Test Div., U. S. Naval Air Test Center (Patuxent River, Md.), Apr. 4, 1957.
11. Anon.: Flying Qualities of Piloted Airplanes. Military Specification, MIL-F-8785 (ASG), Sept. 1, 1954.
12. Klinar, Walter J.: Spinning and Related Problems at High Angles of Attack for High-Speed Airplanes. NACA RM L55L23a, 1956.
13. Klinar, Walter J.: A Study by Means of a Dynamic-Model Investigation of the Use of Canard Surfaces as an Aid in Recovering From Spins and as a Means for Preventing Directional Divergence Near the Stall. NACA RM L56B23, 1956.
14. Boisseau, Peter C.: Low-Speed Roll Effectiveness of a Differentially Deflected Horizontal-Tail Surface on a 42° Swept-Wing Model. NACA RM L56E03, 1956.
15. Paulson, John W., and Boisseau, Peter C.: Low-Speed Investigation of the Effect of Small Canard Surfaces on the Directional Stability of a Sweptback-Wing Fighter-Airplane Model. NACA RM L56F19a, 1956.
16. Hastings, Earl C., Jr.: Minimum Drag of Four Versions of a Swept-Wing Fighter Airplane Obtained From Flight Tests of Rocket-Boosted Models at Mach Numbers From 0.81 to 1.71. NACA RM L56E25a, 1956.
17. Larson, Terry J., Stillwell, Wendell H., and Armistead, Katharine H.: Static-Pressure Error Calibrations for Nose-Boom Airspeed Installations of 17 Airplanes. NACA RM H57A02, 1957.

TABLE I.- PERTINENT CHARACTERISTICS OF TEST AIRPLANE

Wing (not including leading-edge chord-extension):

Area, sq ft	375
Span, ft	35.67
Aspect ratio	3.4
Taper ratio	0.247
Sweepback of quarter-chord line, deg	42.0
Dihedral, deg	-5.0

Geometric wing incidence, relative to fuselage

reference line:

Cruise and high speed, deg	-1.0
Take-off and landing, deg	7.0

Wing-hinge-point location, percent mean geometric chord	39.58
---	-------

Mean geometric chord, in.	141.4
-----------------------------------	-------

Airfoil section parallel to plane of symmetry:

Wing root	NACA 65A006
Wing tip	NACA 65A005

Deflections of leading-edge droop:

Inboard section:

Landing and take-off, deg	25
Cruise, deg	6.75
High speed, deg	0

Outboard section:

Landing and take-off, deg	27
Cruise, deg	7.0
High speed, deg	0

Chord-extension area (both sides), sq ft	10.33
--	-------

Center-section inboard flaps:

Area (both sides), sq ft	13.44
Deflection for landing and take-off, deg	20.0
Deflection for cruise and high speed, deg	0

Ailerons:

Chord, percent of wing chord:

Outboard	28.0
Inboard	23.5
Area, sq ft	20.78

Deflections:

High speed and cruise, deg	±15
--------------------------------------	-----

Take-off and landing:

Both ailerons drooped as flaps, deg	20
As ailerons, deg	+45-15

TABLE I.- PERTINENT CHARACTERISTICS OF TEST AIRPLANE - Concluded

Vertical stabilizer (based on area extending to horizontal tail center line, not including dorsal):

Area, sq ft	109
Span, ft	12.75
Aspect ratio	1.5
Sweepback of quarter-chord line, deg	45.0
Taper ratio	0.25
Mean geometric chord, in.	114.8
Tail length, from 28% wing mean geometric chord to 25% vertical-tail mean geometric chord, in.	168.9
Airfoil:	
Waterline	Modified NACA 65A005.3
Tip	Modified NACA 65A004

Rudder:

Area, sq ft	12.56
Chord, constant, in.	21.28
Maximum deflections:	
High speed and cruise, deg	±6.0
Take-off and landing, deg	±17.0

Horizontal stabilizer (based on area extending to fuselage center line):

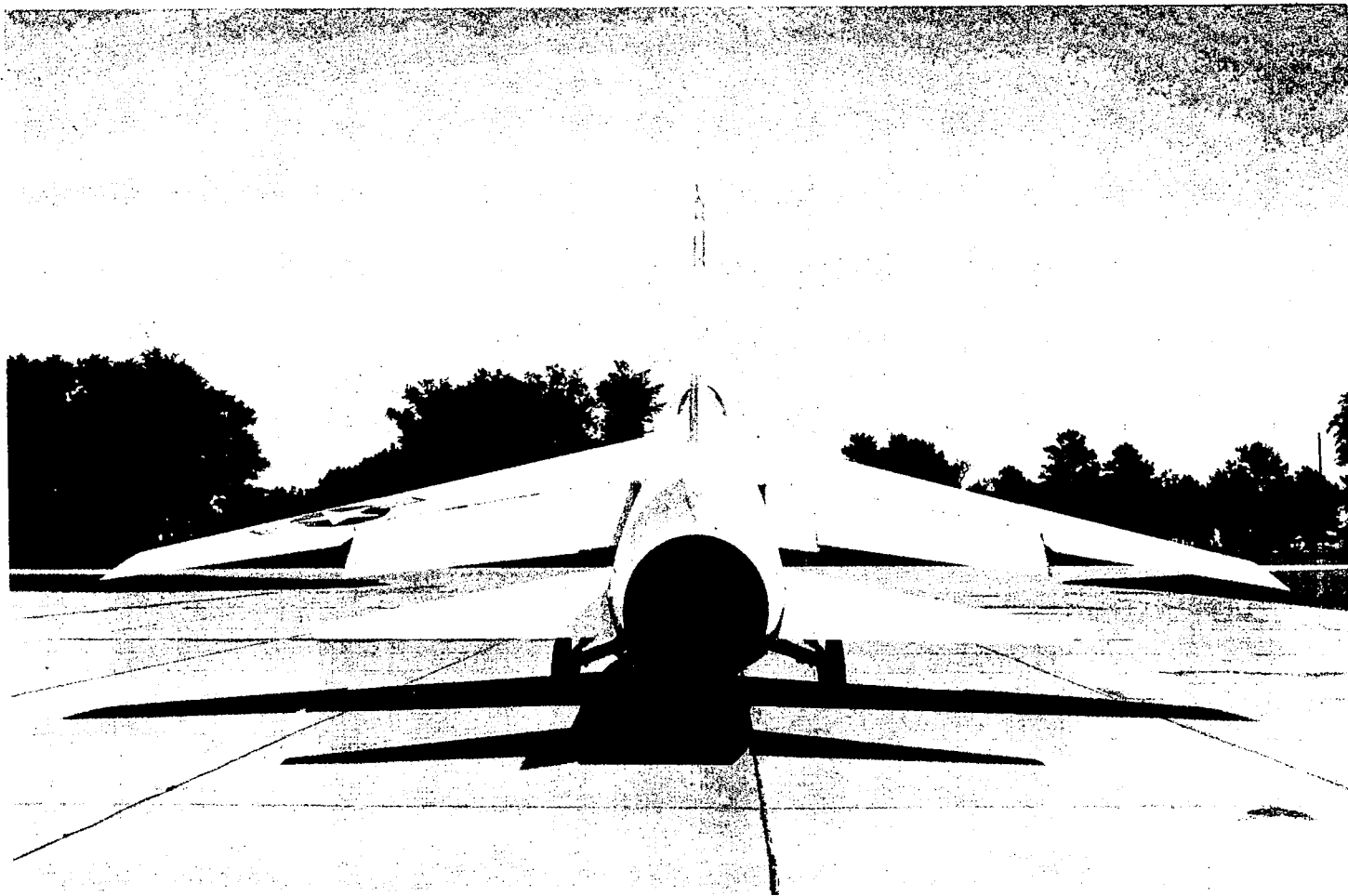
Area, sq ft	93.4
Span, ft	18.1
Aspect ratio	3.5
Taper ratio	0.148
Sweepback of quarter-chord line, deg	45
Geometric dihedral, deg	5.417
Mean geometric chord, in.	73.4
Tail length, from 28% wing mean geometric chord to 25% horizontal-tail mean geometric chord, in.	200.6
Maximum deflections:	
Trailing edge down, deg	8
Trailing edge up, deg	32
Airfoil:	
Root	NACA 65A006
Tip	NACA 65A004



(a) Three-quarter front view.

L-57-2099

Figure 1.- Test airplane in the take-off and landing configuration.



(b) Rear view.

L-57-2102

Figure 1.- Concluded.

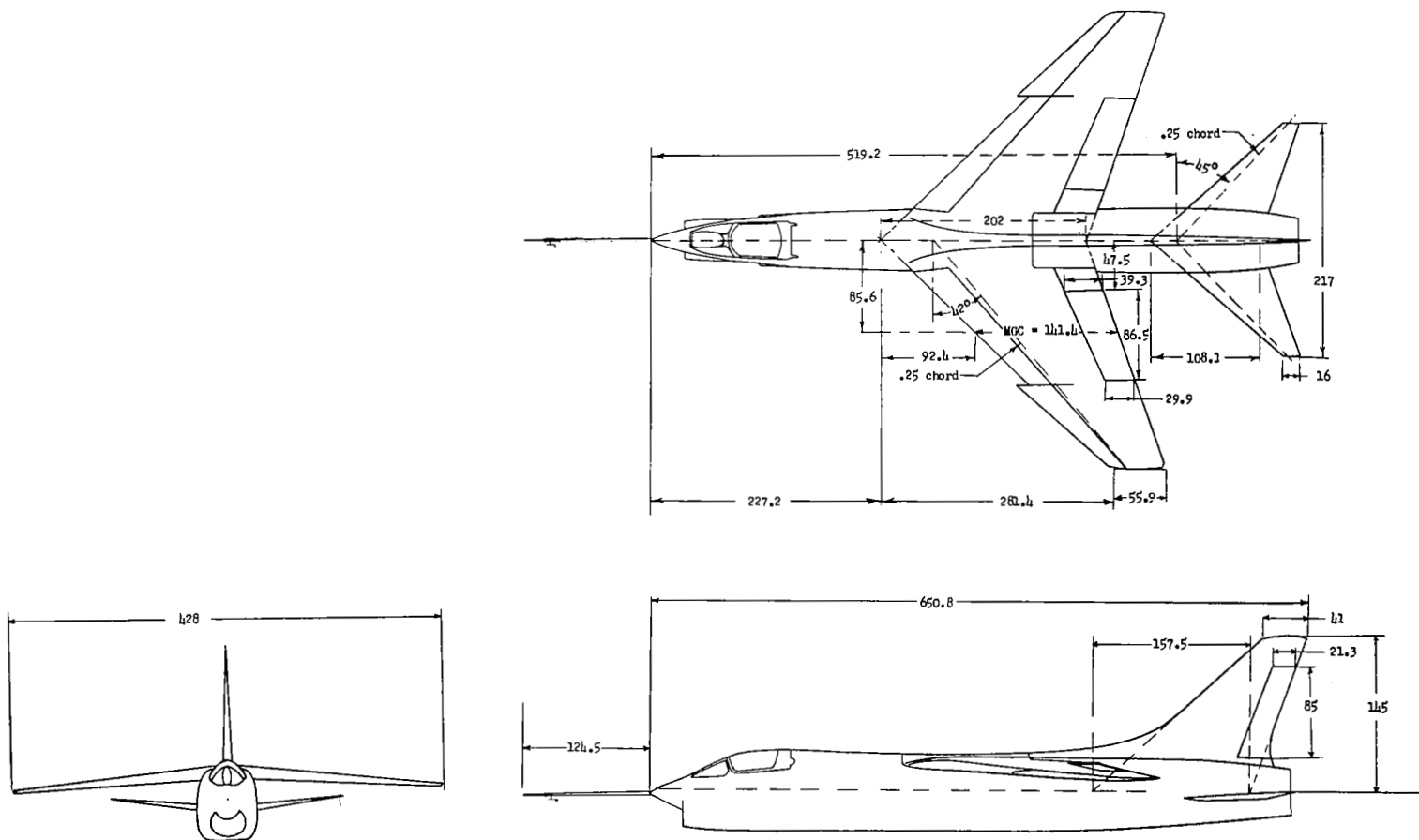
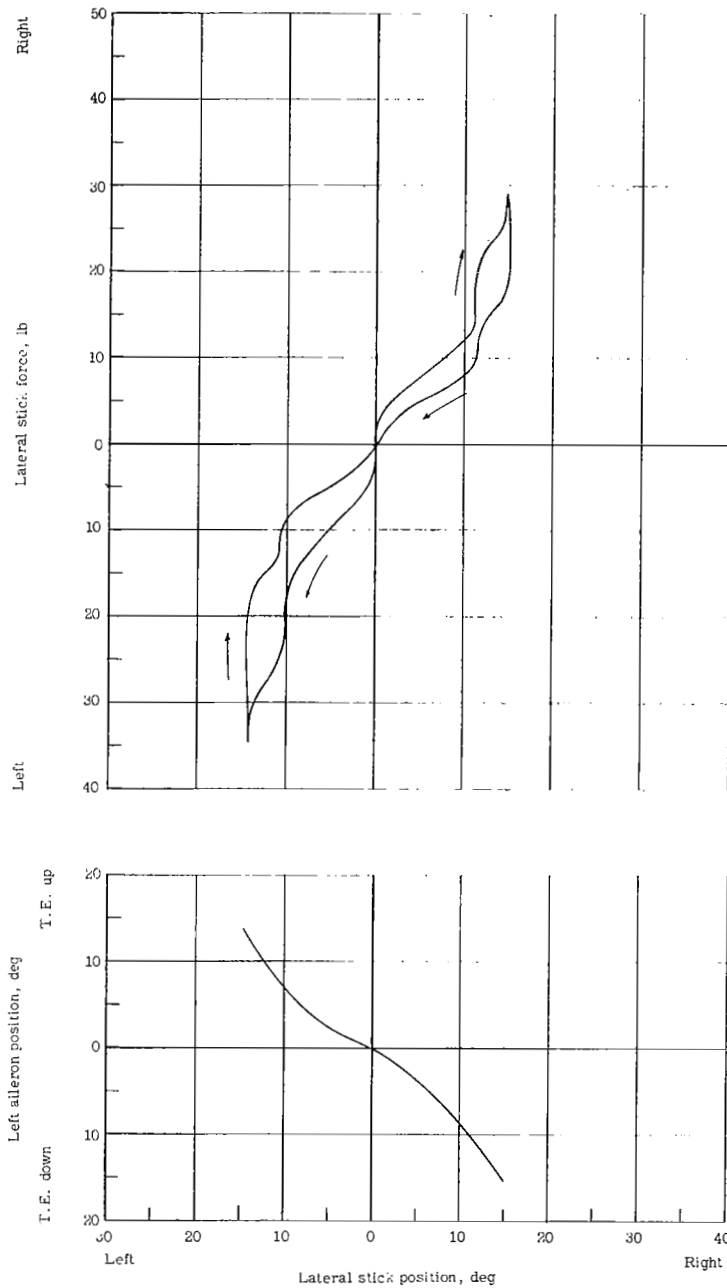
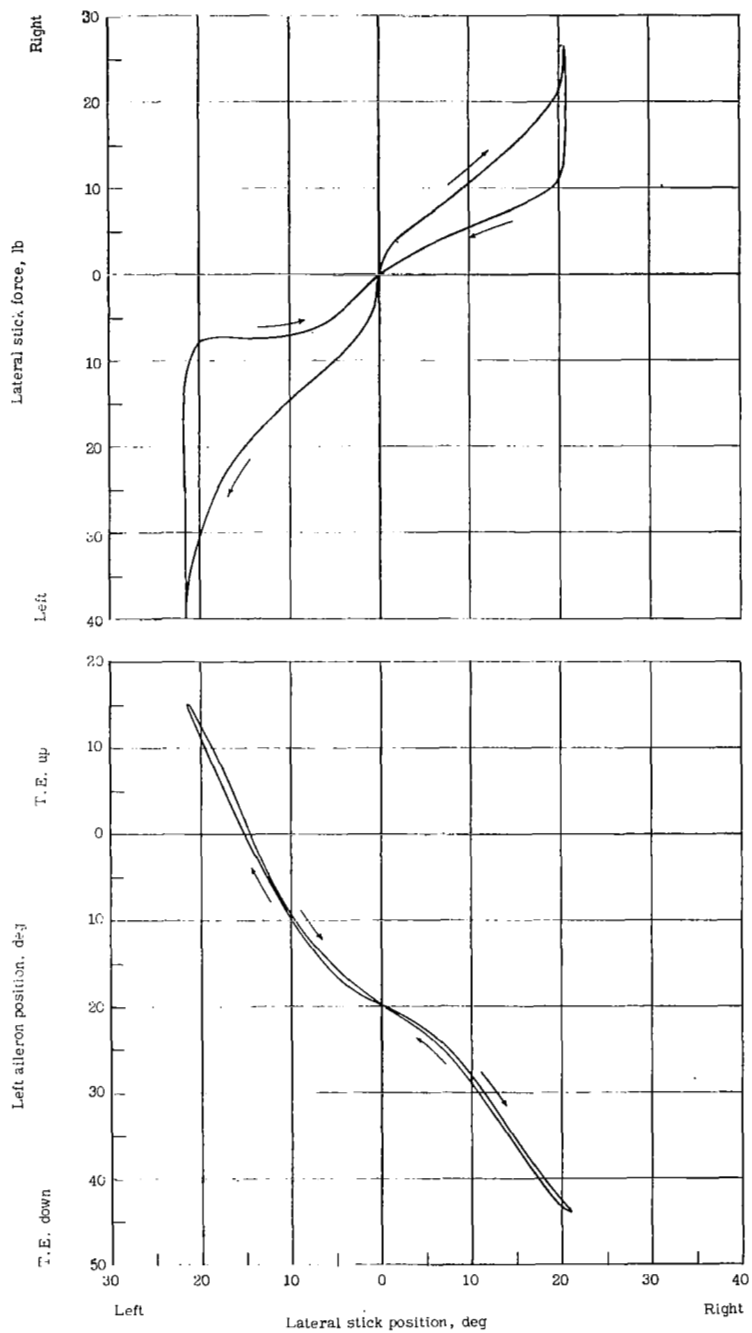


Figure 2.- Three-view drawing of the test airplane. All dimensions are in inches.



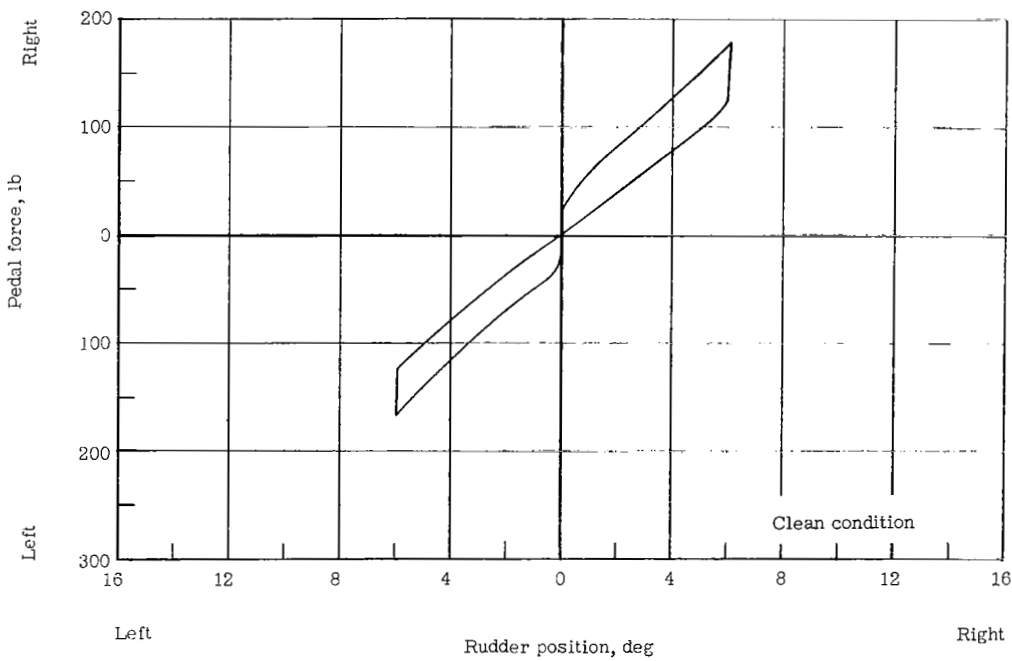
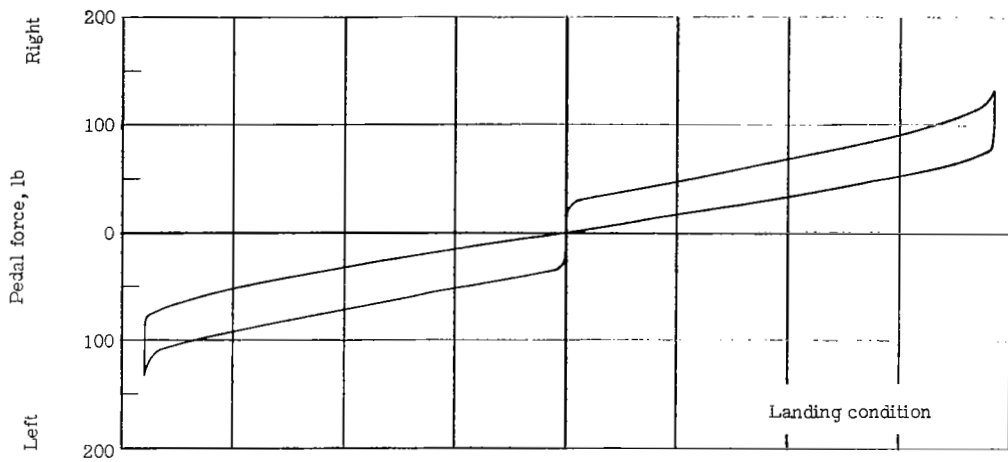
(a) Aileron control system, clean condition.

Figure 3.- Characteristics of the aileron and rudder control systems as measured on the ground. Lateral stick length = $18\frac{3}{8}$ inches.



(b) Aileron control system, landing condition.

Figure 3.- Continued.



(c) Rudder control system.

Figure 3.- Concluded.

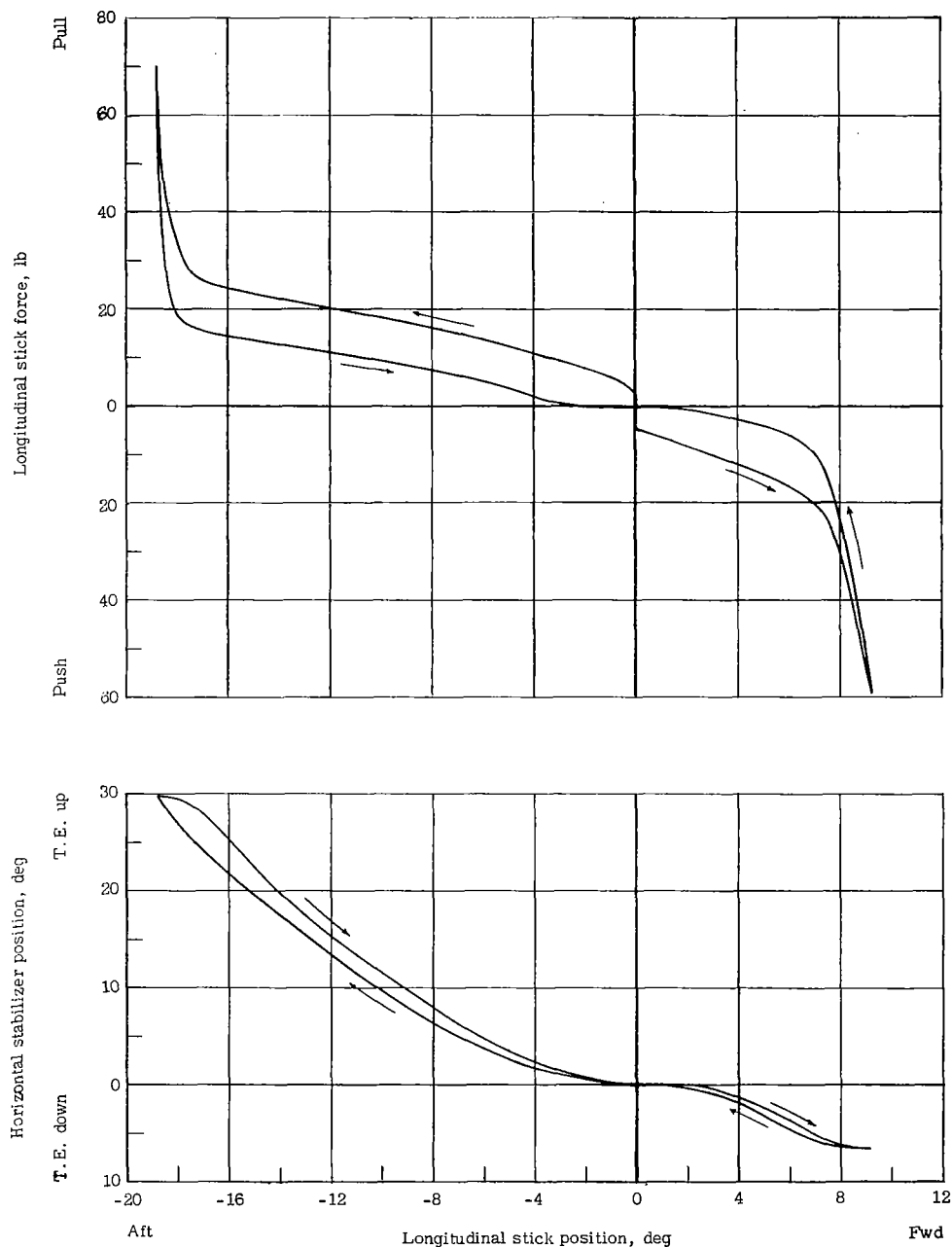


Figure 4.- Characteristics of the longitudinal control system showing the variation of stick force and stabilizer deflection with stick displacement. Longitudinal stick length = $22\frac{3}{8}$ inches.

- NASA Flight Data Point
- Calculated Using
Ref. 17 Fig No. 17
- Chance Vought data

$$\text{Calibrated Mach Number } M_c = M_i + \Delta M$$

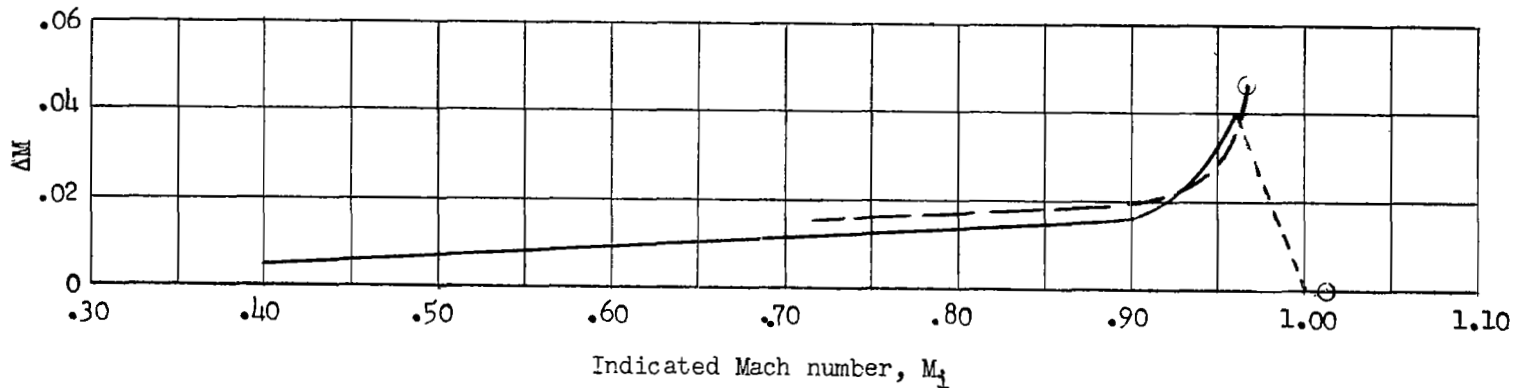
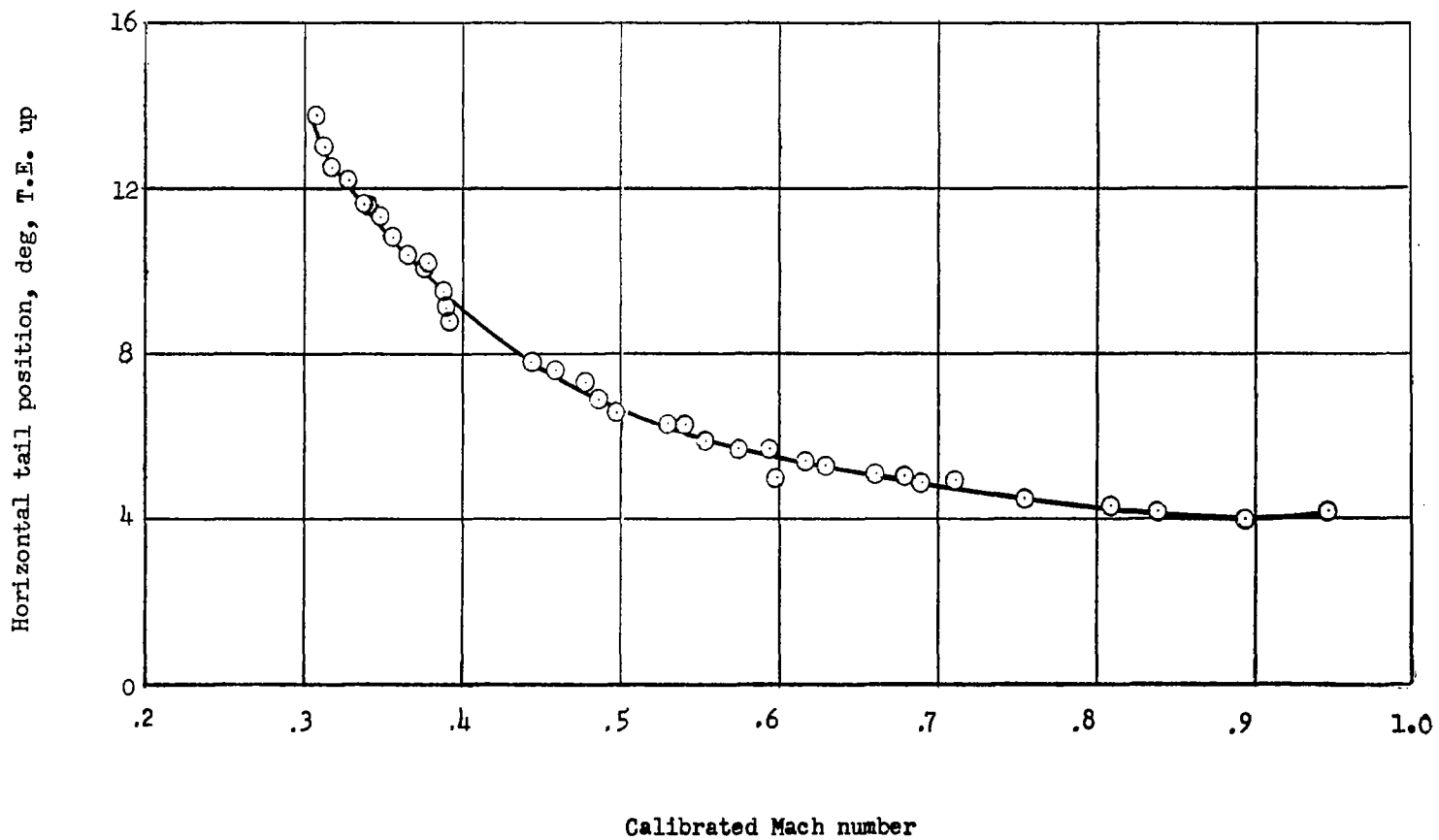
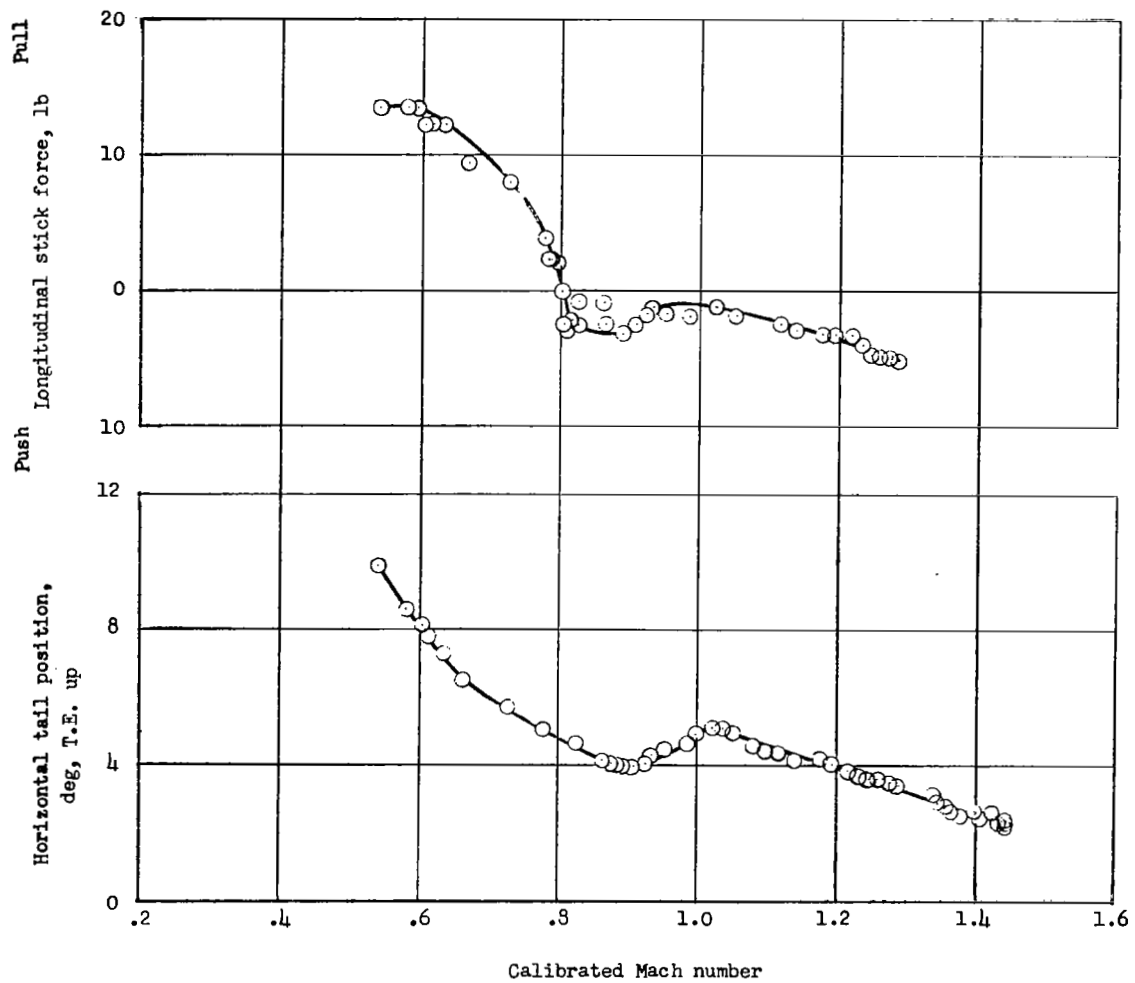


Figure 5.- Mach number calibration used to correct indicated Mach number to calibrated Mach number. Calibration does not exist between $M_i = 0.96$ and $M_i = 1.00$ (shown by short-dash line).



(a) 20,000 feet.

Figure 6.- Variation of stabilizer position and stick force with calibrated Mach number.



(b) 35,000 feet.

Figure 6.- Concluded.

Horizontal tail position , deg, T.E. up

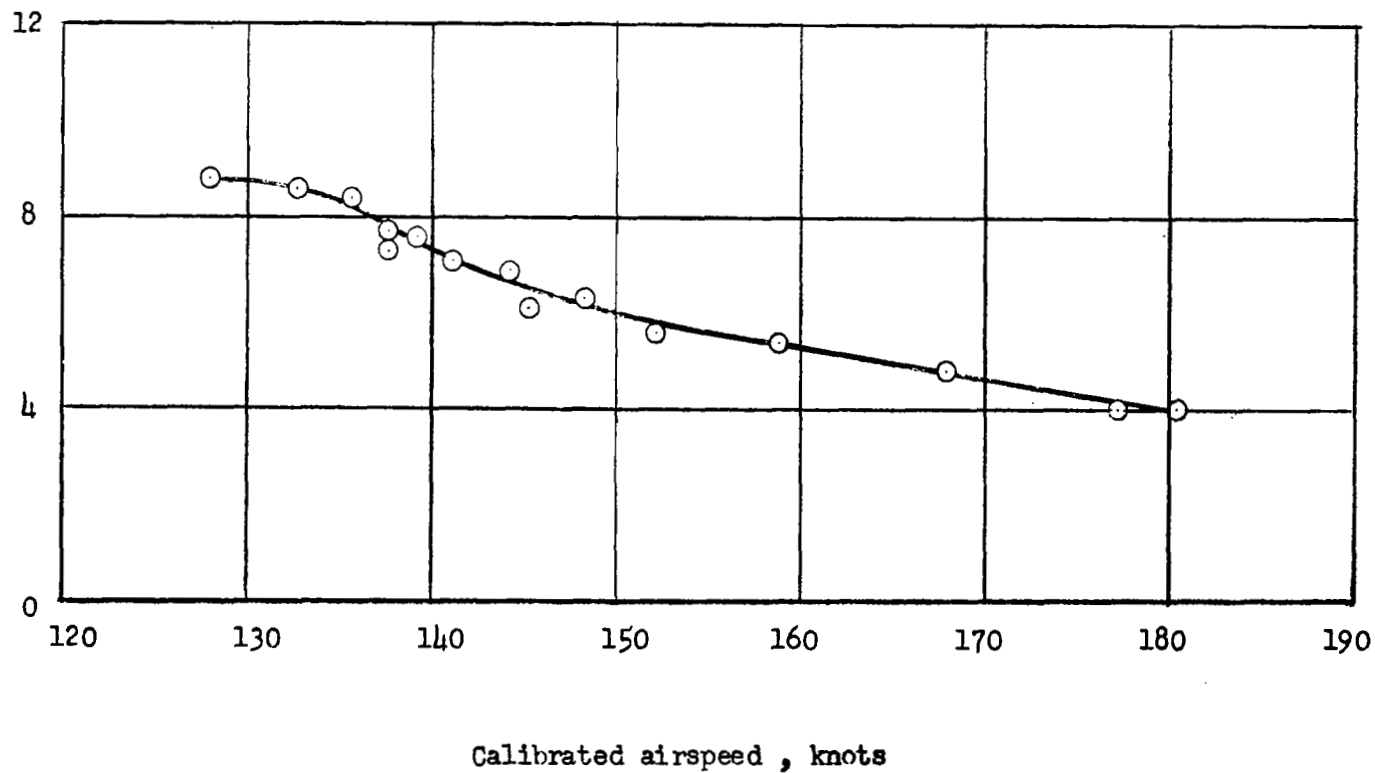
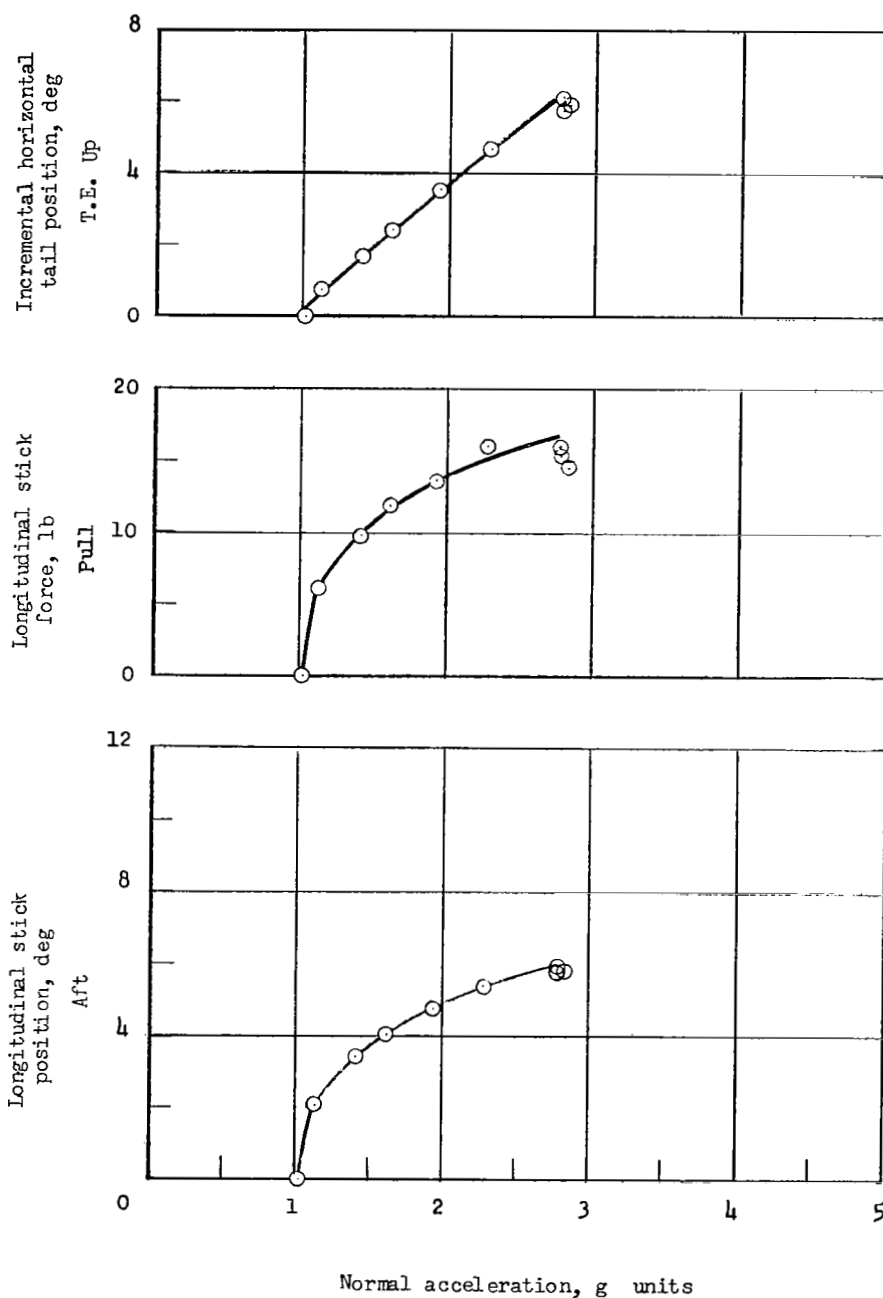
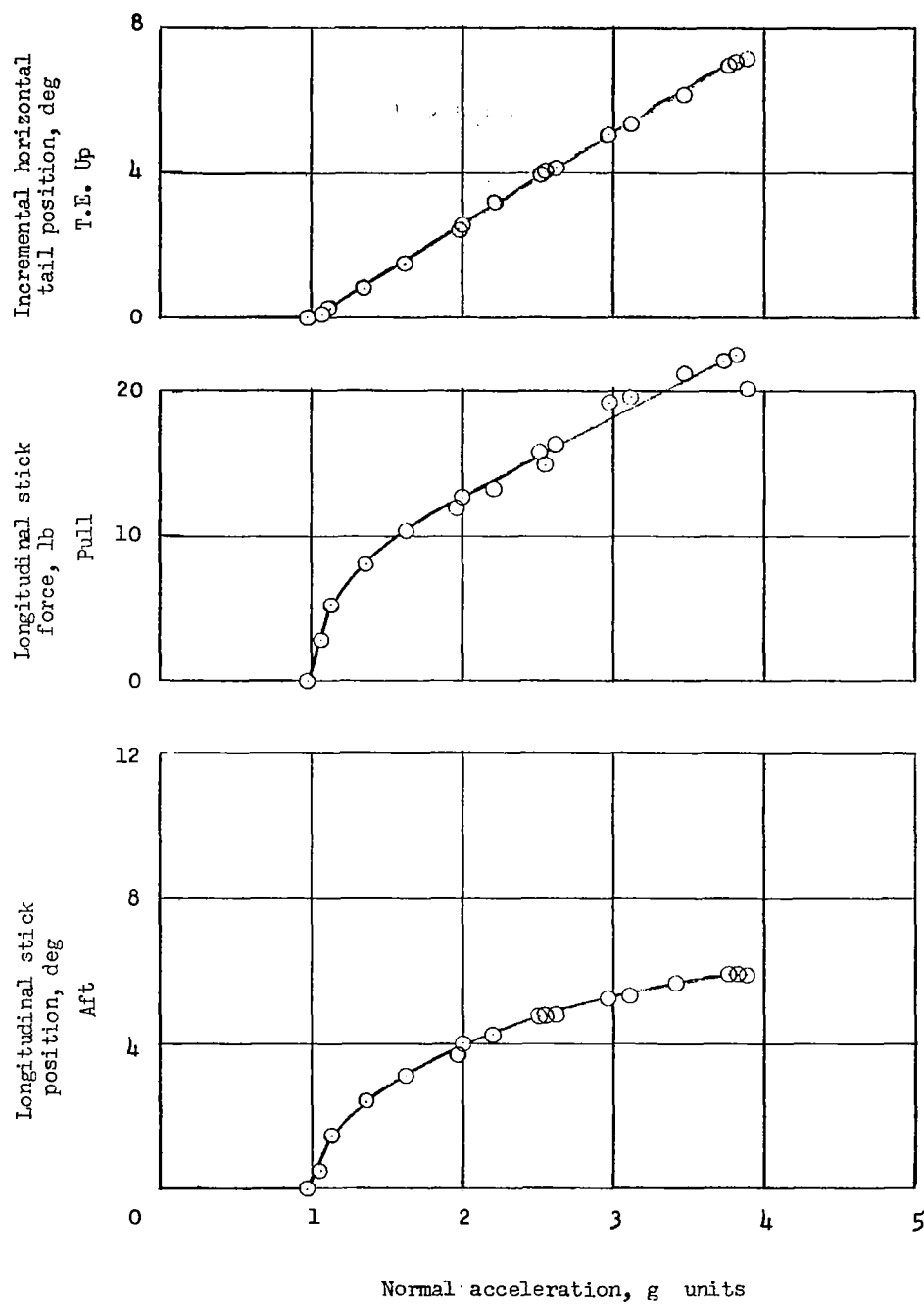


Figure 7.- Variation of horizontal stabilizer position required for trim with calibrated airspeed in the landing condition.



(a) $M_C = 0.90$; altitude = 35,500 feet; cruise droop down.

Figure 8.- Variation of longitudinal stick position, stick force, and horizontal stabilizer position with normal acceleration. Tests made in windup turns.



(b) $M_c = 1.35$; altitude = 29,700 feet; cruise droop up.

Figure 8.- Concluded.

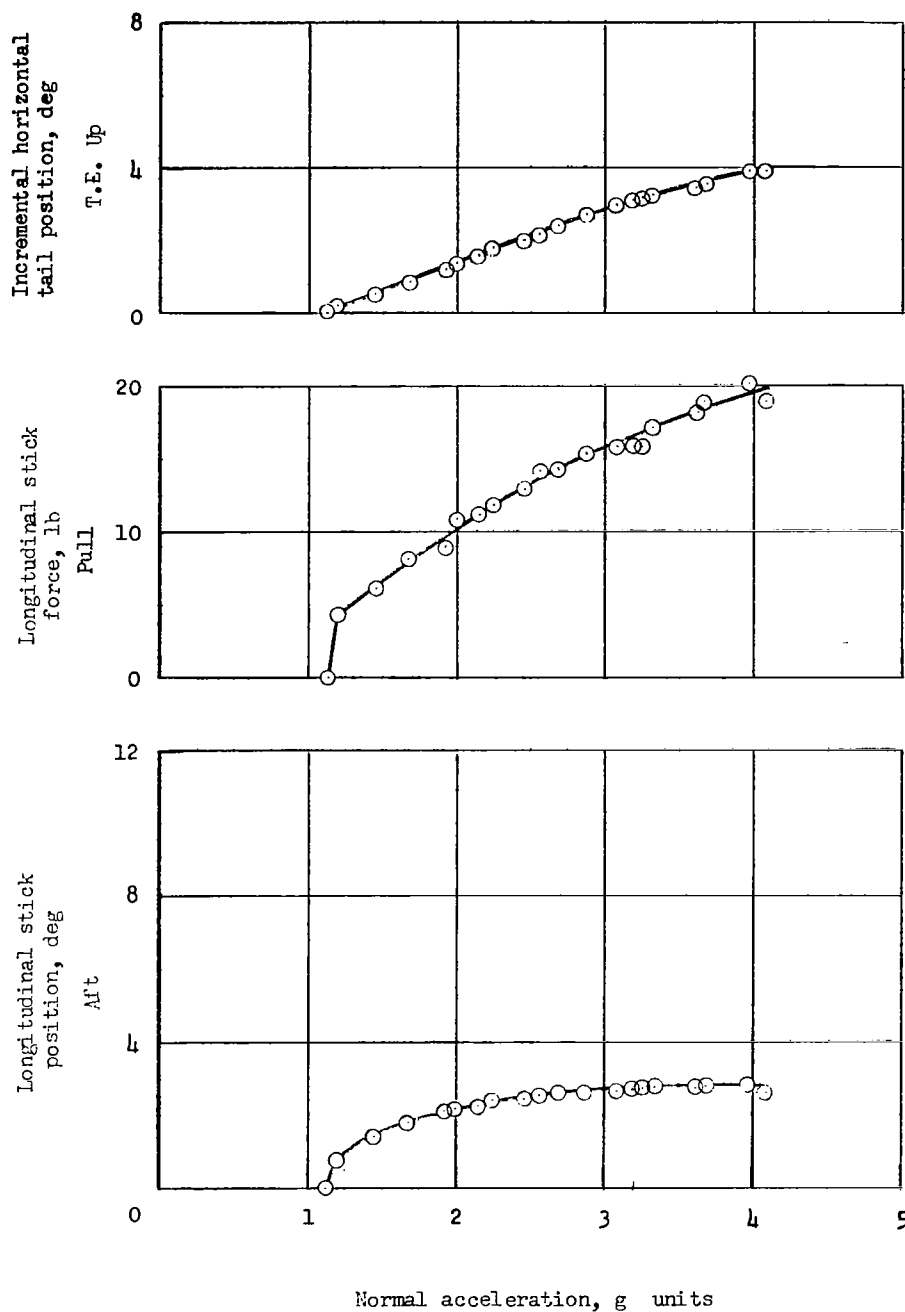


Figure 9.- Variation of longitudinal stick position, stick force, and horizontal stabilizer position with normal acceleration. Tests made in windup turns with cruise droop up at a Mach number of 0.90 and altitude of 14,400 feet.

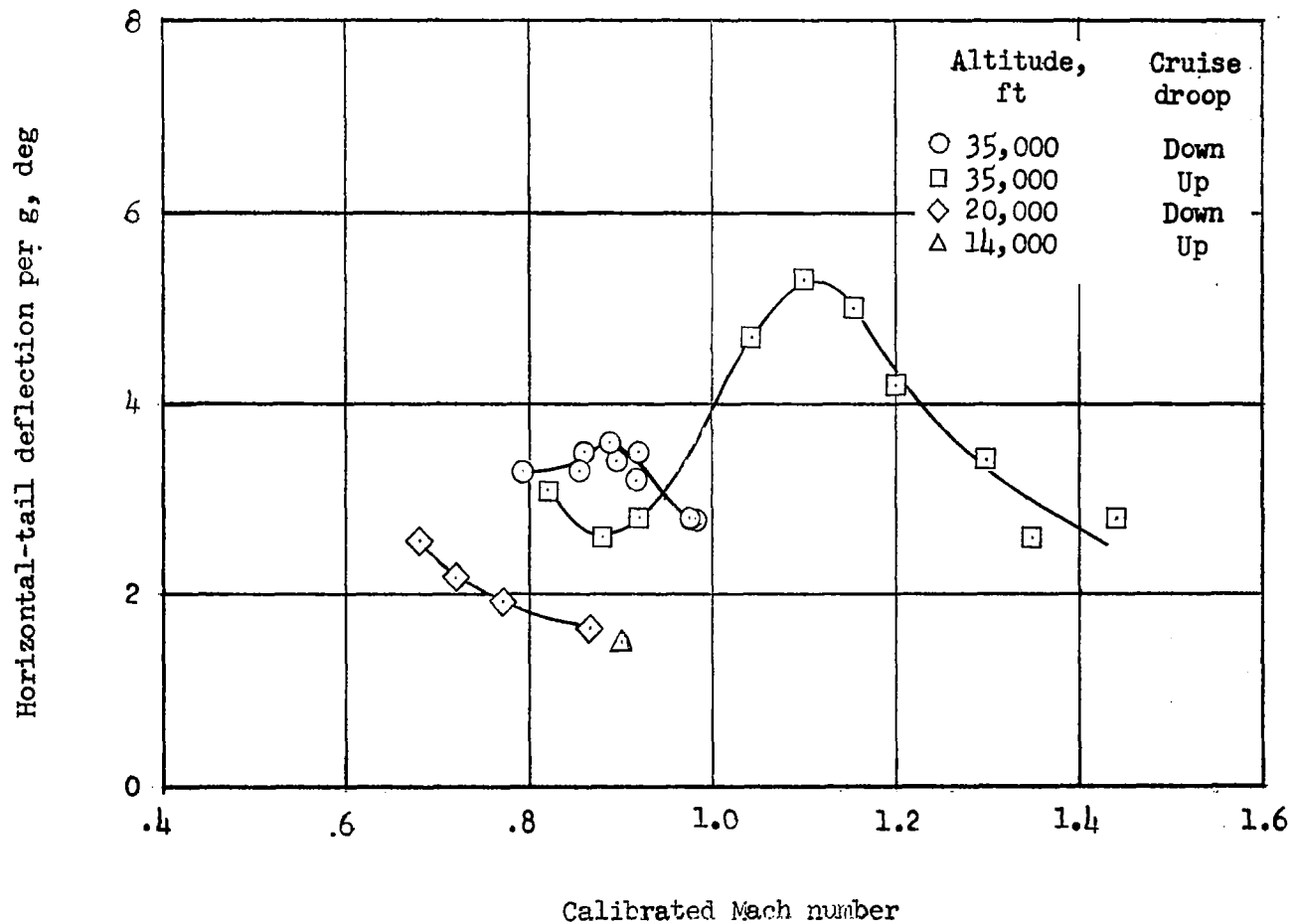
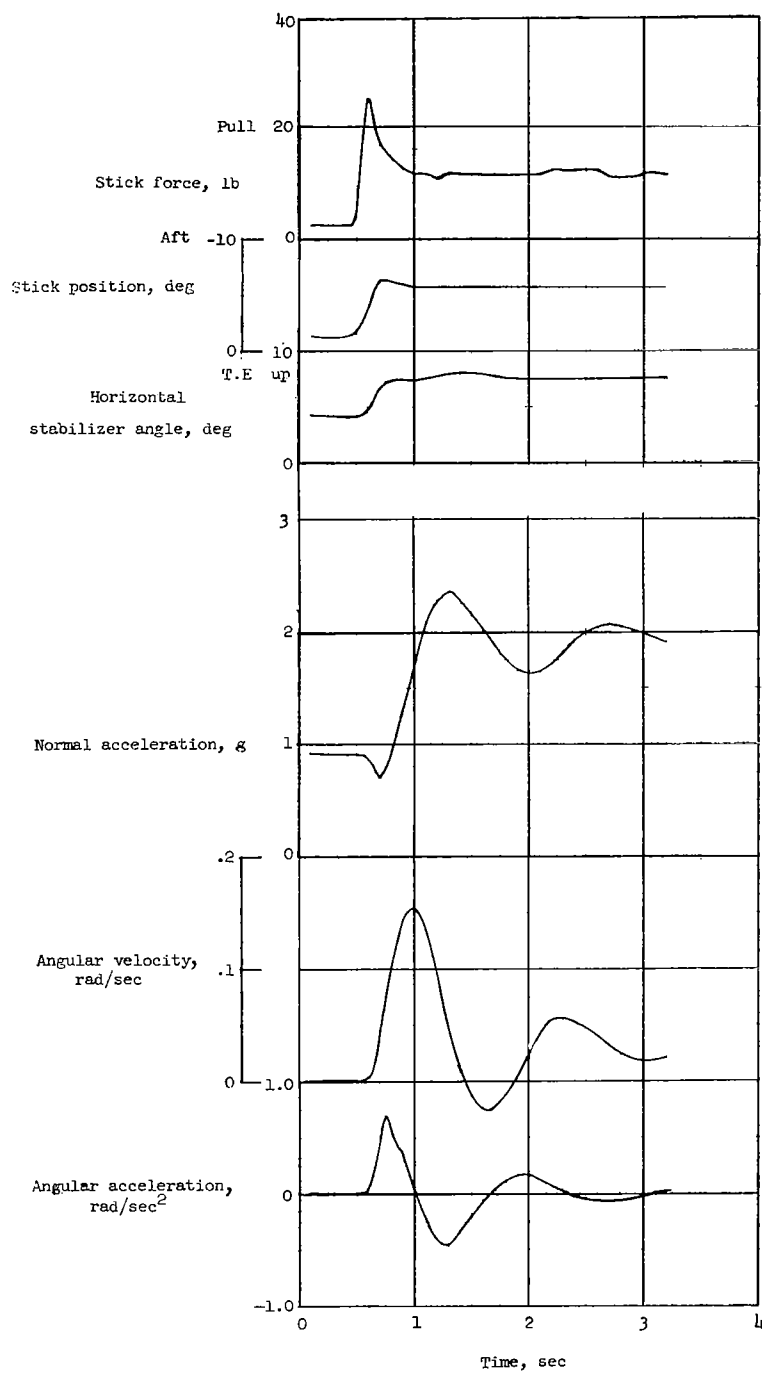
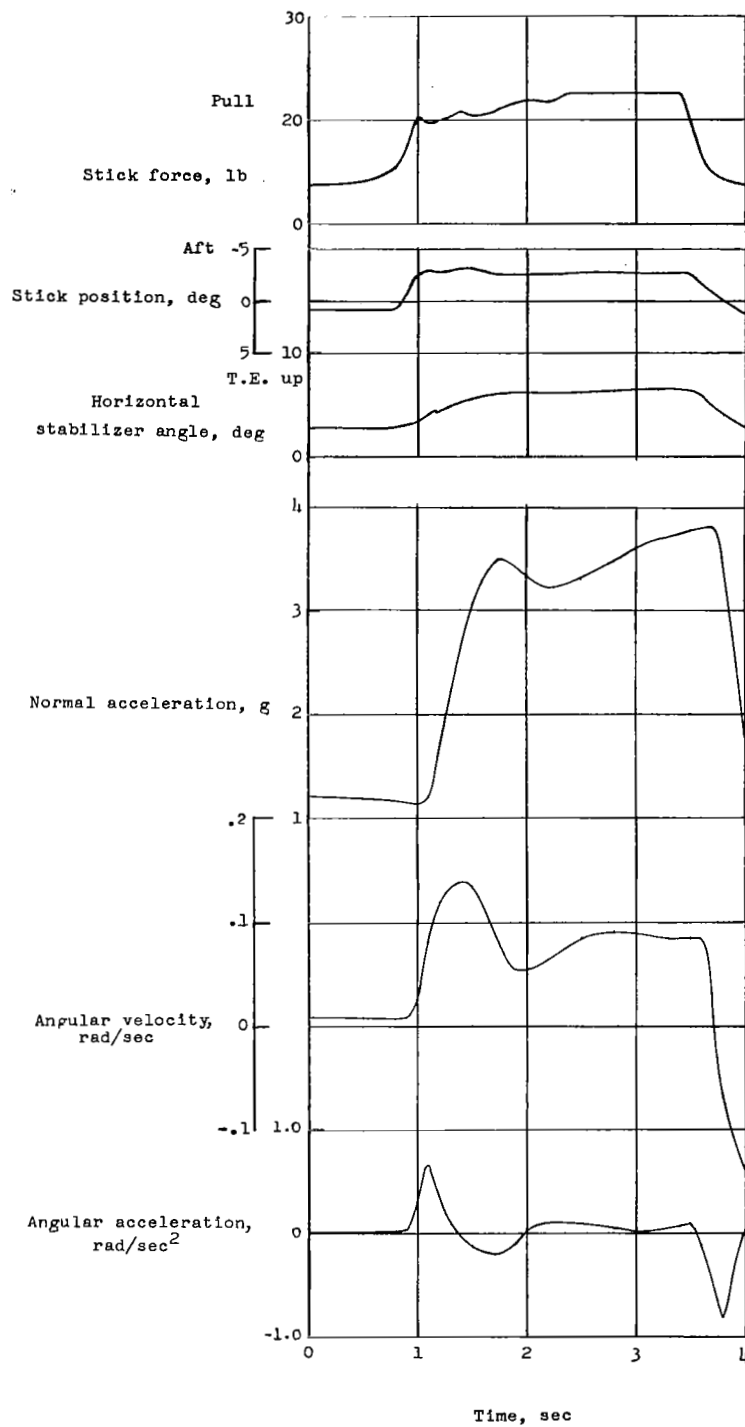


Figure 10.- Summary plot of the variation of horizontal-tail deflection per g as a function of Mach number for several altitudes and the two cruise-droop positions.



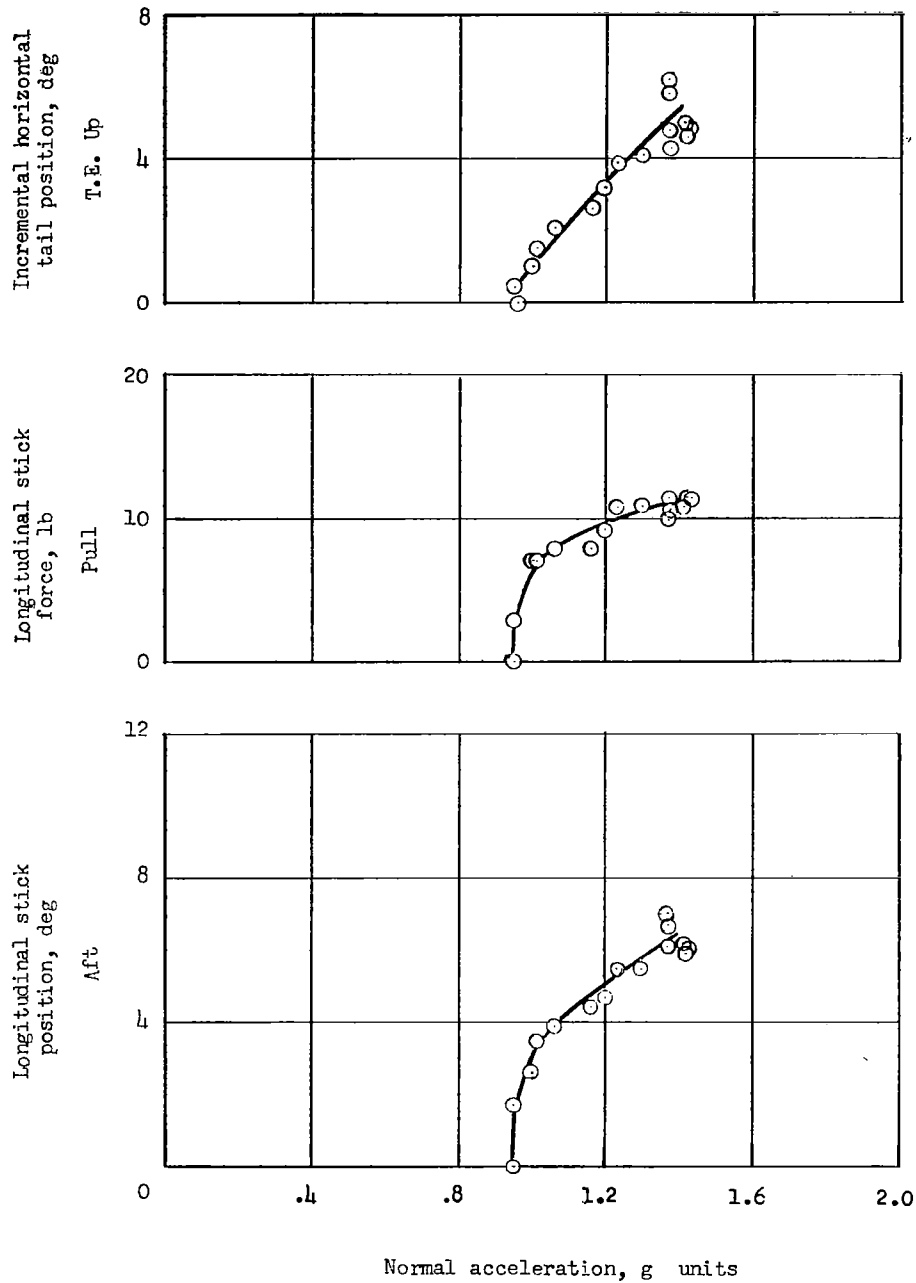
(a) $M_C = 0.98$; altitude = 34,900 feet.

Figure 11.- Time histories of rapid pull-up and hold maneuvers.



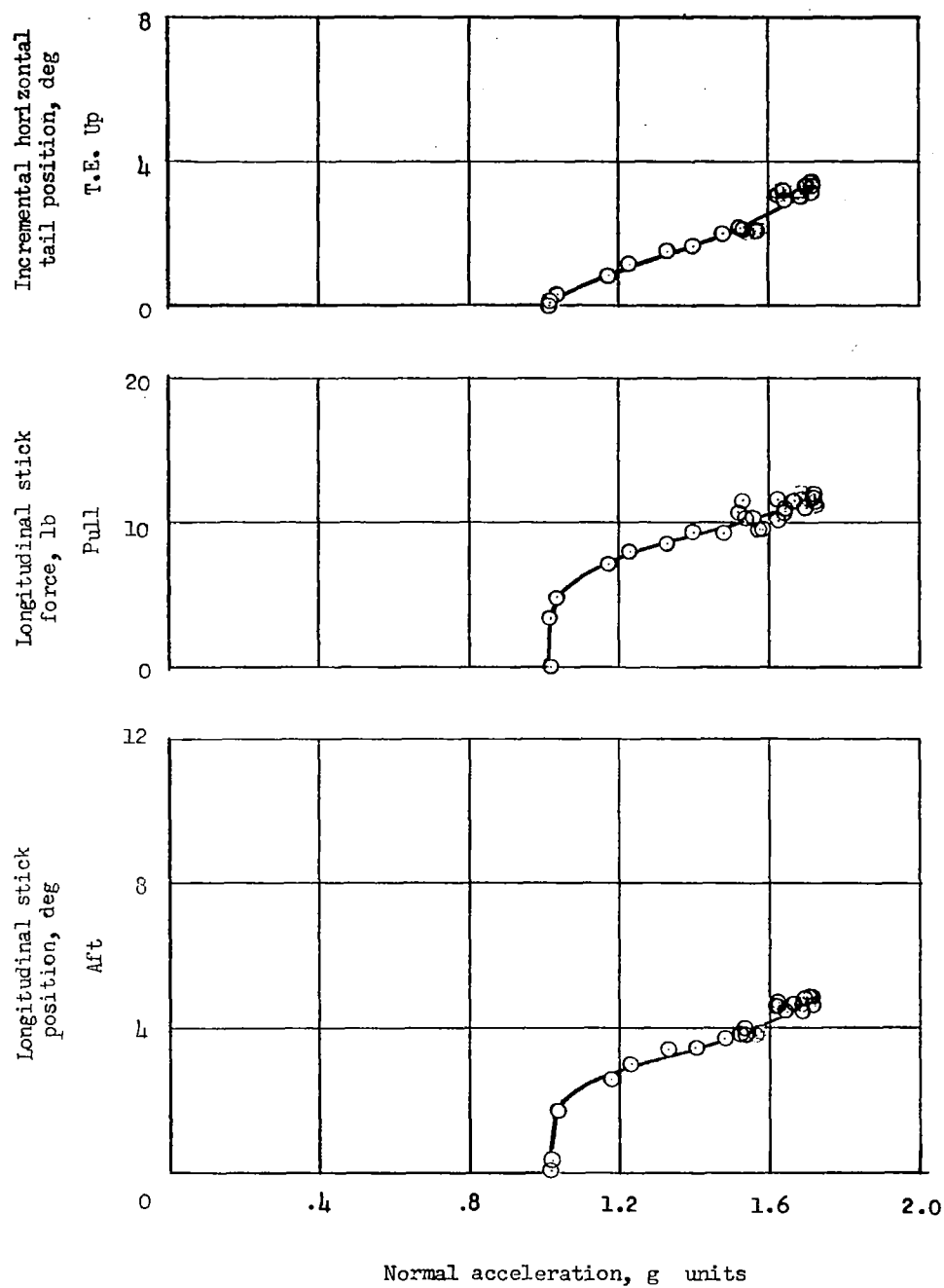
(b) $M_C = 0.93$; altitude = 13,760 feet.

Figure 11.- Concluded.



(a) $V_C = 140$ knots; altitude = 5,000 feet.

Figure 12.- Variation of longitudinal stick position, stick force, and horizontal stabilizer position with normal acceleration in the landing condition.



(b) $V_c = 197$ knots; altitude = 11,000 feet.

Figure 12.- Concluded.

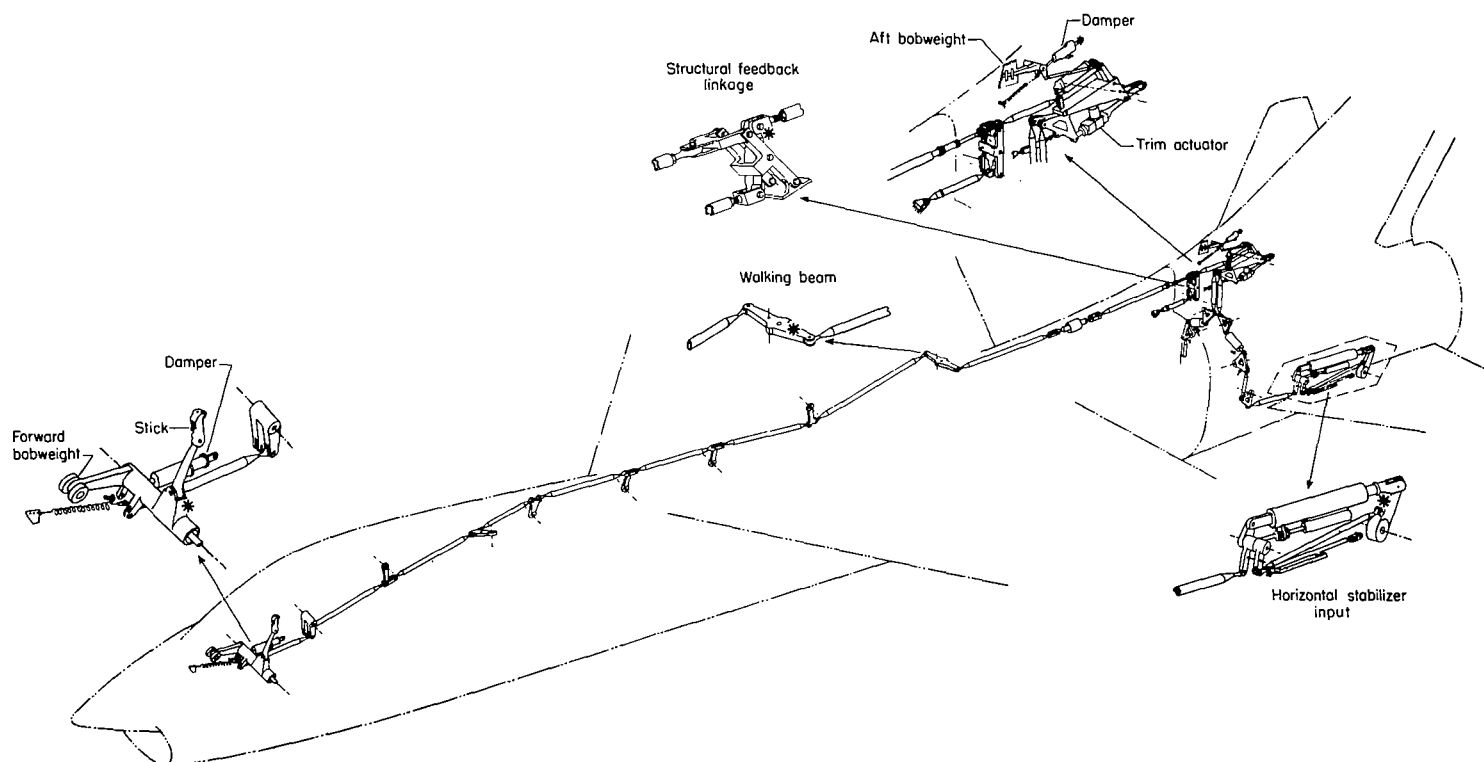
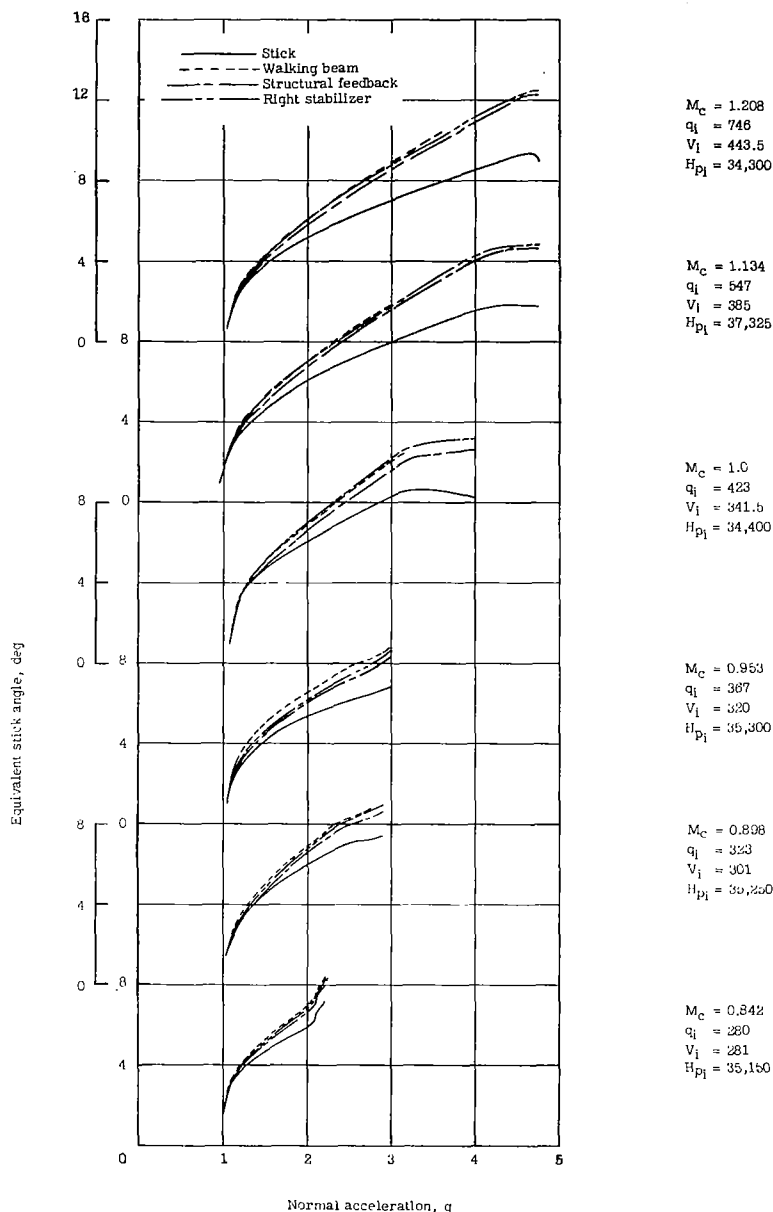
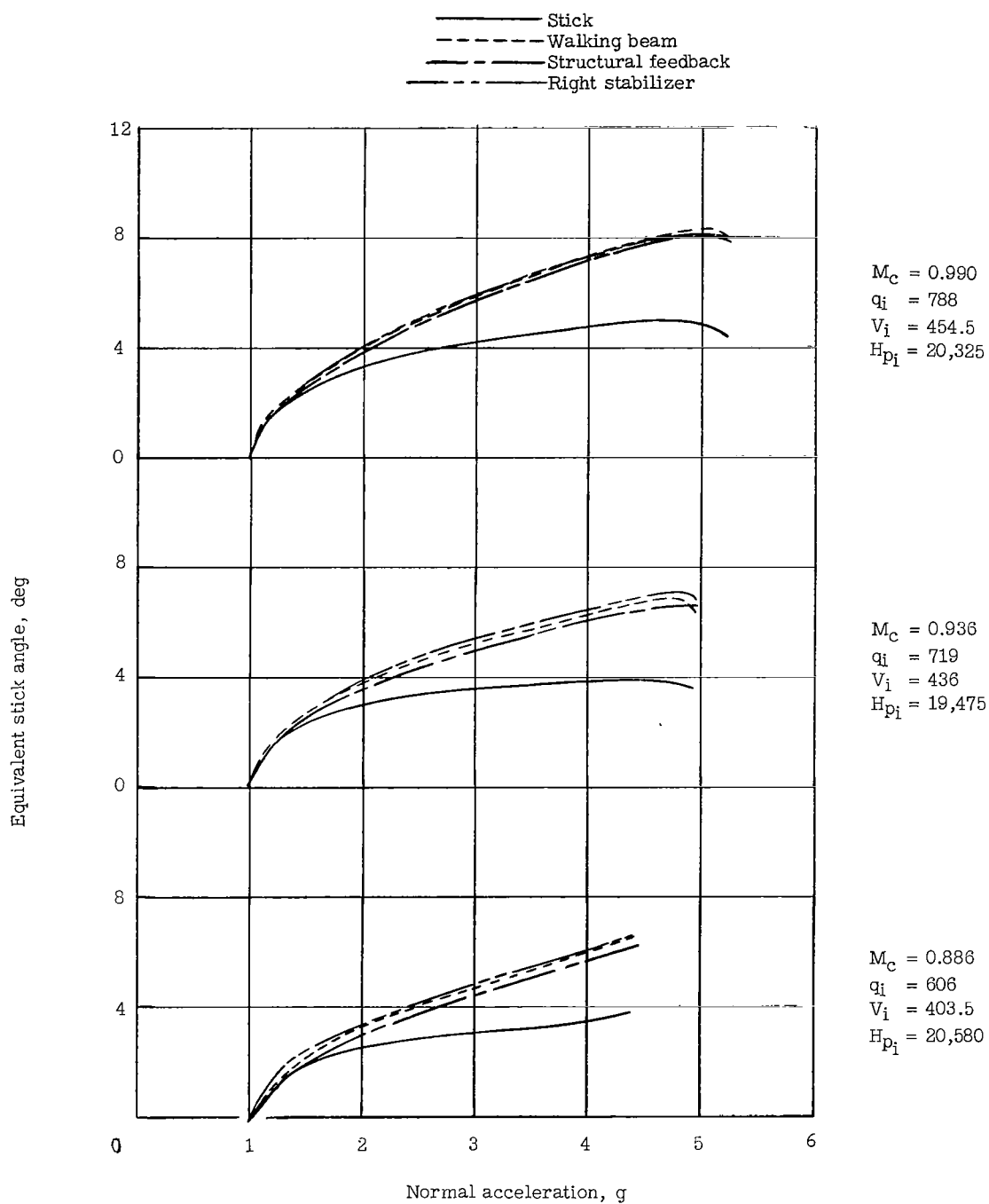


Figure 13.- Schematic drawing of the longitudinal control system of the test airplane. The enlarged drawings indicate the areas where measurements were made. An asterisk on the linkage indicates the point at which the measuring instrument was attached.



(a) Altitude = 35,000 feet.

Figure 14.- Variation of longitudinal stick position, walking beam linkage position, structural feedback linkage position, and right horizontal stabilizer position with normal acceleration. Tests made in windup turns for various Mach numbers at altitudes of approximately 35,000 feet and 20,000 feet.



(b) Altitude = 20,000 feet.

Figure 14.- Concluded.

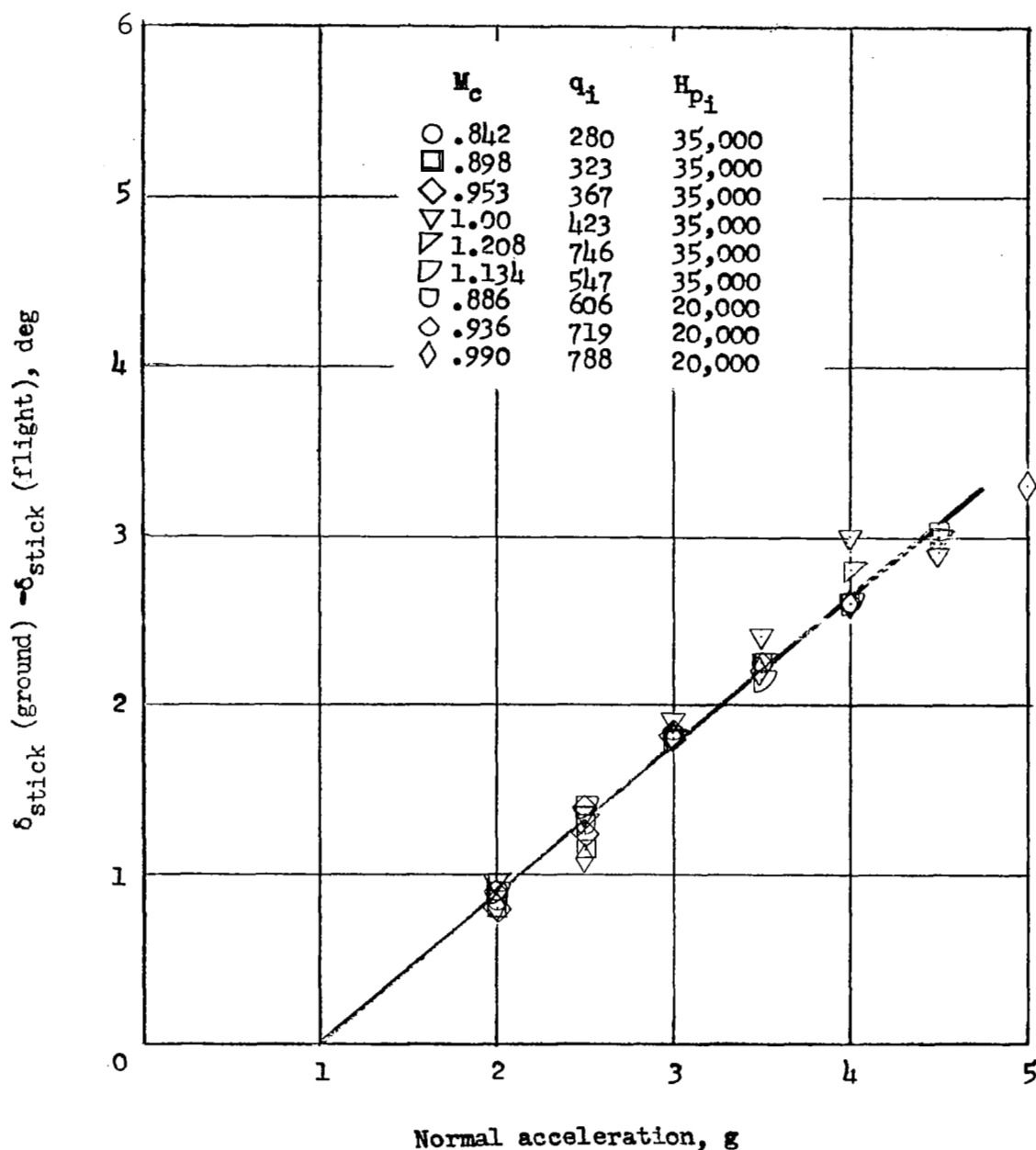


Figure 15.- Summary plot of the structural deformation effects on the longitudinal control system as shown by the variation of the deformation effects in terms of stick angle with normal acceleration as determined by the relative motion between the right horizontal stabilizer and the longitudinal stick position.

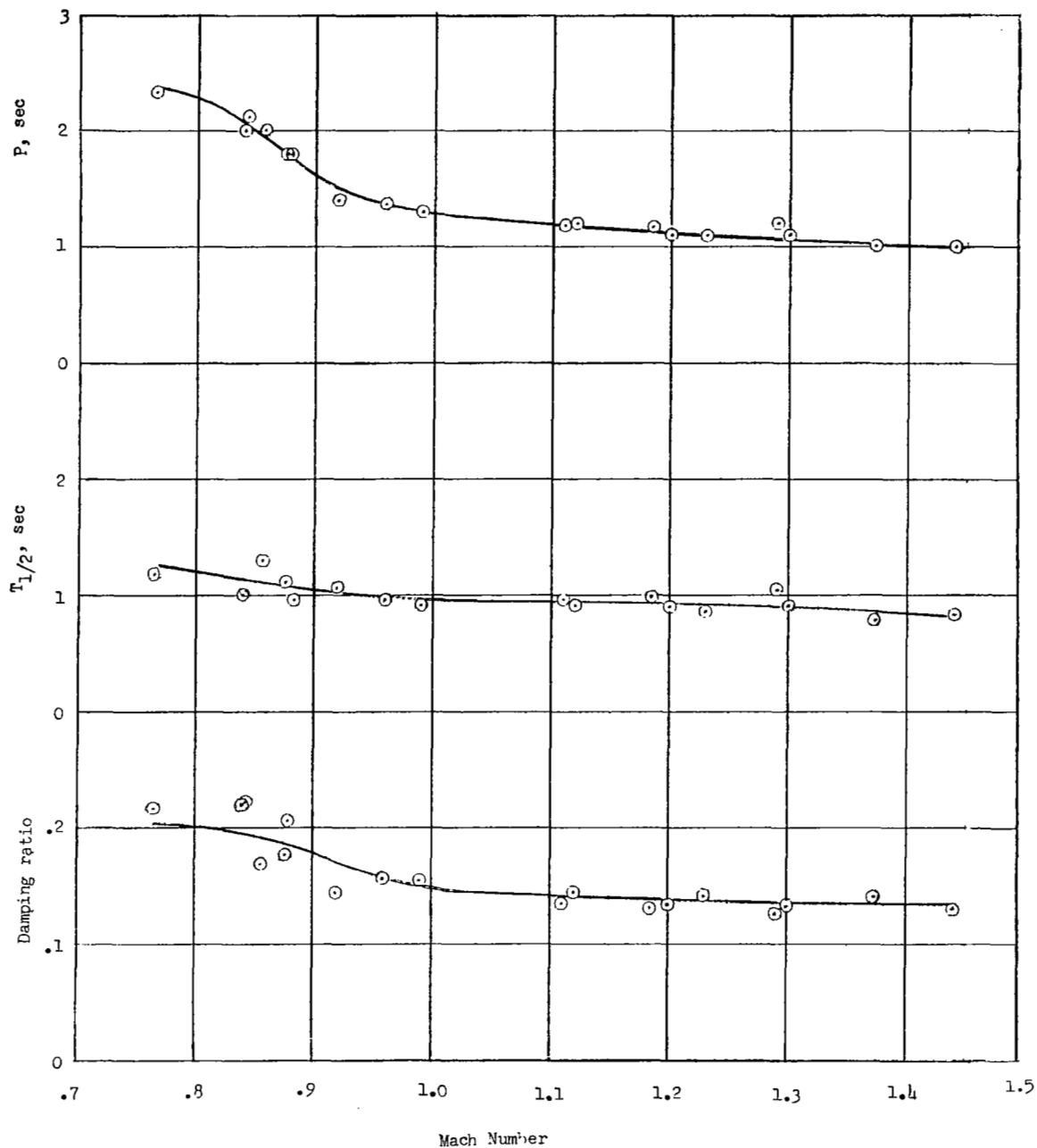


Figure 16.- Characteristics of the short-period longitudinal oscillations showing the variation of the period, time to damp to one-half amplitude, and damping ratio as a function of Mach number at an altitude of approximately 35,000 feet.

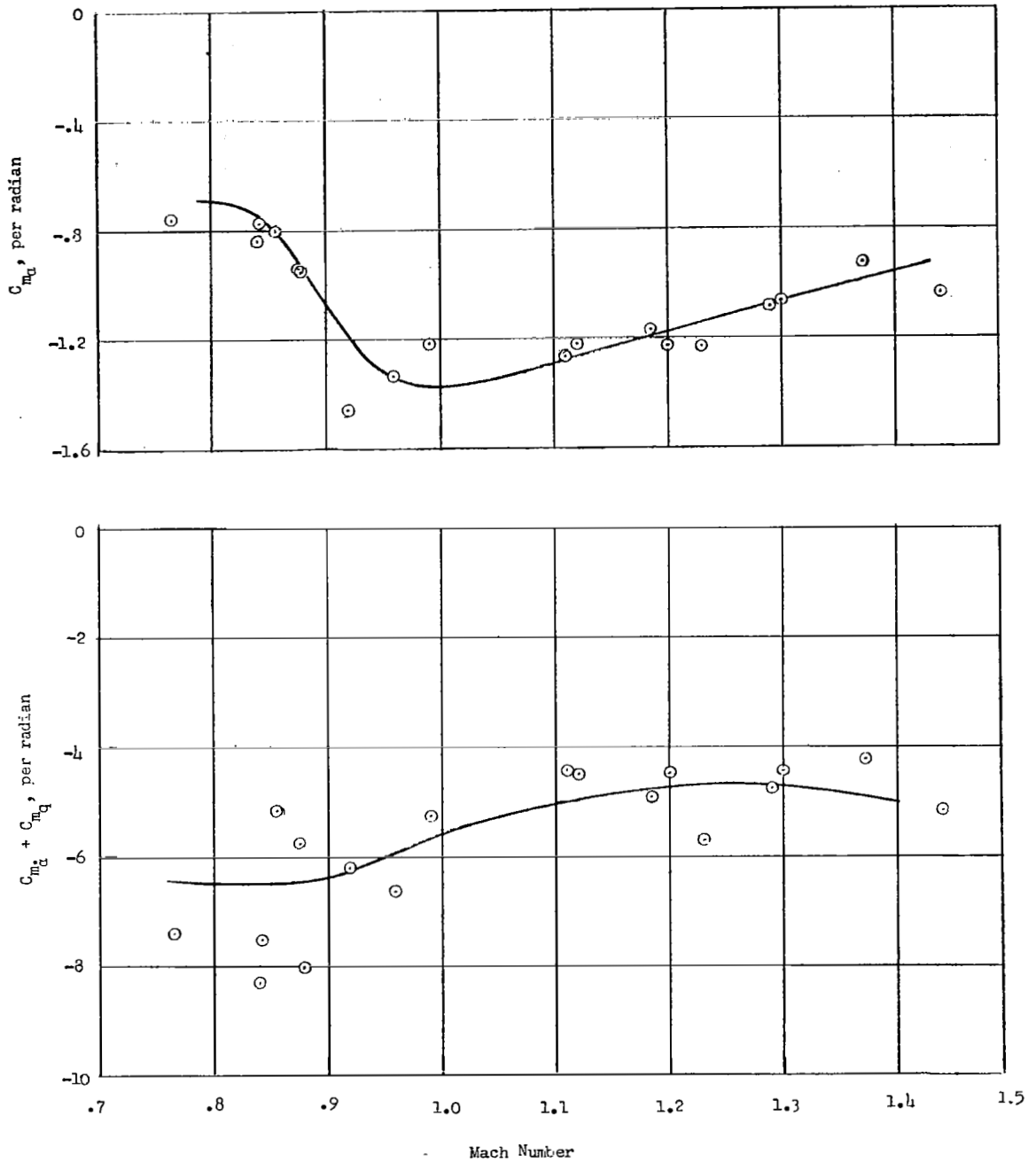


Figure 17.- Variation of C_{m_α} and $C_{m_\alpha} + C_{m_q}$ with Mach number as determined from the period and damping data presented in figure 16. Data obtained at an altitude of approximately 35,000 feet.

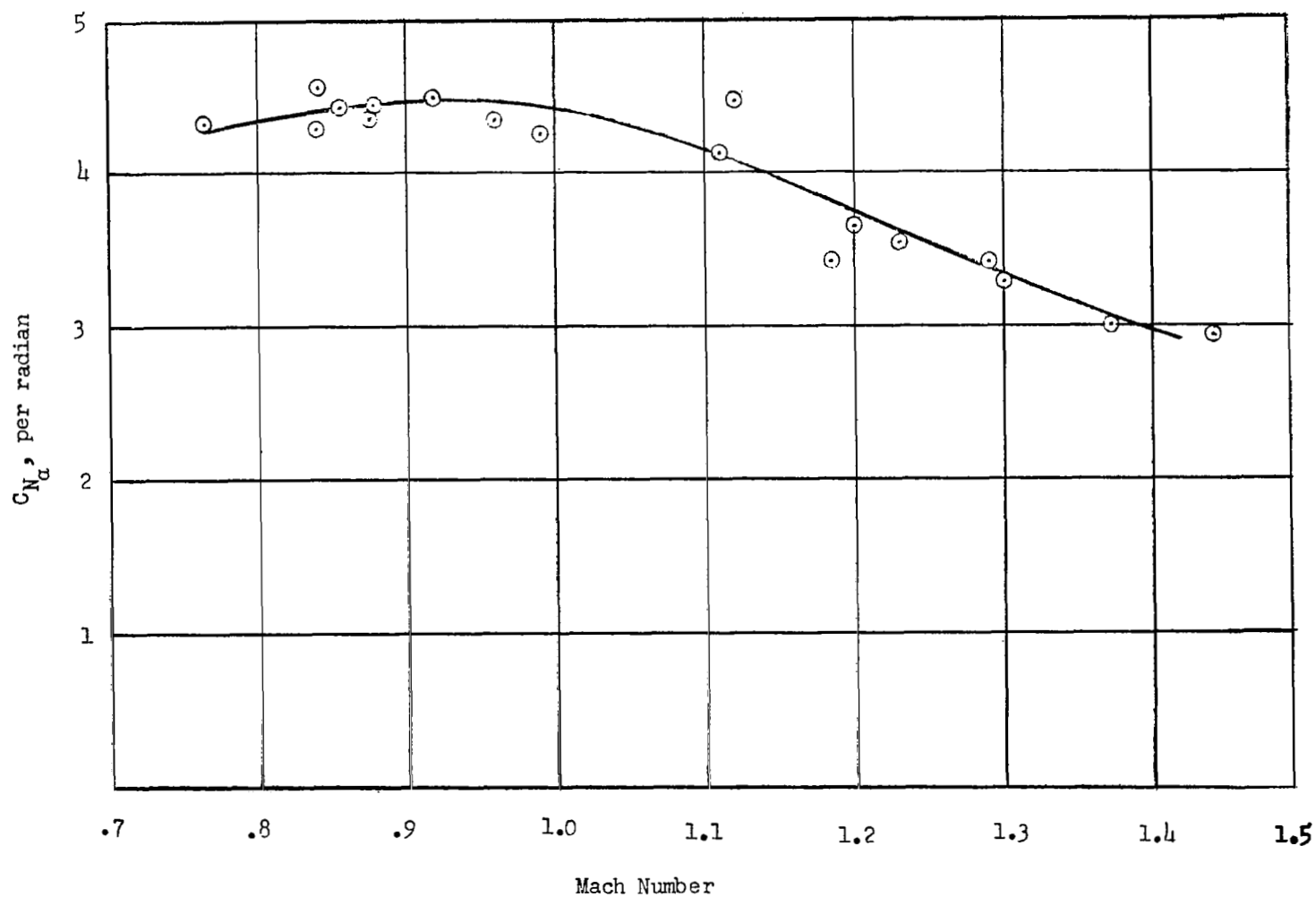


Figure 18.- Variation of C_{N_α} with Mach number as determined from the flight test data. Data obtained at an altitude of approximately 35,000 feet.

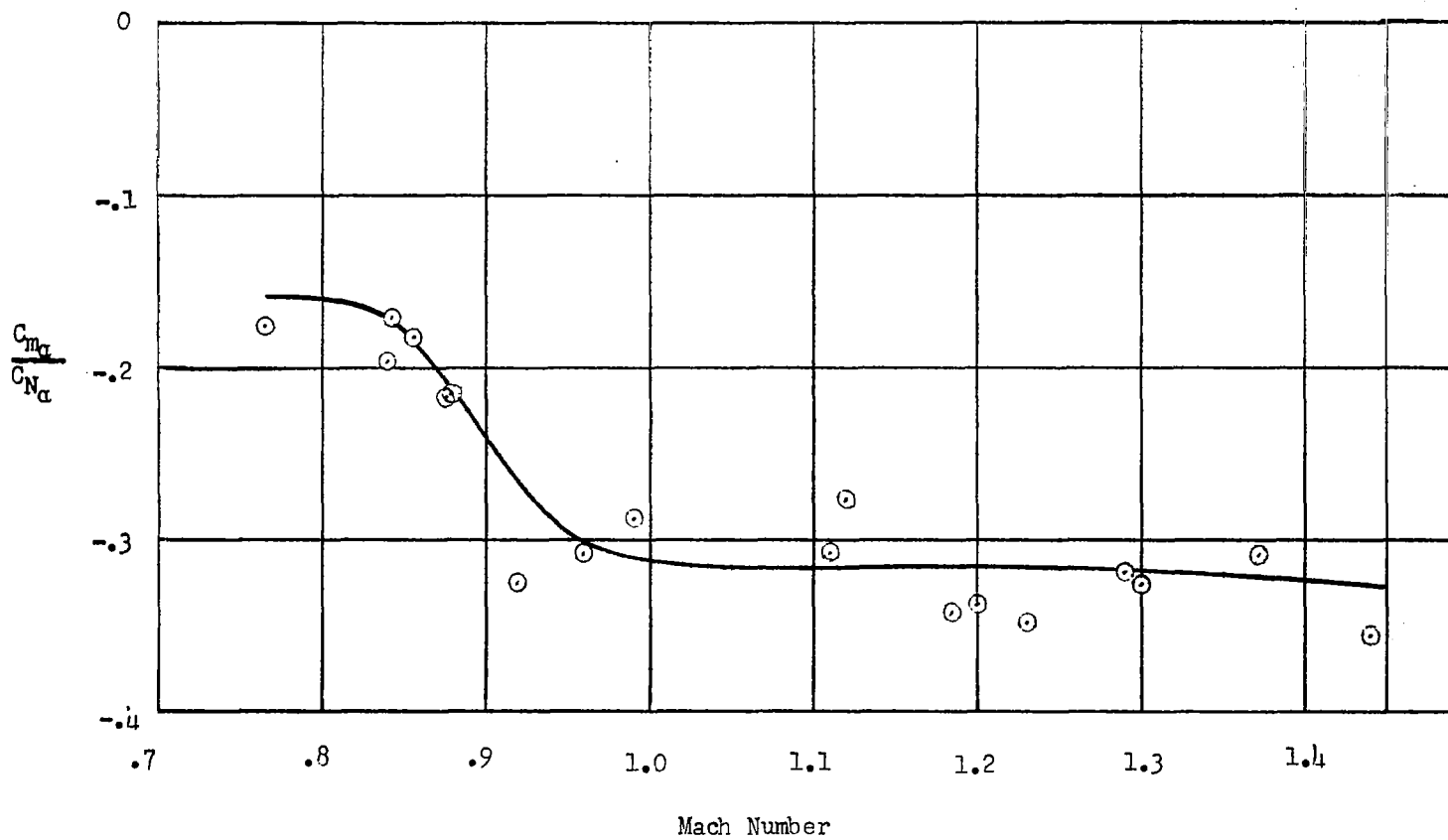
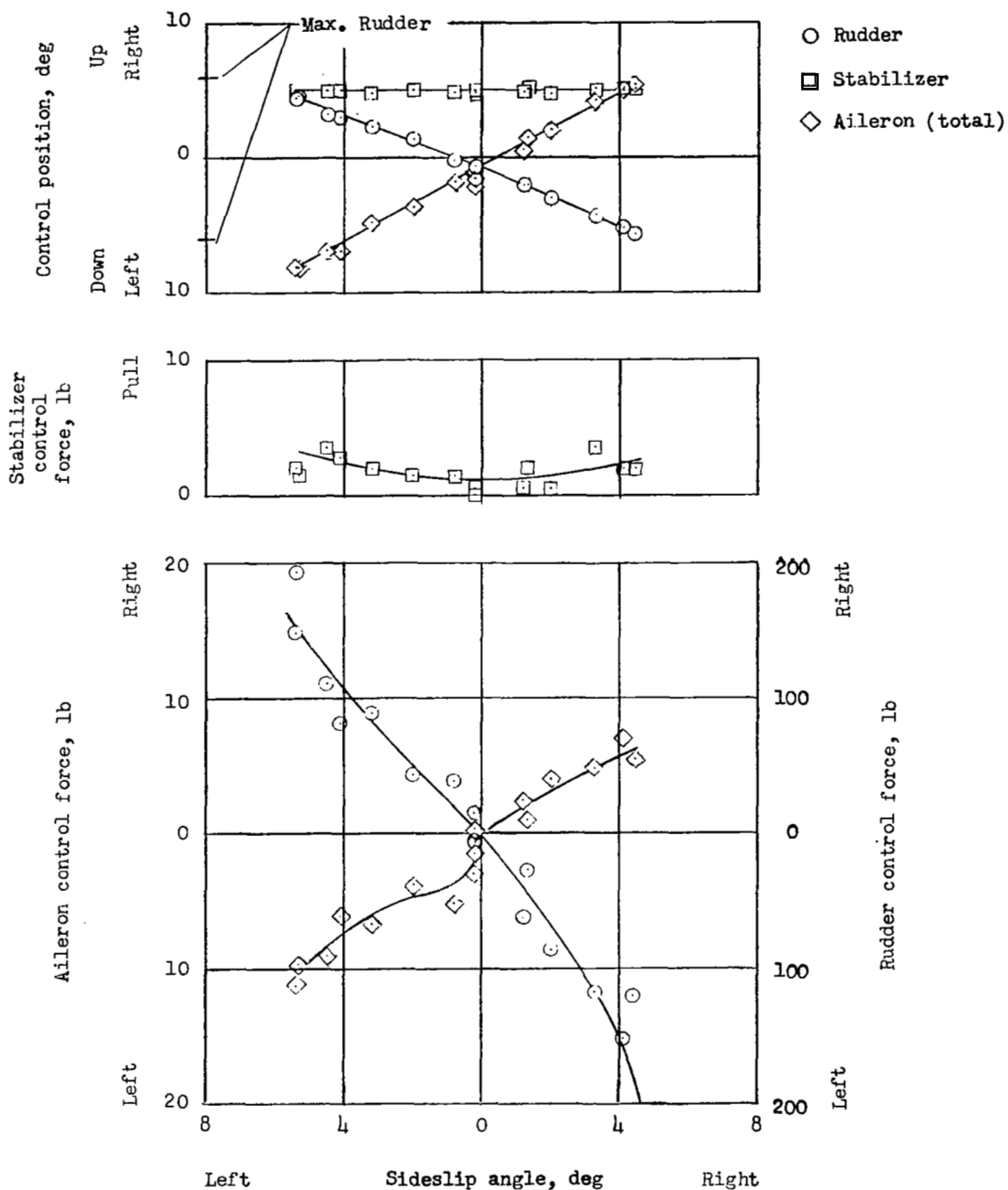
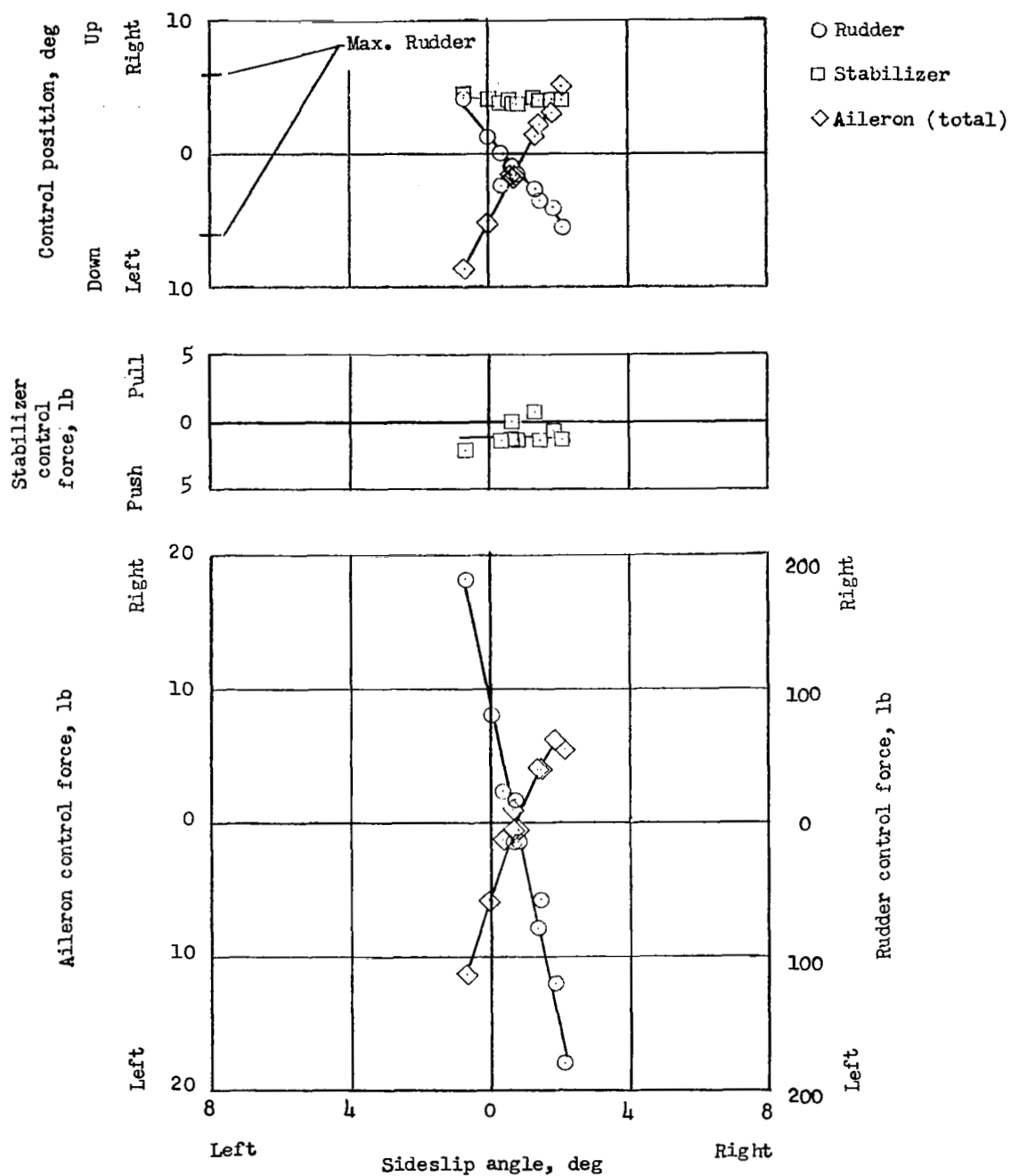


Figure 19.- Variation of aerodynamic-center location with Mach number as obtained from the flight test data. Data obtained at an altitude of approximately 35,000 feet.



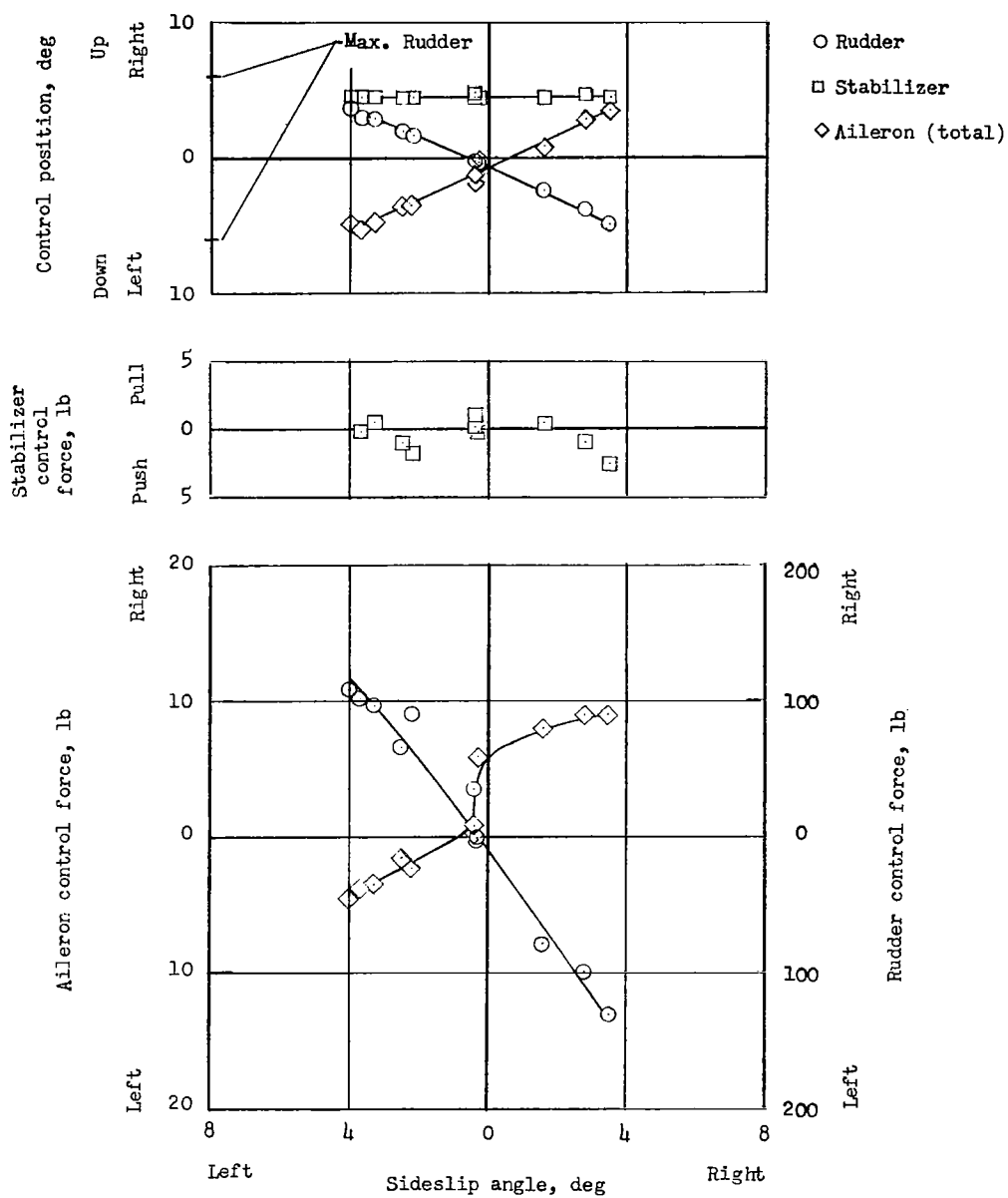
(a) $M_C = 0.83$; altitude = 35,000 feet.

Figure 20.- Static directional stability and control characteristics of the test airplane as indicated by the variation of control positions and forces with sideslip angle for various Mach numbers at altitudes.



(b) $M_C = 1.51$; altitude = 34,500 feet.

Figure 20.- Continued.



(c) $M_c = 0.83$; altitude = 21,000 feet.

Figure 20.- Concluded.

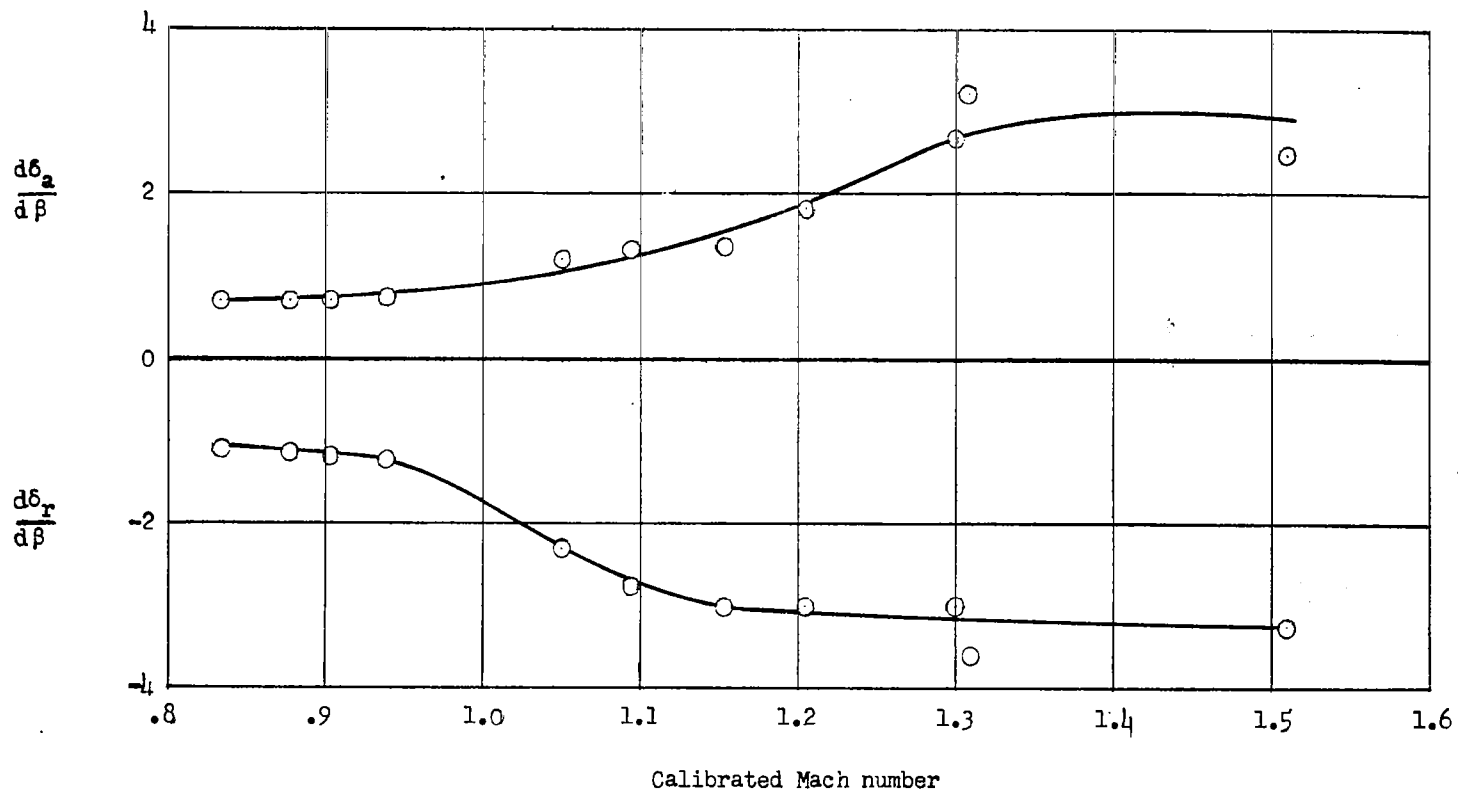
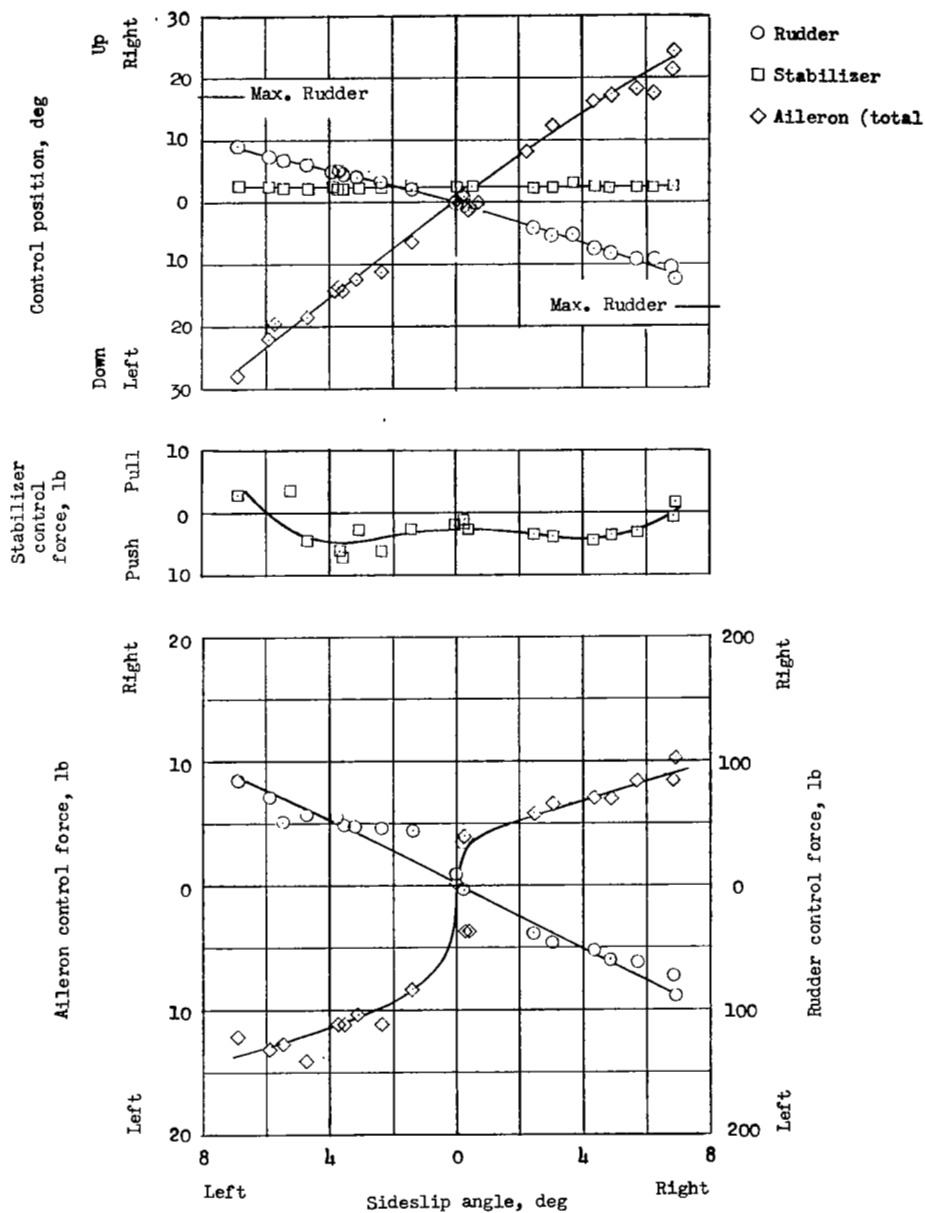
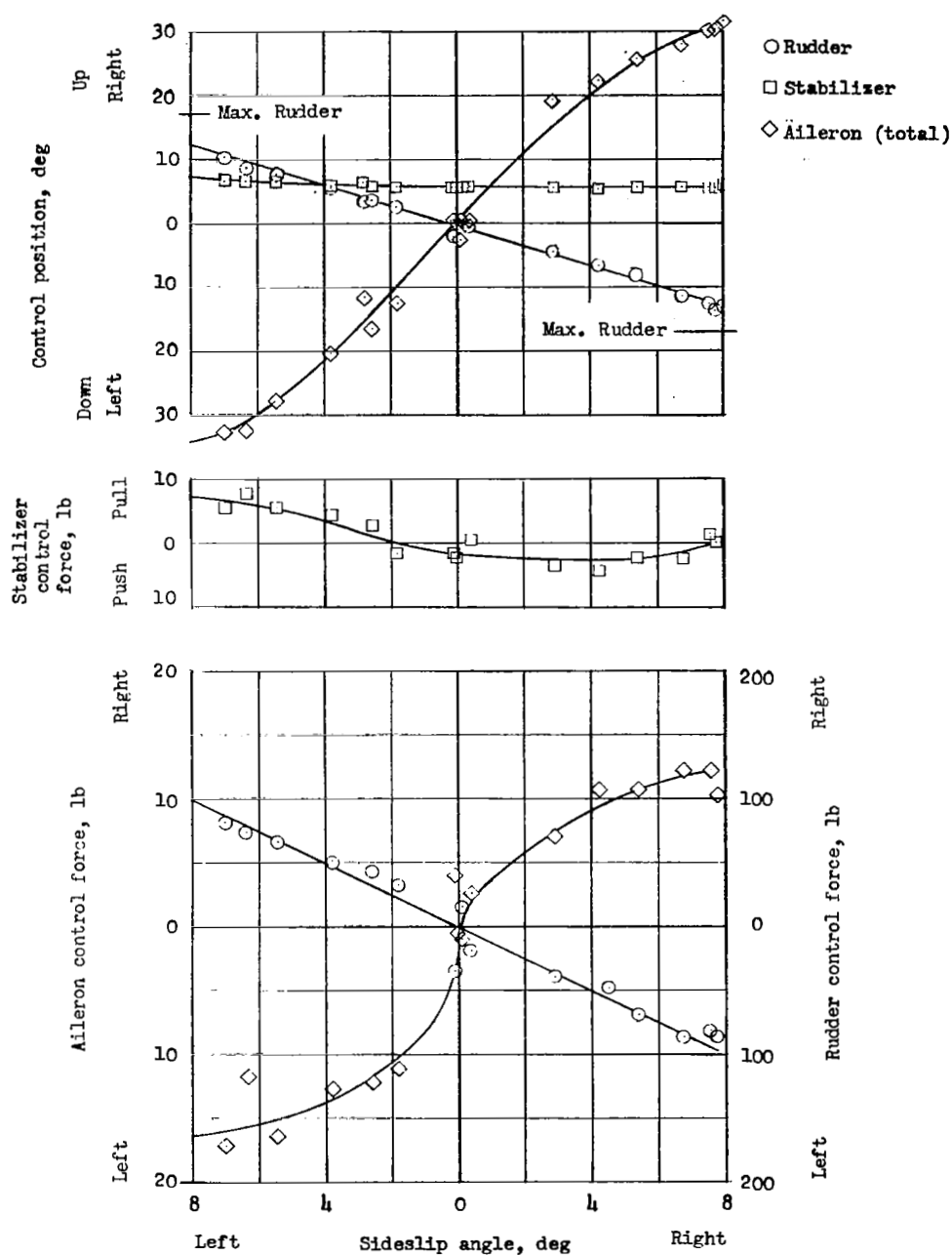


Figure 21.- Variation of the static directional stability parameter $\frac{d\delta_r}{d\beta}$ and the dihedral effect $\frac{d\delta_a}{d\beta}$ with Mach number at an altitude of approximately 35,000 feet.



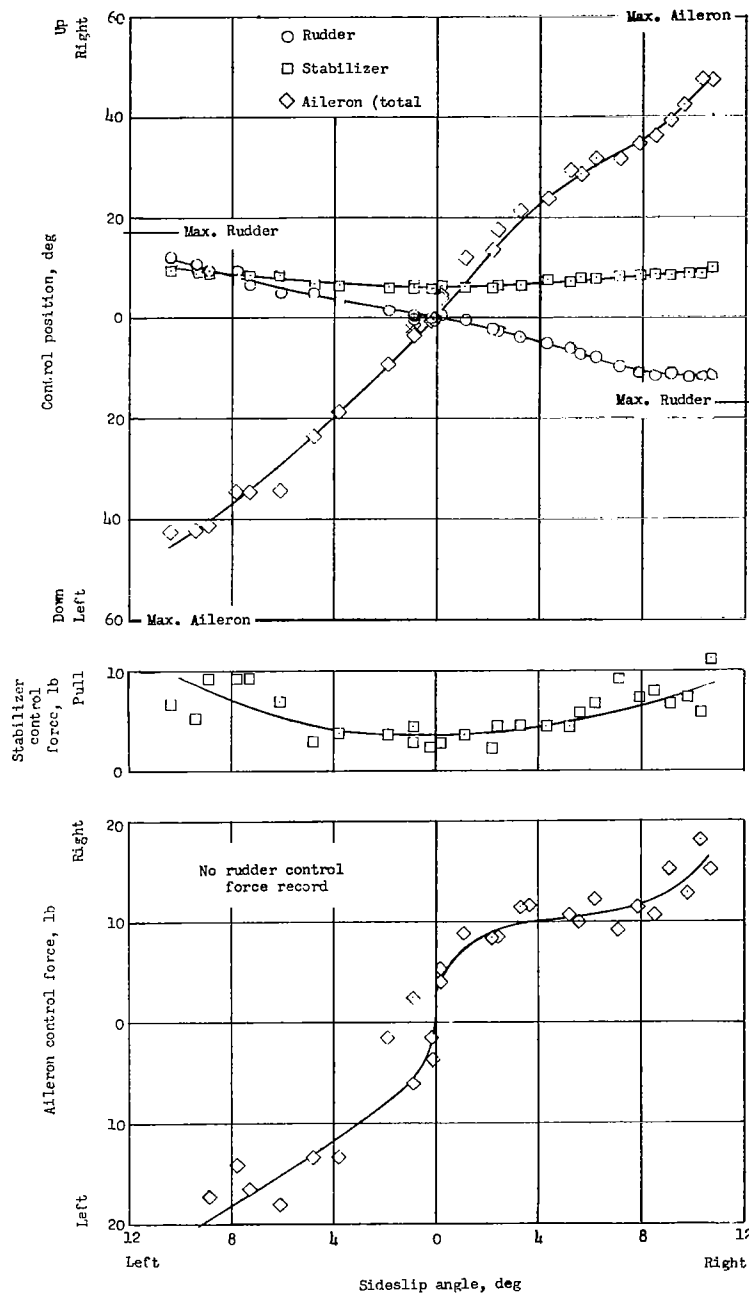
(a) $V = 200$ knots; altitude = 8,500 feet; $C_N = 0.44$; $\alpha_{i,r} = -0.84^\circ$;
 $\alpha_{i,w} = 6.16^\circ$.

Figure 22.- Static directional stability and control characteristics of the test airplane in the landing condition as indicated by the variation of control positions and forces with sideslip angle for three airspeeds.



(b) $V = 150$ knots; altitude = 8,500 feet; $C_N = 0.72$; $\alpha_{i,f} = 4.8^\circ$;
 $\alpha_{i,w} = 11.8^\circ$.

Figure 22.- Continued.



(c) $V = 138$ knots; altitude = 3,300 feet; $C_N = 0.99$; $\alpha_{i,f} = 10.1^\circ$;
 $\alpha_{i,w} = 17.1^\circ$.

Figure 22.- Concluded.

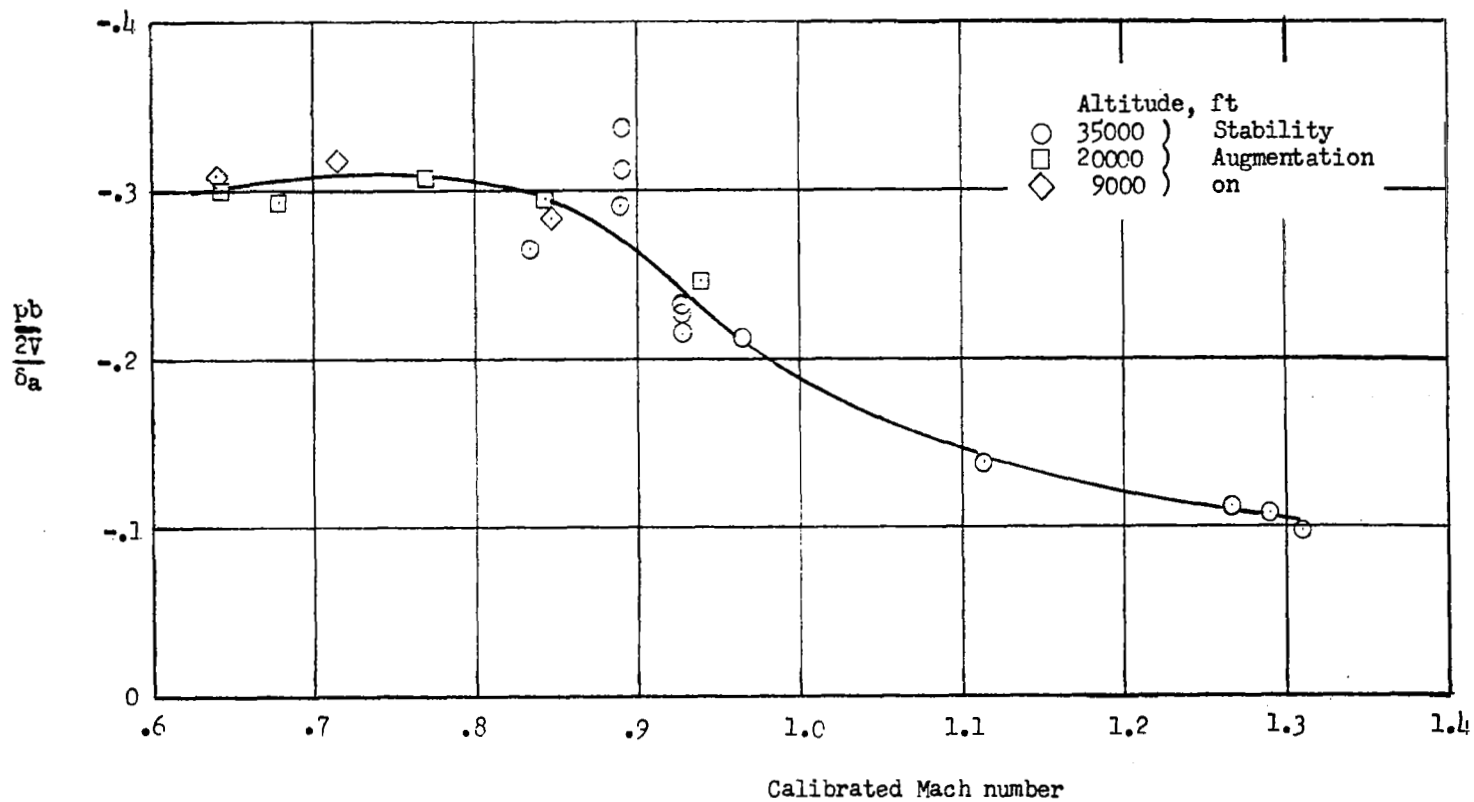


Figure 23.- Variation of helix angle $\frac{pb}{2V}$ with Mach number for a range of altitude from 9,000 to 35,000 feet.

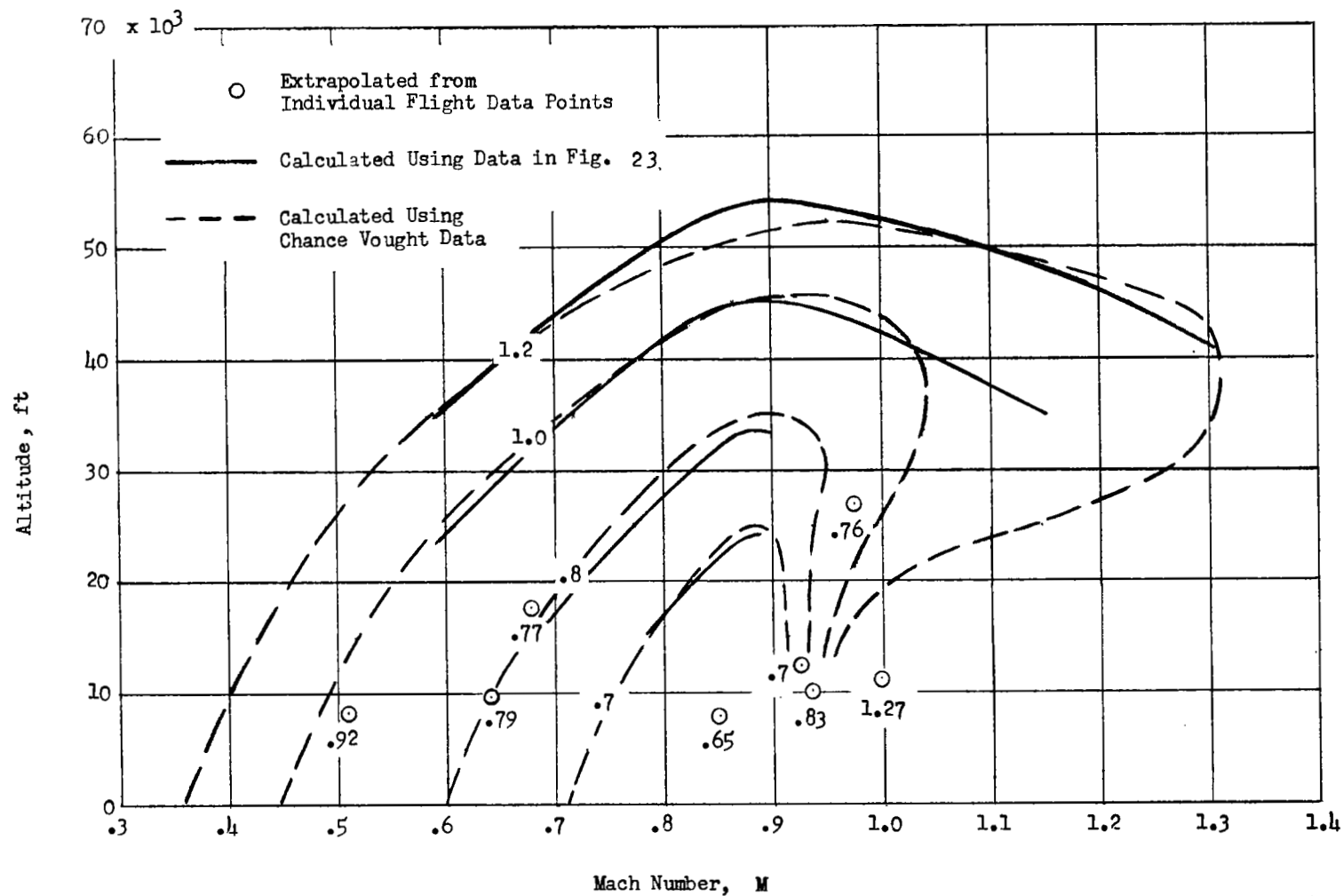


Figure 24.- Plot of the calculated and measured values of the time required to roll through a 90° angle of bank using maximum aileron deflection as a function of altitude and Mach number. Numerals designate time in seconds to roll through a 90° angle of bank.

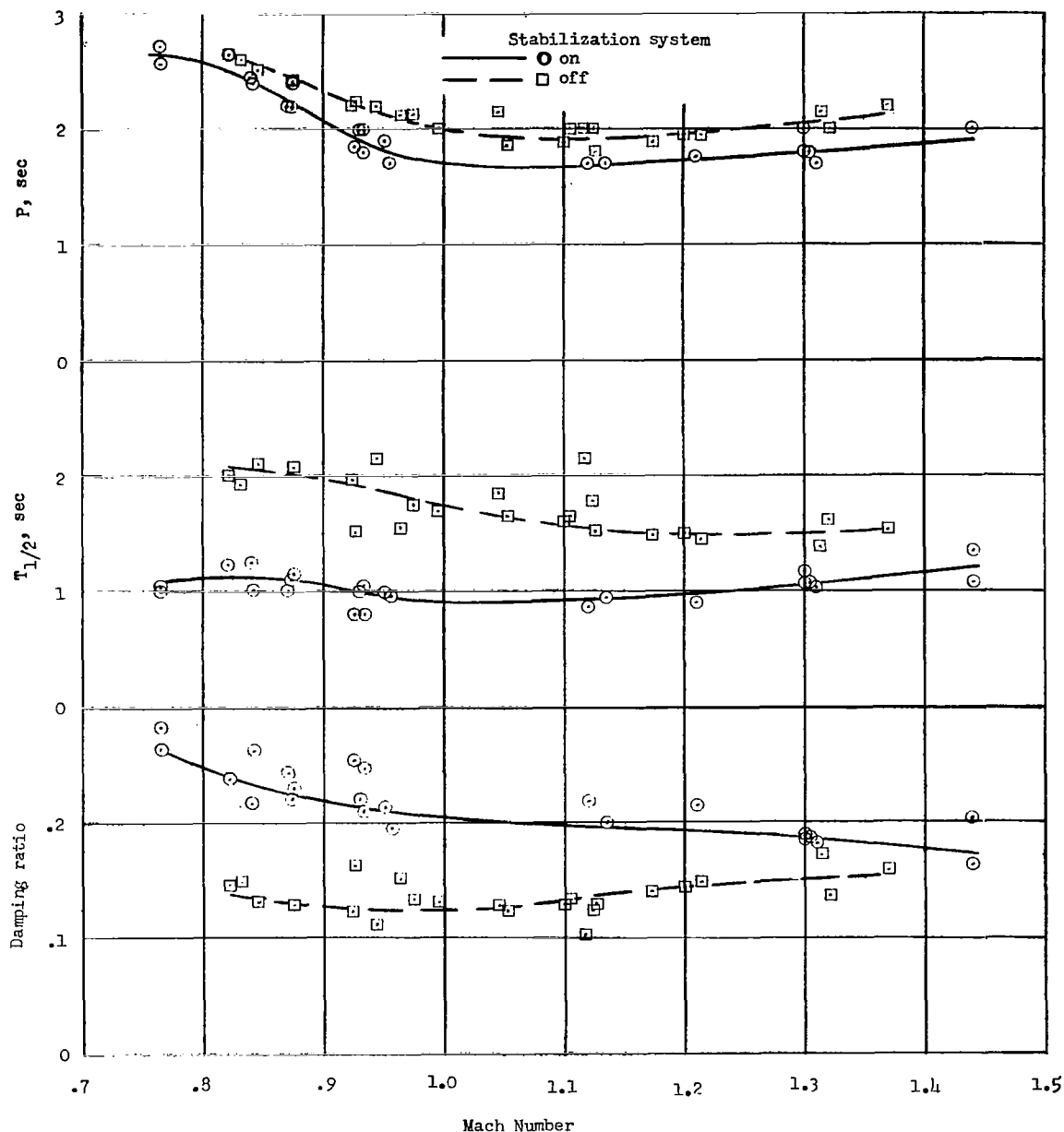


Figure 25.- Characteristics of the lateral directional oscillations showing the period, time to damp to one-half amplitude, and damping ratio as a function of Mach number at an altitude of approximately 35,000 feet. The data are presented for the stabilization system both on and off.

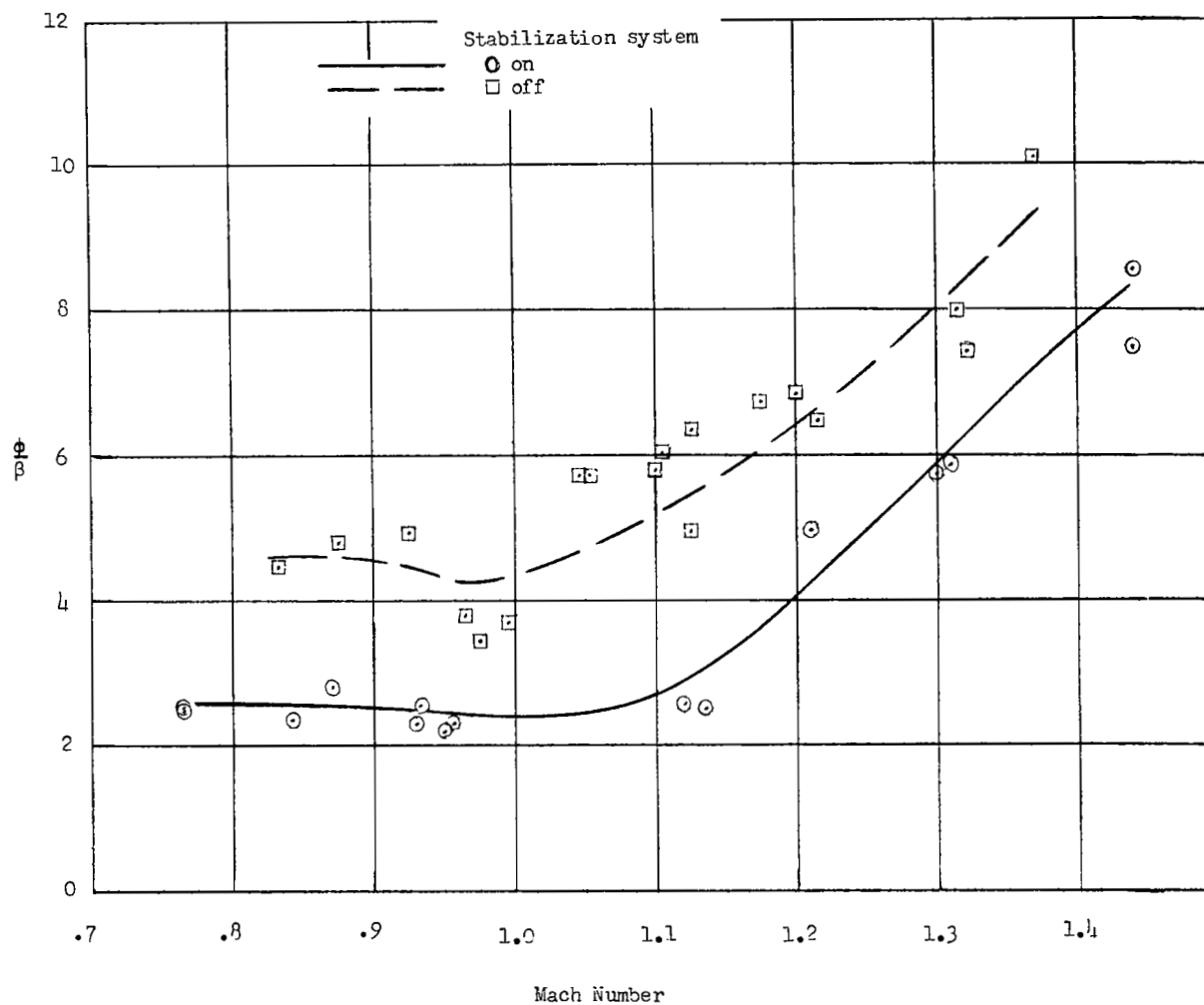


Figure 26.- Roll-to-yaw ratios as measured during the lateral directional oscillations for the stabilization system both on and off. Tests made at an altitude of about 35,000 feet.

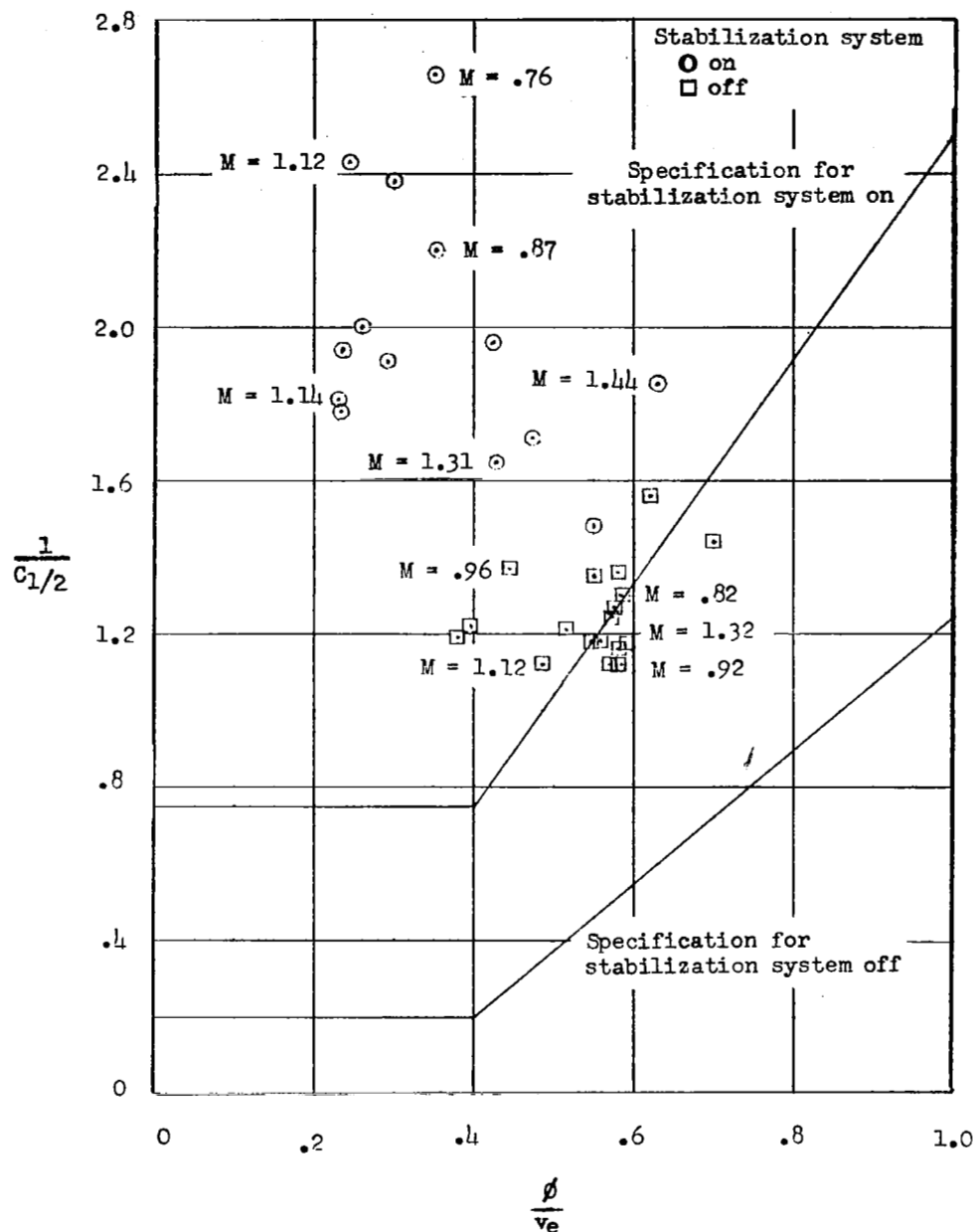


Figure 27.- Damping parameter $\frac{1}{C_{1/2}}$ as a function of the parameter $\frac{\phi}{v_e}$.

Data are presented for the stabilization systems on and off at an altitude of about 35,000 feet; also shown are the requirements as specified in reference 11.

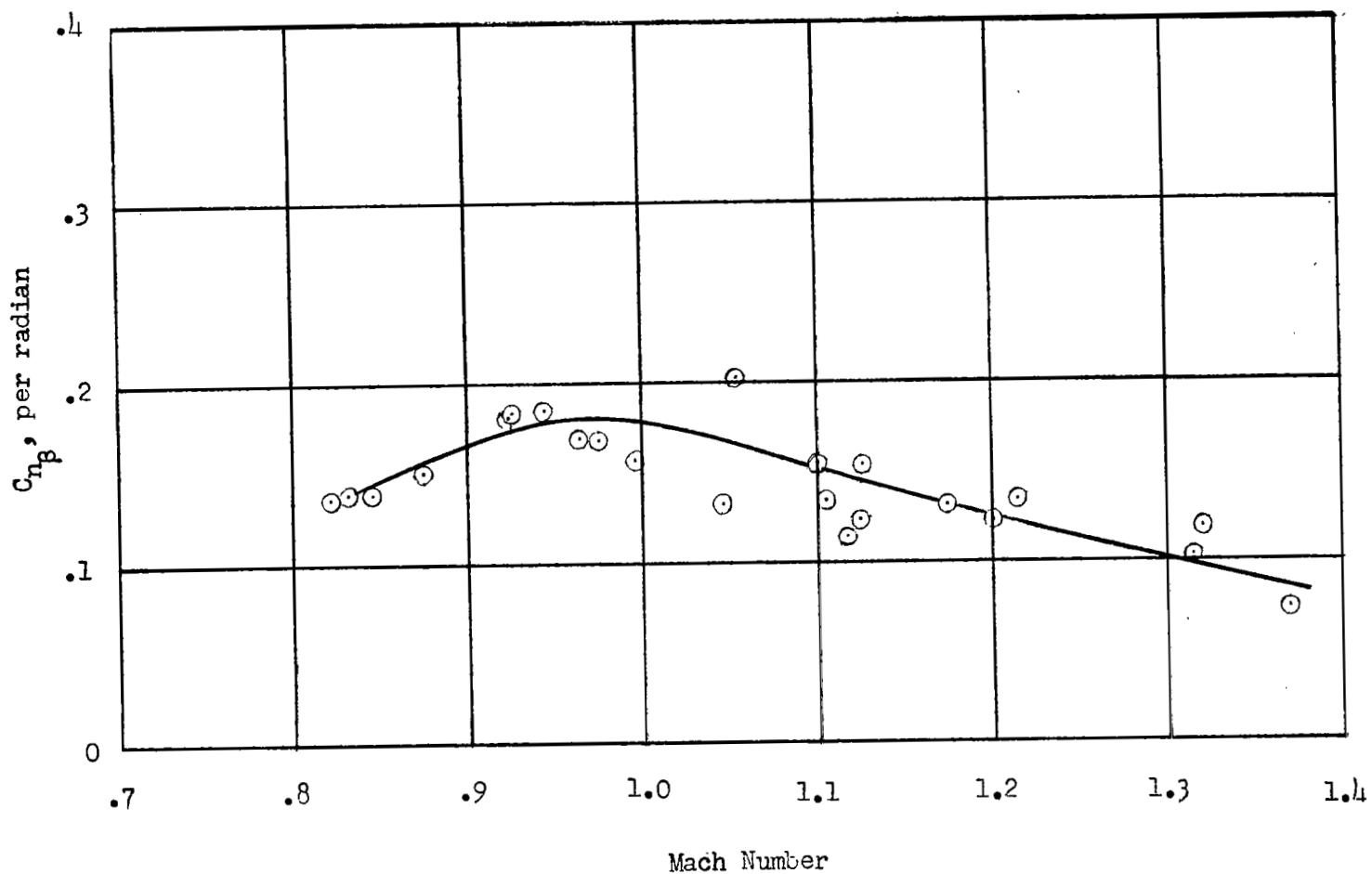


Figure 28.- Variation of the static directional-stability parameter $C_{n\beta}$ with Mach number for the stabilization systems off at an altitude of 35,000 feet. Data obtained from the period and damping data presented in figure 25.

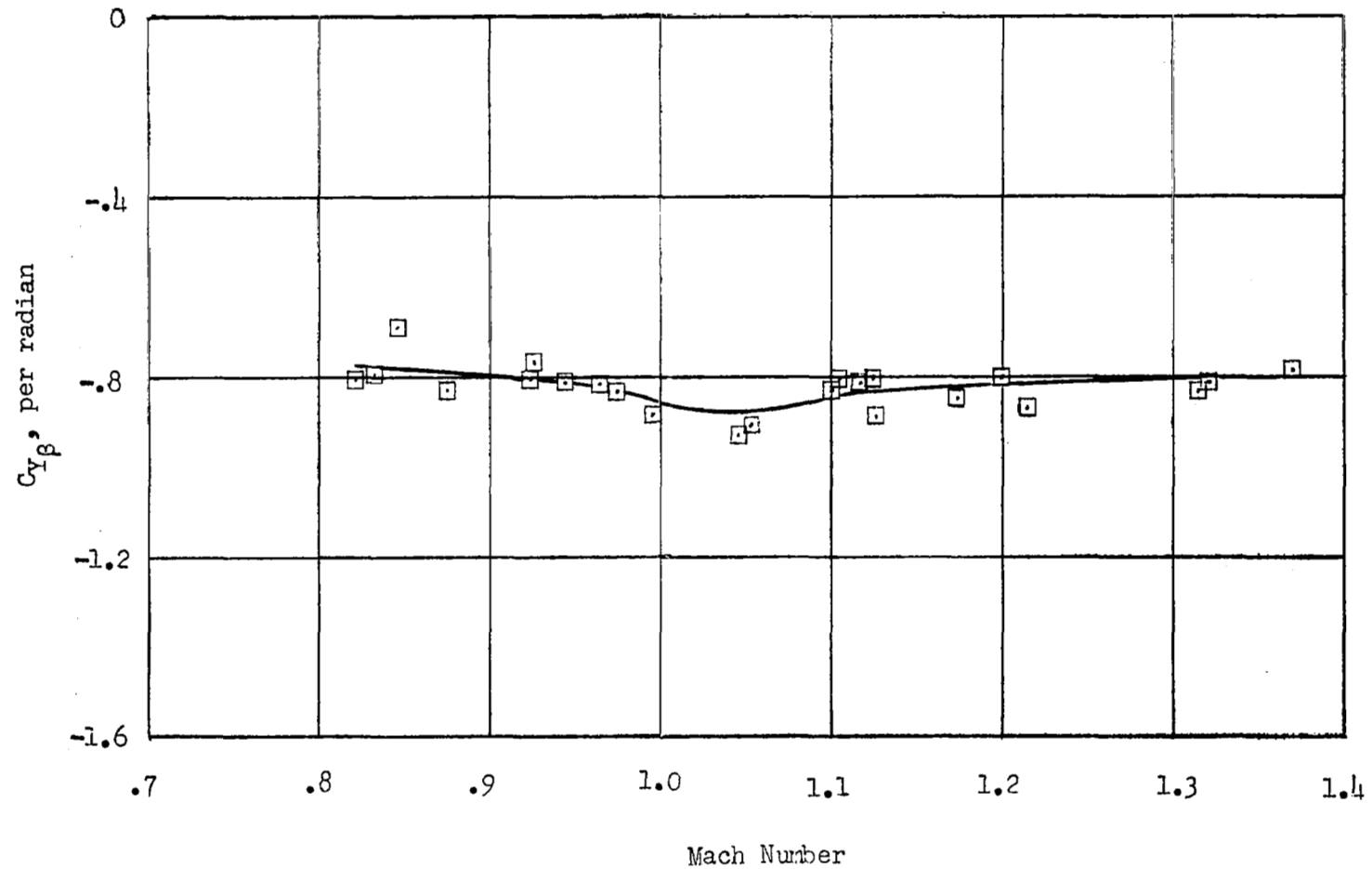
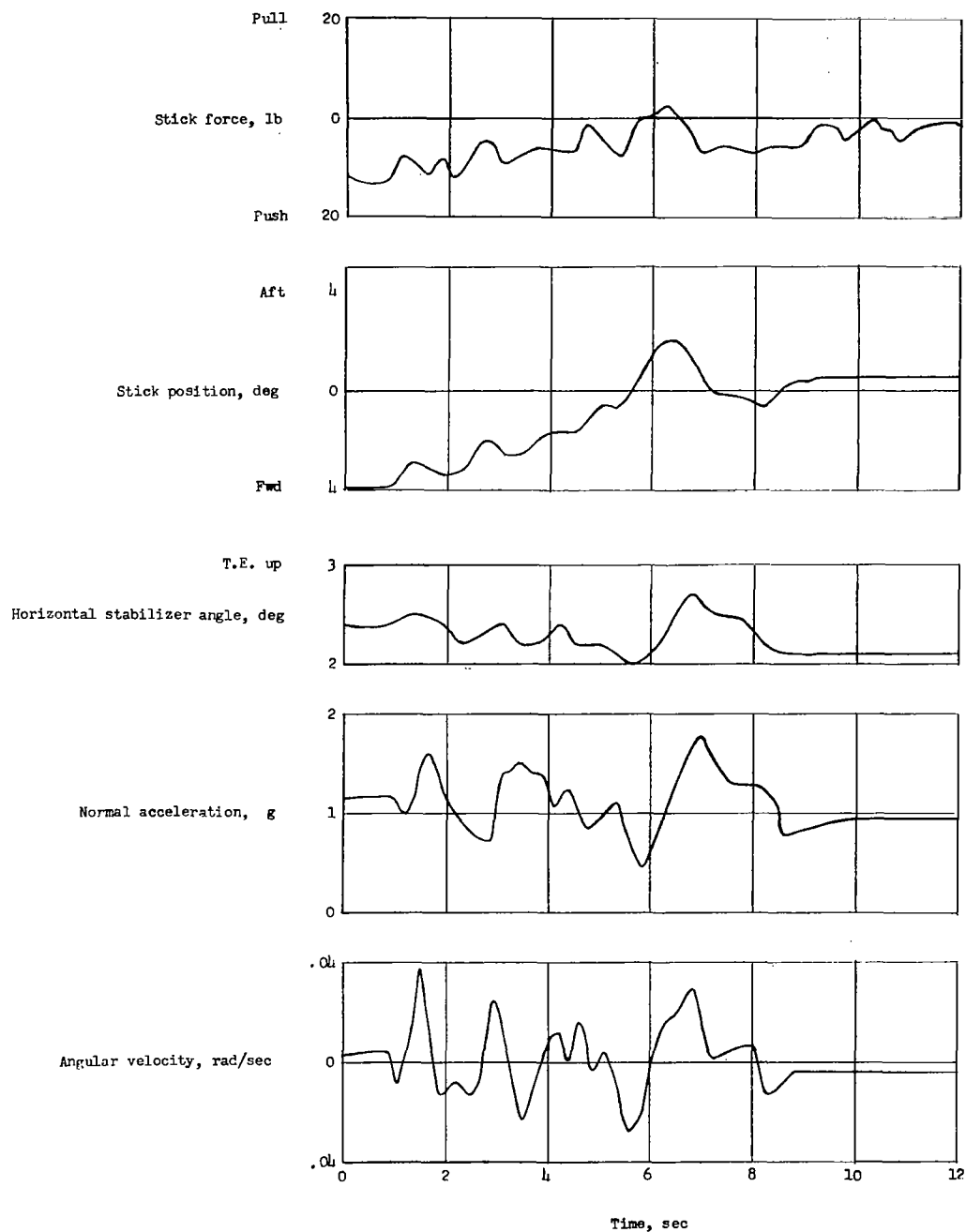
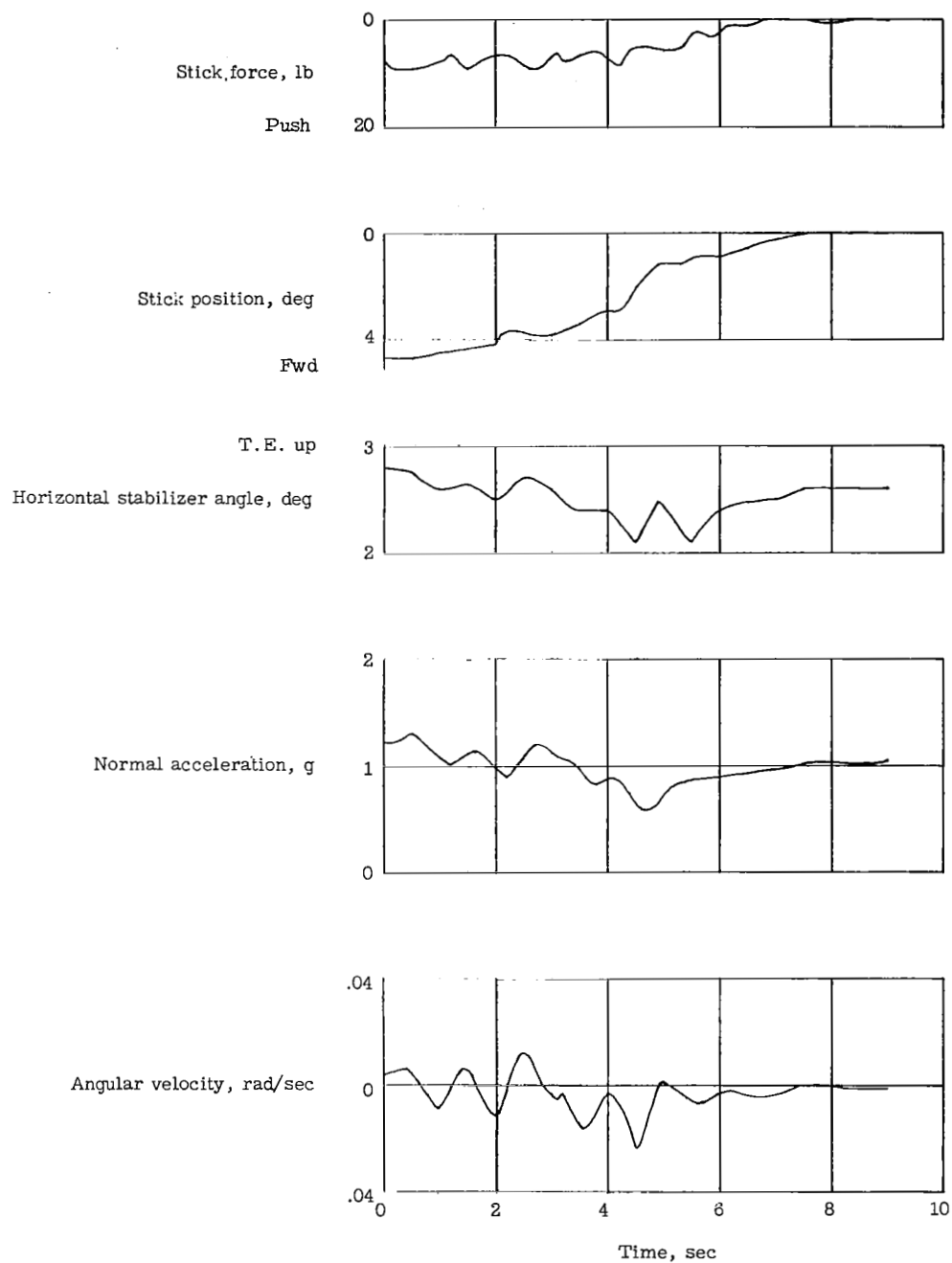


Figure 29.- Variation of the side-force parameter $C_{Y\beta}$ with Mach number for the stabilization system off at an altitude of about 35,000 feet.



(a) Attempt by the pilot to trim the airplane rapidly.

Figure 30.- Time history of attempt to trim the airplane with the normal longitudinal trim system.



(b) Typical example of the pilot's trimming procedure.

Figure 30.- Concluded.

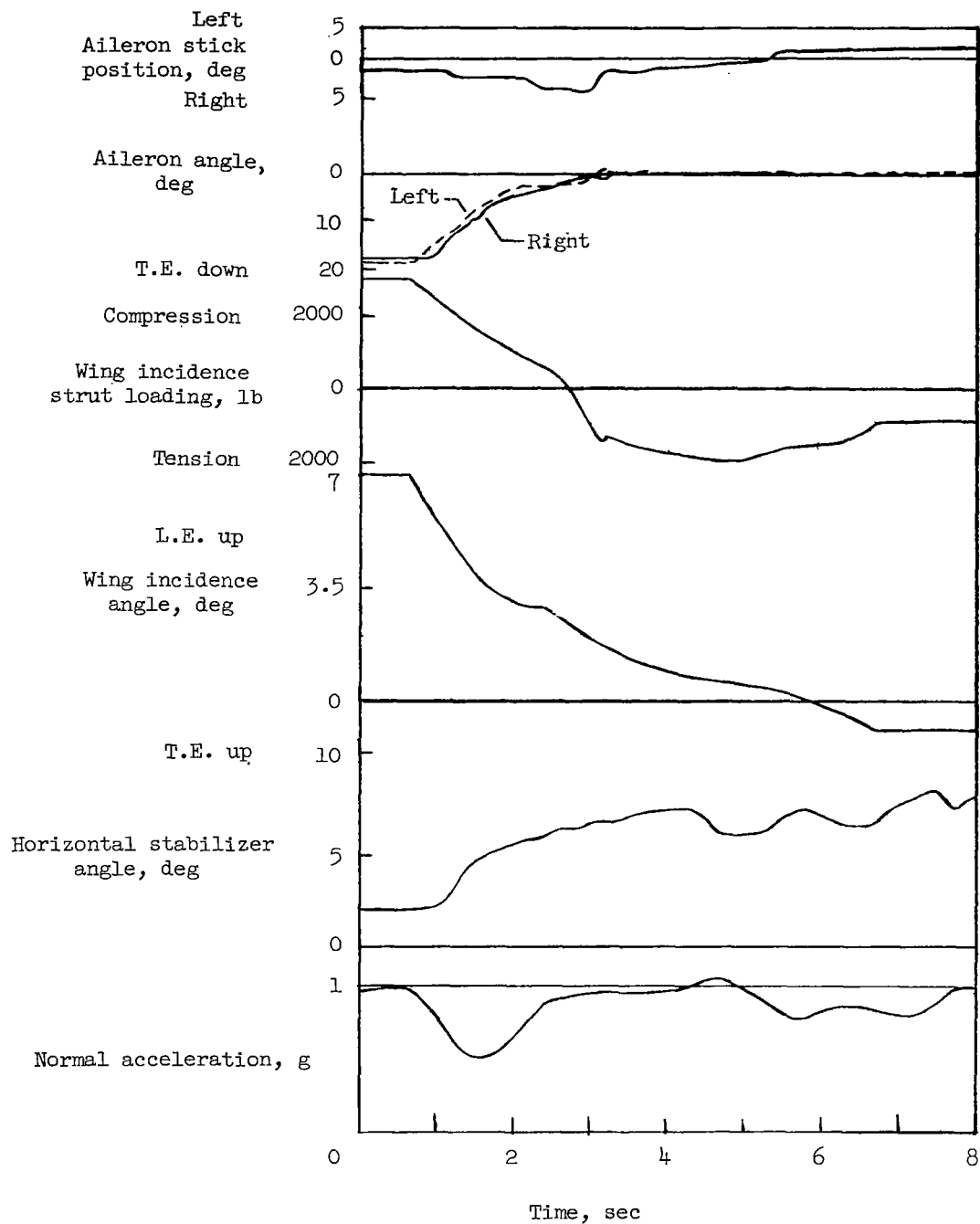


Figure 31.- Time history of a successful operation of the wing from the landing condition to the clean condition. Tests made with the cruise droop down at an indicated airspeed of 201 knots and an altitude of 11,500 feet.

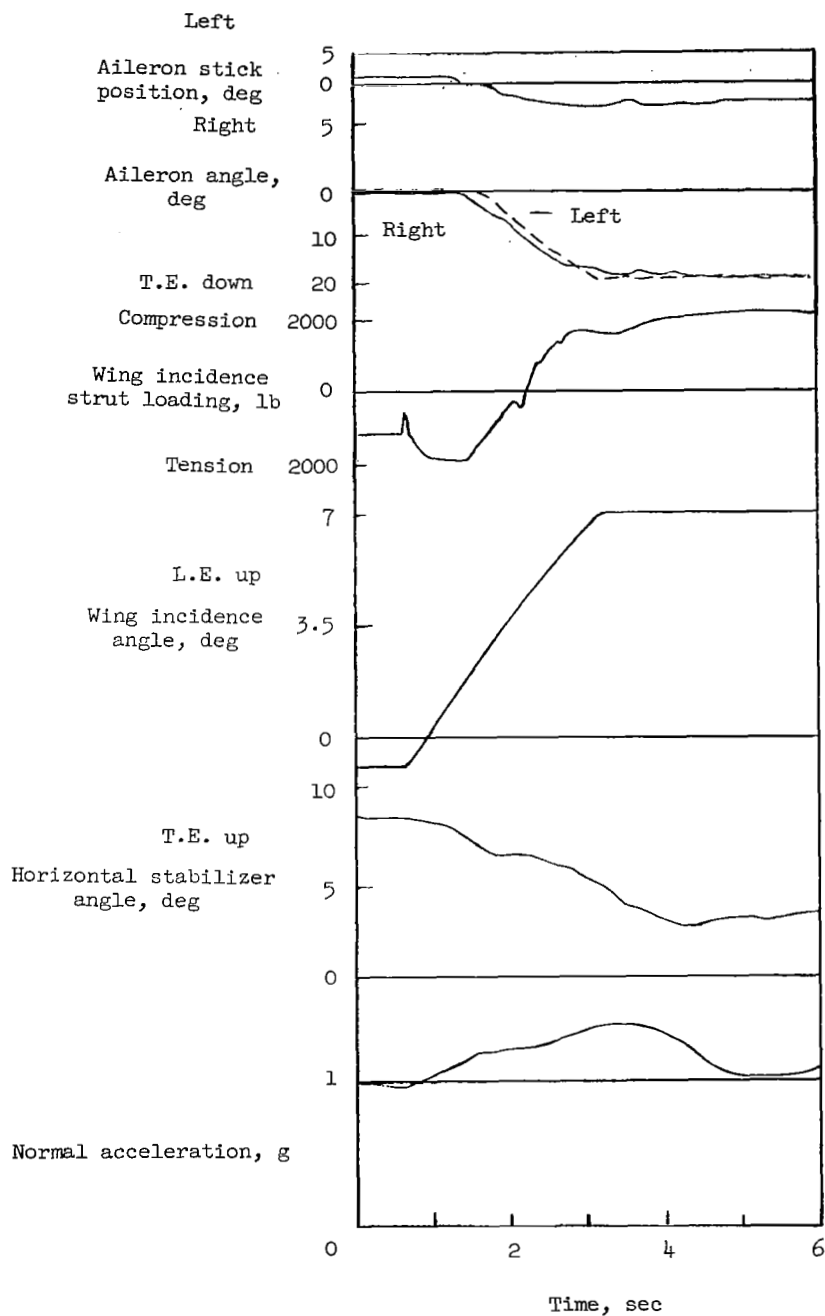


Figure 32.- Time history of the operation of the variable-incidence wing from the clean condition to the landing condition. Tests conducted at an indicated airspeed of 196 knots at an altitude of 11,000 feet.

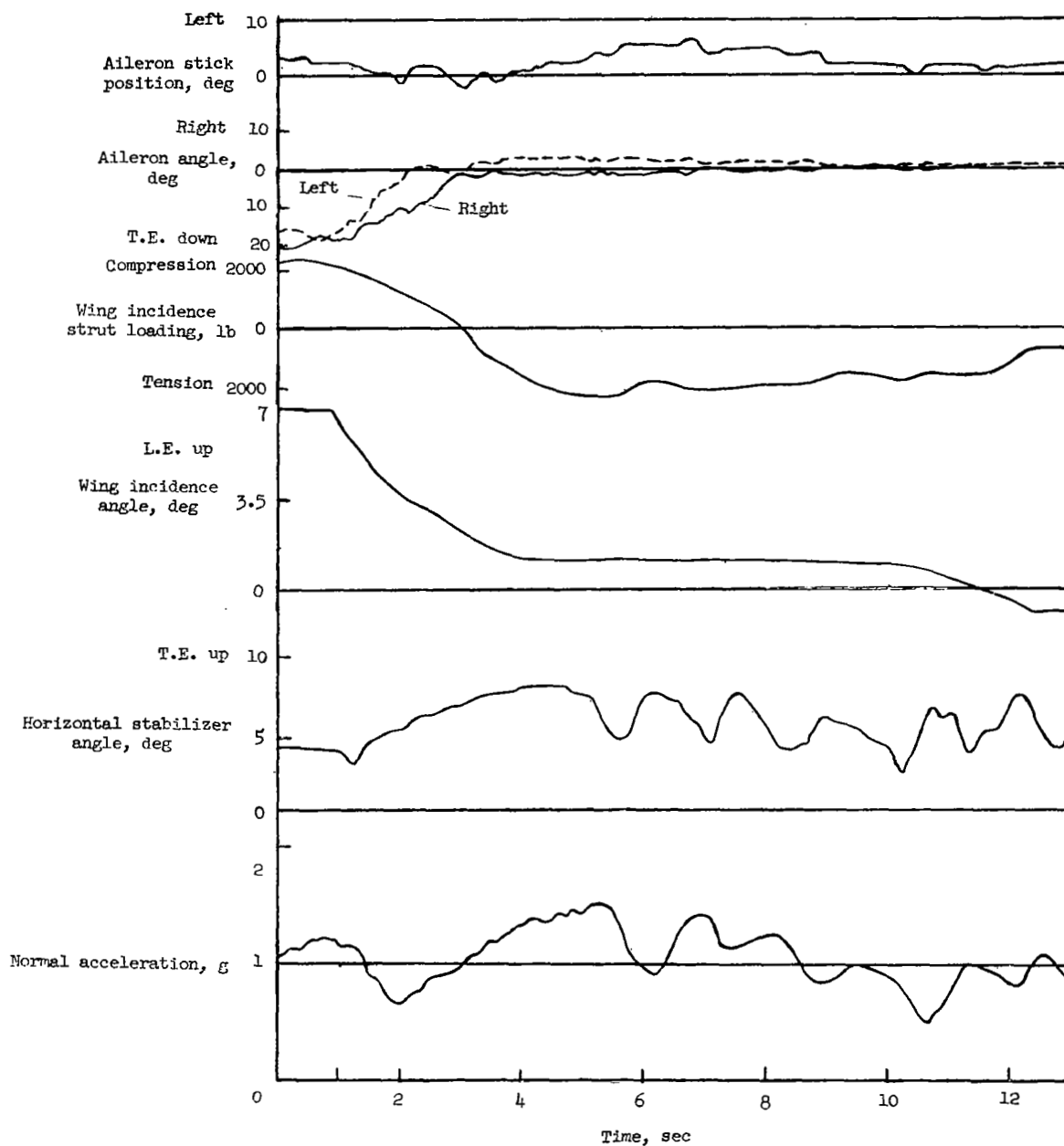


Figure 33.- Time history of the operation of the wing from the full up to the clean condition during a typical take-off. The indicated airspeed varies from about 190 knots to about 220 knots during the tests.

10-7-58L

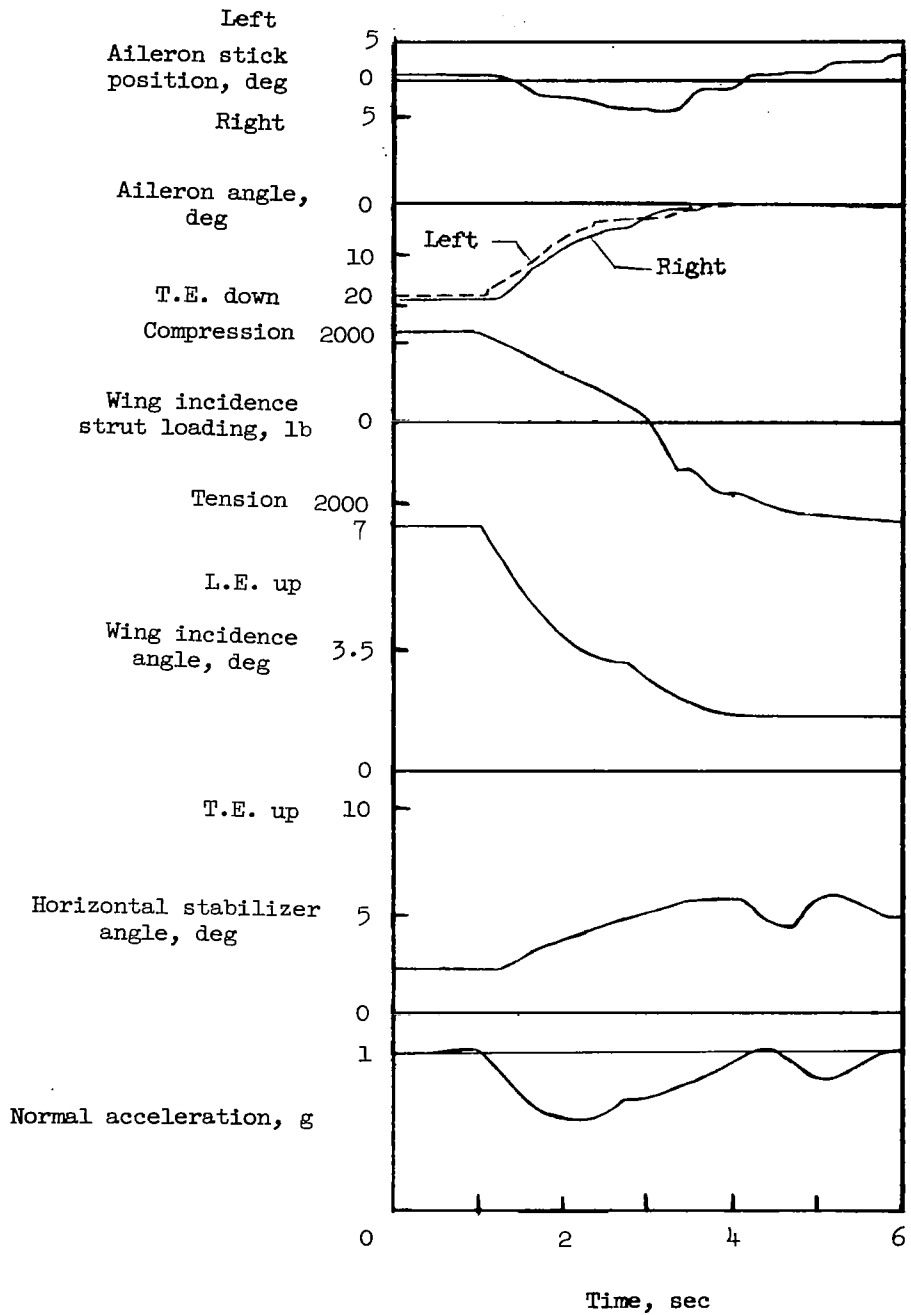


Figure 34.- Time history of an unsuccessful attempt to lower the wing to the clean condition. Tests made with the cruise droop up at an indicated airspeed of 197 knots at 11,500 feet altitude.

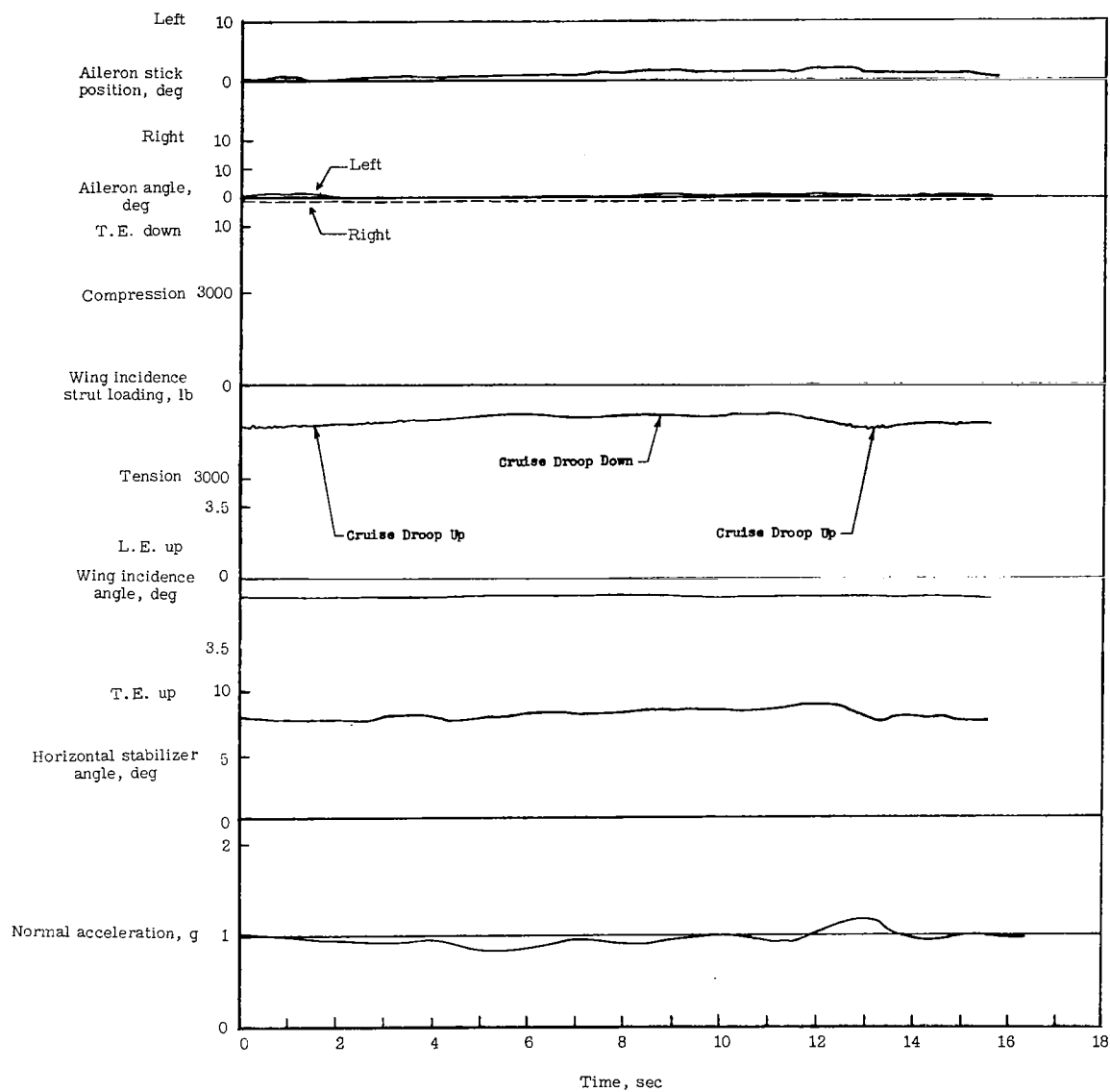


Figure 35.- Time history of the operation of the cruise droop at an indicated airspeed of about 178 knots and an altitude of 15,800 feet.

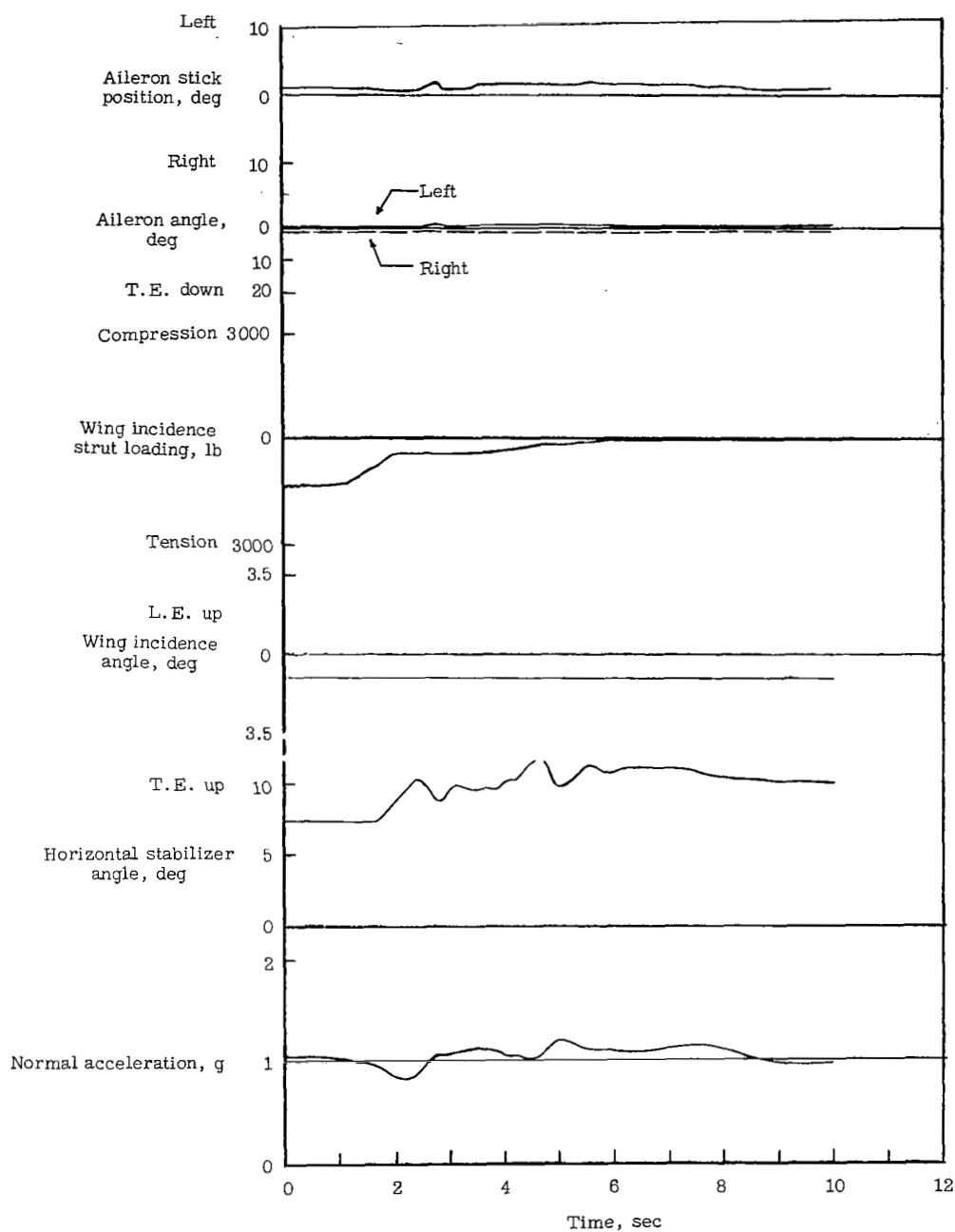
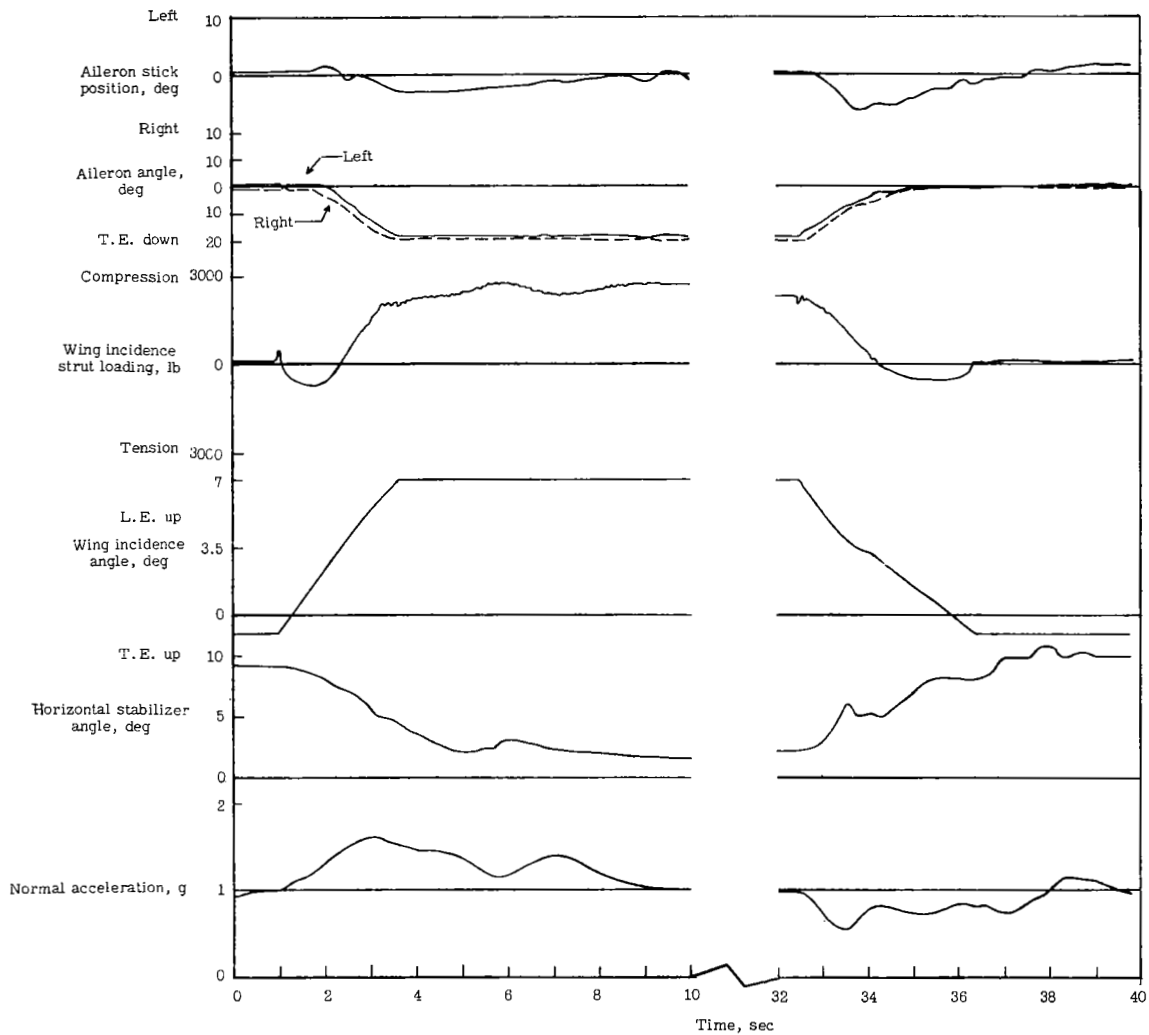


Figure 36.- Time history of the operation of the leading-edge droop from the full-up position to the landing-droop position with the wing in the down and locked position. Tests conducted at an indicated airspeed of about 186 knots at an altitude of 15,800 feet.



(a) Wing-up cycle; $V_i = 198$ knots; 15,500 feet. (b) Wing-down cycle; $V_i = 181$ knots; 16,000 feet.

Figure 37.- Time history of the operation of the variable-incidence wing with the leading-edge droop locked in the landing-droop position during the entire cycle.